The Impacts of Aviation Emissions on Human Health through Changes in Air Quality and UV Irradiance

by

Elza Brunelle-Yeung

B.Eng. in Mechanical Engineering, McGill University, 2007

Submitted to the Department of Aeronautics and Astronautics
in Partial Fulfillment of the Requirements for the Degree of

Master of Science in Aeronautics and Astronautics

at the

MASSACHUSETTS INSTITUTE OF TECHNOLOGY

[illegible]
May 2009

Author.....
Department of Aeronautics and Astronautics
May 22, 2009

Certified by.....
Ian A. Waitz
Jerome C. Hunsaker Professor of Aeronautics and Astronautics
Department Head
Thesis Supervisor

Accepted by.....
David L. Darmofal
Professor of Aeronautics and Astronautics
Associate Department Head
Chair, Committee on Graduate Students

ARCHIVES

The Impacts of Aviation Emissions on Human Health through Changes in Air Quality and UV Irradiance

by

Elza Brunelle-Yeung

B.Eng. in Mechanical Engineering, McGill University, 2007

Submitted to the Department of Aeronautics and Astronautics
in Partial Fulfillment of the Requirements for the Degree of

Master of Science in Aeronautics and Astronautics

Abstract

World-wide demand for air transportation is rising steadily. The air transportation network may be limited by aviation's growing environmental impacts. These impacts take the form of climate impacts, noise impacts, and health impacts, the latter of which are addressed in this thesis.

Aircraft emissions released into the atmosphere have an impact on human health. In the context of assessing the environmental impacts of aviation-related policies, costs and benefits on human health must be considered. Two different models were developed as tools to assess the impacts of aircraft emissions on human health. The first model estimates the changes in skin cancer incidences and mortalities due to changes in ozone column caused by aircraft NO_x emissions. The second model estimates changes in health endpoints related to changes in ambient concentrations of particulate matter ($PM_{2.5}$) by estimating changes in elemental carbon, primary and secondary organic PM, secondary sulfates, and secondary nitrates. The air quality model discussed herein is the second iteration in the development of a response surface model (RSM) based on a set of 25 simulations done with the Community Multiscale Air Quality model (CMAQ), a more complex atmospheric chemistry model.

The increase in adult premature mortalities in the U.S. caused by air quality impacts of aviation emissions in year 2005 is estimated at 210 deaths per year (90% confidence interval: 130 - 340). This considers only those emissions that occur below 3000 feet above ground level as is consistent with

current regulatory practice for aviation. The monetized value of the mortality and morbidity effects using RSM v2 outputs is estimated at $1.4 billion in year 2000 US dollars (90% confidence interval: $550 million - $2.8 billion). Of these total impacts, 4 % are found to stem from emissions of volatile organic compounds and volatile particulate matter from organics, another 12 % from emissions of sulfur dioxide and volatile particulate matter from sulfur, 70 % from nitrogen oxide emissions, and 14% from non-volatile particulate matter emissions

The net benefit from subsonic aircraft NO_x in year 2002 on nonmelanoma skin cancer incidence and associated mortality in the U.S. is estimated at $130 M (90 % confidence interval : $68 – $220 M) in 2000 dollars. This corresponds to the prevention of approximately 6,200 new basal cell carcinoma cases (BCC) (90 % confidence interval: 3,800 – 9,100), 2,900 new squamous cell carcinoma cases (SCC) (90 % confidence interval: 1,700 – 4,200), and 20 nonmelanoma skin cancer (NMSC) premature mortalities (90 % CI : 13 – 28). The monetary benefits due to the prevention of 20 cases of premature mortality represent 96 % of total skin cancer benefits.

Acknowledgments

In the course of preparing this Master's thesis at MIT, I received encouragement, support, guidance and counsel from the following people, all of whom have made the process all the more enjoyable. I have had the pleasure of working with the most incredible people, and have grown tremendously from this experience.

My advisor Professor Ian Waitz tops the list. His dynamism and natural ability for motivating his students (and just about anyone within a ten kilometer radius) has kept me positively motivated and excited about my research. Ian's deep knowledge allows him to provide his students with great technical insight. His mentorship has been invaluable to me. I am convinced that Ian is the best advisor that anyone could ever hope for. Working under his supervision has been extremely educational, fulfilling, and inspirational. His managerial style is one that I aspire to possess one day.

The continuous moral support and encouragement that my parents, Olivette Brunelle and Chi Im Yeung, have shown me throughout my studies have been an important boost for me. I am forever grateful for their love and all that they do for me.

Working with my labmates has been a fantastic experience. I sincerely thank all of them for their positive attitudes, their patience, and the sense of family that we share. Special thanks are due to Stephen Kuhn with whom I tackled the new RSM and CMAQ work. His efficiency and initiative were especially notable. We made a great team. I thank Rhea Liem for her kindness, her friendship, and her collaborative help in the assessment of the AQ model. I thank Anuja Mahashabde to whom I looked up to for her experience and great problem-solving skills. Thanks go to Doug Allaire for his expertise in assessment methods and for his camaraderie. Steven Barrett's words of wisdom often shone like beacons in the fog, providing invaluable atmospheric chemistry guidance. Special thanks to Julien Rojo, Tudor Masek, and Chris Sequeira for their mentorship, their generous willingness to help despite being miles away with jobs, and their friendship. Mina Jun, Alice Fan, Pearl Donohoo, Jim Hileman, Chelsea He, Chris Dorbian, Andrew March, Bastien Martini, and Russell Stratton, thank you for making my PARTNER experience so fun!

The AHEF section of this thesis could not have been made possible without the collaboration of ICF International's Rawlings Miller and Mark Wagner. The generosity of their time given and their enthusiasm for the project has been remarkable.

I would also like to thank the MIT Aeronautics and Astronautics Department for making my time at MIT absolutely memorable. I find the sense of community within the department to be phenomenal.

Finally, a warm thank you goes out to my close friends and family for their unrelenting support. Thank you for caring so much!

Table of Contents

List of Figures

List of Tables

1 Introduction

1.1 Context

World-wide demand for air transportation is rising steadily. While the expansion of the world's air transportation network is faced with infrastructure barriers, such as scarcity of undeveloped land around airports on which to build new runways, the expansion may also be limited by aviation's growing environmental impacts. These impacts can be found in the form of climate impacts, noise impacts, and health impacts, the latter of which are addressed in this thesis. Environmental considerations which may limit the growth of air transportation include: the level of tolerated noise in communities proximate to airports, the rules and standards governing ambient particulate matter concentrations, and a country's targets for reducing greenhouse gases.

Aircraft differ from ground-level sources of pollution in that their emissions are vertically distributed in the atmosphere at varying altitudes. The atmospheric chemistry and dispersion occurring at high altitudes lead to health effects being felt beyond the immediate vicinity of the airport. Policymakers world-wide are faced with the challenge of taking into consideration not only the economic impacts of potential regulations and policies on the air transportation industry but also of the associated environmental benefits or costs.

International standards for commercial aviation emissions and noise are recommended by the International Civil Aviation Organization (ICAO), a United Nations agency, and more specifically the Committee on Aviation Environmental Protection (ICAO/CAEP). The environmental standards set forth by ICAO are then promulgated within the United Nations' member states by independent regulatory bodies. In the United States, the U.S. Environmental Protection Agency (EPA) is responsible for setting the standards, and the Federal Aviation Administration (FAA) is responsible for ensuring compliance while maintaining safety and efficiency in the system. Air transportation in Europe is governed by the European Aviation Safety Agency (EASA), whose objectives are aviation safety as well as environmental protection. Aircraft manufacturers and air carriers are legally required to abide by the requirements of their governing regulatory body in order to operate.

Policymaking guidelines typically mandate a full cost-benefit analysis (CBA) to evaluate the benefits versus the implementation costs of a proposed regulation or policy. In the context of evaluating a policy's health benefits or costs, a valuation scheme must be adopted. Often a controversial issue, monetary values are assigned to the number of lives saved and weighed against the monetary costs of a policy. This valuation-based policy-making procedure is one adopted by many regulatory bodies world-wide.

The objectives of this thesis are to provide and assess two reduced order models capable of estimating the costs and benefits of aviation emissions on human health, both of which are to be used in the context of policymaking. The first model estimates health costs related to changes in UV irradiance and consequent changes in skin cancer incidences and mortalities. The second model estimates health costs related to changes in air quality and associated changes in health endpoints. These models form an integral part of the Aviation Environmental Portfolio Management Tool (APMT), a suite of environmental impact assessment tools developed for the U.S. FAA.

An overview of APMT follows in Section 1.2 providing further context behind the development of the health impact models. Background information explaining how aircraft emissions affect human health is given in Section 1.3. The overall structure of this thesis can be found in Section 1.4.

1.2 Aviation Environmental Portfolio Management Tool (APMT)

The Aviation Environmental Portfolio Management Tool (APMT) is a tool suite designed to evaluate the economic impacts of an air transportation policy or scenario (Waitz et al., 2006a, Waitz et al., 2006b). APMT is being developed and used by the Partnership for AiR Transportation Noise and Emissions Reduction (PARTNER), an FAA Center of Excellence headquartered at the Massachusetts Institute of Technology.

Figure 1 illustrates the distinct blocks composing the APMT. The APMT Environmental Design Space models aircraft and engine technology. The APMT Economics block models global commercial aviation demand and airline behavior. The APMT Aviation Environmental Design Tool produces emissions inventories and noise contours based on these specifications and on given flight paths and procedures. Emissions inventories include for example kilotonnes of non-volatile particulate matter, NO_x, and SO_x emitted at a given airport for all flights during the landing, take-off and taxi cycles. Inventories are then input into the APMT Impacts block where impacts on climate, health and noise are estimated and monetized.

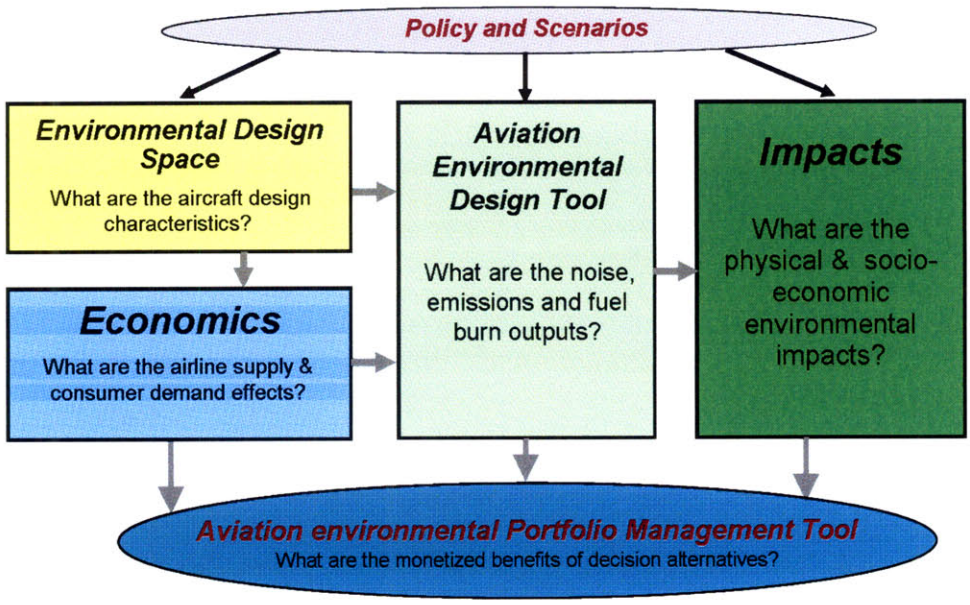

Figure 1: Aviation Environmental Portfolio Management Tool (APMT) Architecture.

1.3 Health Impacts of Aviation

Aircraft propulsion is the result of the combustion of fuel within an engine. The exhaust of the engine contains carbon dioxide (CO_2), carbon monoxide (CO), unburned hydrocarbons (HC), nitrogen oxides (NO_x), water vapor (H_2O), sulfur oxides (SO_2), oxygenated hydrocarbons, black carbon including smoke or soot, as well as volatile and non-volatile particulate matter (PM). Particles such as non-volatile PM can be breathed by humans causing negative health impacts. Similarly, other aircraft exhaust components such as NO_x and SO_x react with the atmosphere's chemical components forming secondary particulate matter, which is also harmful for human health. The U.S. Environmental Protection Agency (EPA) has defined fine particulate matter, $PM_{2.5}$, as particulate matter having a diameter of 2.5 micrometers or less and coarse particulate matter, PM_{10}, as PM having a diameter of 10 micrometers or less.

When humans breathe in particulate matter, the smallest particles get lodged within their lungs and cause serious health problems. Health endpoints related to $PM_{2.5}$ include asthma, chronic bronchitis, restricted activity days, respiratory hospital admissions, cardiovascular hospital admissions, even premature mortality in infants and adults. Regulations such as the Clean Air Act (CAIR), and the National Ambient Air Quality Standards for Particle Pollution Rule have been implemented in the aim of reducing ambient $PM_{2.5}$ concentrations.

Despite the clear negative health impacts of $PM_{2.5}$ described previously, aircraft emissions may also yield certain health benefits. Subsonic aircraft flying at altitudes between 9 and 13 km in altitude emit NO_x, an ozone precursor, in the upper troposphere. The net resulting increase in ozone leads to a decrease in UV radiation (UVR), namely of the UV-B type, reaching the surface of the Earth. Biological effects of UV radiation on humans include skin cancer and ocular damage. The increase in ozone due to aircraft NO_x emissions could therefore contribute to a decrease in skin cancer incidence.

Beyond the health impacts of aircraft emissions, negative health effects related to aircraft noise also exist. Though noise-related health effects are in large part still under investigation, a recent study by Franssen et al. has found a correlation between exposure to aircraft noise and the use of

cardiovascular disease medication, sleep inducing drugs, as well as poor general health (Franssen et al., 2004).

1.4 Thesis Structure

The methods used to evaluate and monetize the impacts of an aviation scenario or policy on human health, as implemented in the APMT Benefits Valuation Block, are described in Chapters 2 and 3 of this thesis. Chapter 2 treats the assessment of the impacts of subsonic aviation on skin cancer incidence in the United States, with results being compared to those of an EPA model which has similar capabilities. Chapter 3 presents the assessment of the impacts from aircraft emissions in the landing and takeoff cycles on human health in the United States. Modifications to the APMT Impacts - Air Quality model are described. Finally, model limitations and suggestions for future work are offered.

2 Impact of Subsonic Aviation on Nonmelanoma Skin Cancer Incidence in the United States

Chapter 2 addresses the impacts of aircraft emissions on the Earth's ozone leading to changes in ultra-violet (UV) irradiance reaching the ground and consequently on human skin cancer cases. We begin the chapter with some background on the topics of atmospheric ozone changes and UV induced skin cancers. Section 2.2 provides a literature review of aviation-related changes in ozone column as well as a review of literature behind the skin cancer impact pathway used in APMT. Section 2.3 presents in greater detail the APMT skin cancer impact pathway, including a characterization of uncertainty for each parameter. The results of two impact analyses calculating changes in nonmelanoma skin cancer incidences in the U.S. due to subsonic aviation are given in Section 2.4 for years 1992 and 2002. The U.S. EPA's Atmospheric and Health Effects Framework (AHEF) model is explained in Section 2.5 along with the results of a comparative analysis between the AHEF and the APMT reduced-order model, for the year 2002 subsonic aviation case. The chapter is concluded with a discussion on model limitations and avenues for future work.

2.1 Background

2.1.1 Net increase in ozone

Since the discovery of the ozone hole over Antarctica in 1985 by a British Antarctic Survey team, anthropogenic chemical pollutants such as chlorofluorocarbons (CFCs) have been found to cause a depletion of the Earth's ozone layer. The ozone depletion which began in the 1970's has been a major concern for human health as the ozone layer constitutes an indispensable shield from the sun's harmful UV rays for all living organisms. The ozone layer is situated in the stratosphere, between 10 and 40 km above ground level. A reduction in the ozone layer means higher doses of ultraviolet radiation reaching the ground, leading to negative health impacts for the Earth's population. The internationally agreed upon *Montreal Protocol on Substances that Deplete the Ozone Layer* was signed in 1987 by ICAO members in the aim of banning man-made substances known to

contribute to ozone depletion. Despite the success of the Montreal Protocol in reducing ozone-depleting substances, the 2008 British Antarctic Survey Science Briefing (BAS, 2008) reveals that,

> *"the original compounds are so stable and long-lived that an ozone hole will exist each Antarctic spring for at least another 50 years. (...) in the Northern Hemisphere, winter stratospheric ozone amounts have fallen by 10 to 15%. Depletion is generally even greater in the Southern Hemisphere as a direct consequence of the deep Antarctic ozone hole. There has been little ozone depletion over the tropics and globally the depletion averages out at about 4%."*

Reductions in the Earth's ozone layer are not confined to the Antarctic and are therefore a global concern.

In contrast to ozone-depleting substances, subsonic aircraft NO_x emissions in the upper troposphere and lower stratosphere (UTLS region) between 9 and 13 km act as an ozone precursor (Liu et al., 1987, Crutzen, 1973). Several analyses have been done to assess the impact of NO_x emissions from commercial aviation on the global ozone profile. Complex non-linear chemical reactions in the atmosphere with the aircraft NO_x lead to an increase of O_3 concentration in the troposphere and a decrease in the lower stratosphere. The net change of O_3 due to aviation is nonetheless considered to be positive (Köhler, 2008; Gauss, 2006; Grewe, 2002; IPCC, 1999; Brasseur, 1998) with values ranging from 3 to 11 ppbv. Köhler et al. (2008) attribute result differences among studies to "emissions inventory and model formulations such as the chemistry schemes, convective transport schemes, and wet deposition schemes employed."

Different units can be used to measure changes in the Earth's ozone. As a gas, ozone mixing ratio can be expressed as parts per billion volume (ppbv). This measure is most suited for studying O_3 concentrations near the ground. When looking at the total ozone column in the atmosphere, scientists usually use the Dobson Unit (DU). If the ozone found vertically over a certain area is hypothetically spread evenly at a pressure of 1 atm and at 0 °C, one DU corresponds to an O_3 thickness of 0.01 mm. The global average ozone thickness is about 300 DU.

Ultraviolet radiation (UVR) was divided into three types based on wavelength by the Comission Internationale de l'Éclairage (McKinlay, 1987): UV-C, 200–290 nm, UV-B, 290–320 nm, and UV-A, 320–400 nm. While the Earth's ozone layer absorbs all of the sun's UV-C radiation, only partial

amounts of UV-B rays are absorbed and no UV-A rays are absorbed. For this reason, biological effects of UV-A and UV-B radiation are of particular interest when it comes to assessing the impacts of changes in the ozone layer.

2.1.2 Skin Cancer

2.1.2.1 Nonmelanoma

Biological effects of UV radiation on humans include sunburn, skin cancer and ocular damage among others. Ultraviolet radiation is known to be absorbed by different biological molecules of the skin such as DNA and melanin. The result can be damage at the molecular level, leading to skin cancer, more specifically through gene mutations (Hussein, 2005). There exist two general categories of skin cancers in which UVR plays a role: cutaneous malignant melanoma (CMM) and nonmelanoma skin cancer (NMSC).

There are two distinct types of nonmelanoma skin cancer: basal cell carcinoma (BCC) and squamous cell carcinomas (SCC). BCC is not only the most common type of NMSC at an estimated 80% of diagnosed NMSC cases (Epstein, 1996), but it is also the most common type of cancer in humans (Tang et al., 2007). SCC incidence rates are lower than those of BCC; however, most NMSC mortalities are related to SCC. Recent estimates from the American Cancer Society estimate the annual number of new BCC cases to be between 800,000 and 900,000 Americans while the number of SCC cases is estimated between 200,000 and 300,000 (ACS, 2008a).

2.1.2.2 Melanoma

Originating in the melanocytes of the skin, cutaneous malignant melanoma (CMM) has been found to be less prevalent than NMSC, but yet more difficult to treat (ACS, 2008b). The American Cancer Society estimates the number of new CMM cases in the U.S. for year 2009 to be about 68,720 and the number of CMM mortalities to be approximately 8,650. The etiology of CMM and the exact UV-A/UV-B action spectrums remain ongoing topics of research in the skin cancer field.

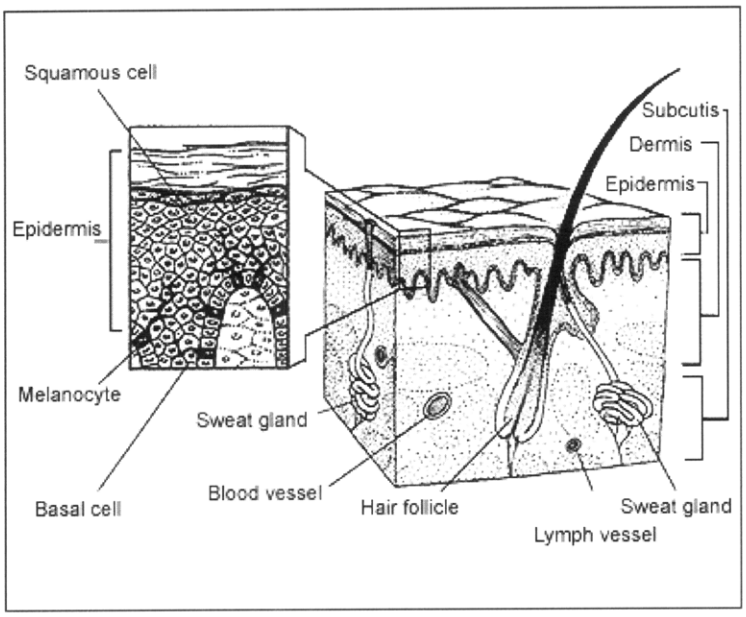

Figure 2: Cross-section of human skin. Shown are basal cells and squamous cells in which NMSC originates. Melanocytes, the cells affected by CMM, are also shown. Image source: American Cancer Society[1].

[1] American Cancer Society, *What is melanoma skin cancer?*, [online] URL: http://www.cancer.org/docroot/CRI/content/CRI_2_2_1X_What_is_melanoma_skin_cancer_50.asp?sitearea=. Web accessed March 2009.

2.2 Literature Review

2.2.1 Ozone Variations Due to Global Aviation

Since the mid-nineties, several analyses have been done using 3-D global chemistry and transport models (CTMs) to estimate the change in O_3 caused by aircraft NO_x emissions released in the atmosphere. The response in atmospheric concentrations of O_3 is non-linear with respect to NO_x. The altitude at which the NO_x is emitted as well as the background NO_x concentration both influence the change in O_3 resulting from the complex atmospheric reactions. An excerpt from Gauss et al. succinctly describes the chemistry behind the aviation-induced changes in O_3 (Gauss et al., 2006):

> *"The implication of NOx emissions for ozone levels depends strongly on the altitude of the emissions for both chemical and dynamical reasons. As aircraft emissions occur near the tropopause, only small shifts in flight altitude will lead to large changes in the fraction of emissions released into the stratosphere, where pollutants accumulate more efficiently due to less vertical mixing and the absence of washout processes. Secondly, the chemical production of ozone per emitted NOx molecule is a non-linear function of ambient levels of NOx (Brasseur et al., 1998; Jaeglé et al. 1998, 1999) and the availability of hydrocarbons (Brühl et al., 2000; Kentarchos and Roelofs, 2002), which in turn largely depend on altitude. In the sunlit troposphere and lower stratosphere, NOx leads to efficient ozone production through oxidation of carbon monoxide, methane, and higher hydrocarbons. At higher altitudes in the stratosphere this source becomes less important due the limited availability of hydrocarbons, while catalytic ozone depletion cycles involving NOx (Crutzen, 1970; Johnston, 1971) gain importance, and the injection of NOx actually destroys ozone rather than producing it."*

Additional details on the effects of transportation emissions on atmospheric ozone, both in terms of depletion and production, are given in Fuglestvedt et al. (2009). The authors highlight different types of emissions from air transportation vehicles which can lead to ozone depletion: HCFCs from refrigeration units used to transport frozen goods, and halons from fire extinguishers on aircraft. NO_x emissions are cited to lead to ozone production, as seen previously (Fuglestvedt et al., 2009).

The net change in ozone column due to global aviation NO_x emissions is positive. Due to differences among the studies including the use of different inventories, CTMs, and modeling methods, variations exist among estimates from different studies. There have been two reports published based on the results of multiple models (multi-model assessment): the Intergovernmental Panel on Climate Change (IPCC) *Aviation and the Global Atmosphere* report (Penner et al., 1999) and the EU project TRADEOFF final report (Isaksen et al., 2003). Recent studies by Köhler et al. (Köhler et al., 2008) and Gauss et al. (2006) compared their results to those of the IPCC and TRADEOFF reports.

Table 1 highlights the main differences in estimates of O_3 changes due to aviation. The net total ozone increase due to aviation NO_x emissions is estimated at about 0.4 % in the Northern Hemisphere, as published in the IPCC report and as quoted by Fuglestvedt et al. in *Transport impacts on atmosphere and climate: Metrics* (Fuglestvedt et al., 2009). This includes changes in the troposphere and stratosphere. Aircraft emissions are reported to be responsible for a 20 % increase in NO_x concentration in the Northern Hemisphere.

Both Köhler et al. (2008) and Gauss et al. (2006) attribute Köhler et al.'s higher changes in O_3 to higher inventories in the baseline (0.68 Tg/year versus 0.594 Tg/year) as well as the downward bias of the plume chemistry employed in the Gauss study.

Although the studies from Table 1 found that O_3 changes are non-linear with NO_x emissions, we can nonetheless do a cursory comparison of results using linear scaling based on inventory nitrogen. We find that results of Köhler et al. (2008) are within the range of IPCC 1999 results and that Gauss et al. (2006) values are lower. Gauss et al. included plume chemistry which is thought to contribute to a decrease in NO_x catalytic efficiency (Gauss et al., 2006; Köhler et al., 2008). Gauss et al. use Oslo-CTM-2, a newer version of the model used for the IPCC best estimate which has both tropospheric and stratospheric chemistry. However, no latitudinal distinction of the results of this study was available, only average changes for the entire Northern Hemisphere.

This work uses the average change in O_3 total ozone column over three latitude bands, 20-30 °N, 30-40 °N, and 40-50 °N to estimate changes in skin cancer incidence caused by subsonic aviation NO_x emissions via changes in the atmospheric ozone column. Data sources for O_3 column changes used in the analyses presented in Section 2.4 of this report are: 1) latitudinal best estimates from the

IPCC 1999 *Aviation and the Global Atmosphere* report defined as the results from the Oslo-CTM (UiO); 2) latitudinal O_3 changes from Köhler et al. (2008) study.

Table 1: Literature review of estimated changes in ozone column due to world-wide air traffic.

Study	Model	Inventory/ Year	Inventory Nitrogen (Tg/year)	Global ΔO_3			Comments
				(ppbv)	(DU)	(Tg)	
IPCC, 1999	6 models[2]	NASA1992	0.5	n/a	0.37 to 0.64	4 to 7	Either tropospheric models with no stratospheric processes or stratospheric model with omission of important tropospheric processes.
Isaksen, 2003	5 models[3]	ANCAT 2000	0.59	3 to 6	n/a	n/a	Model results differ by a maximum factor of 2. Largest observed mass
Gauss, 2006	Oslo CTM-2	TRADEOFF 2000	0.594	4 to 5	0.339	3.71	Includes plume chemistry, reduction of NO_x. Differs from IPCC Oslo CTM by including tropospheric and stratospheric chemistry.
Köhler, 2008	p-TOMCAT & SLIMCAT	AERO2K 2002	0.68	6	0.81	8.8	No inclusion of plume chemistry for NO_x. Possible upward bias.

[2] Refer to IPCC 1999 report, *Chapter 4 Modeling the Chemical Composition of the Future Atmosphere* for model descriptions.
[3] Refer to *TRADEOFF Final Report*, Isaksen (2003), for model descriptions.

2.2.2 Skin Cancer Impact Analysis

2.2.2.1 Action Spectrum

There is general consensus in the scientific community that BCC and SCC in humans is related to UVR exposure. The cause-effect relationship has been confirmed by both animal testing and epidemiolocial studies in humans (IARC, 1992, Scotto et al., 1991). UV-B was shown to induce mutations of the p53 tumor suppressor gene commonly found in SCC and BCC tumors (Brash et al., 1991, Ziegler et al., 1993). Scientists consider this to be proof that UVR exposure is directly responsible for SCC and BCC (de Gruijl and Van der Leun, 1994, Longstreth et al., 1994).

Although the IPCC *Aviation and the Global Atmosphere* (Penner et al., 1999) report uses erythemal dose rate (UV_{eff}) to measure the efficacy of solar radiation, it is not the most appropriate or recent method for studying the potential for skin cancer. Indeed, UV_{eff} is associated with the action spectrum for sunburn, as compared to the action spectrum for skin cancer. The concept of action spectrum represents the weighted sum of wavelengths of the UV spectrum by the effectiveness of cancer initiation. Aside from the erythemal action spectrum, there exists a DNA-h action spectrum which uses DNA damage to measure the efficacy of solar radiation (Setlow, 1974). The DNA-h action spectrum is not specific to skin DNA, but rather to human DNA damage in general. Through experiments with hairless mice, an action spectrum for human carcinogenesis of the NMSC type has been derived (de Gruijl and Van der Leun, 1994). Referred to as the Skin Cancer Utrecht-Philadelphia (SCUP), this action spectrum was corrected to account for differences in UV-transmission rates in human and murine skin. The resulting corrected action spectrum, "SCUP-h", is recognized as the most appropriate action spectrum for SCC and BCC available to date (EPA, 2001, ICF, 2006, Kyle et al., 2008)

At present, the exact action spectrum of UV-B and UV-A on CMM is not completely understood (Norval et al., 2007, van der Leun et al., 1998). Some reports even conclude that ozone has a very minor effect on CMM, since UV-A, which is not filtered by ozone, was found to be the main risk factor (Grant et al., 2007, Setlow, 1999). However, other reports refer to two different studies on newborn mice to suggest that UV-B also plays a part in human melanoma formation (Perlis and Herlyn, 2004, Norval and Gruijl, 2007). Due to the lack of consensus on the issue, it is difficult to estimate the impact of a change in ozone on melanoma incidence. Therefore, the APMTresults

section of this thesis does not include an estimate for changes in melanoma skin cancer incidence and mortality.

2.2.2.2 Amplification Factors

Radiation Amplification Factor (RAF)

The ozone layer constitutes a shield from UVR by absorbing radiation depending on its wavelength. A change in the concentration of atmospheric ozone leads to a change in the ozone layer's property to absorb UV-R. This has a direct impact on the amount of UVR reaching the ground. In other words, variations in the Earth's ozone column (measured in DU) lead to changes in ambient UV exposure (E_{am}). For a given action spectrum, the radiation amplification factor (RAF) gives the percent increase in ambient exposure to the action spectrum's UV range (E_{am}) per percent decrease in O_3 (de Gruijl and Van der Leun, 1994):

$$RAF = \frac{-\frac{dE_{am}}{E_{am}}}{\frac{dO_3}{O_3}} \qquad (1)$$

Radiation amplification factors are derived based on the UVR action spectrum of a given effect. A full derivation of the RAF from an action spectrum is given by de Gruijl and Van der Leun (1994). RAFs for various action spectrums ranging from erythema to inhibition of phytoplankton photosynthesis have been compiled in Table 1.1 of the 1998 United Nations *Environmental Effects of Ozone Depletion* assessment report (van der Leun et al., 1998). As per Kelfkens et al., RAFs vary by less than 6% from the average for latitudes between 0°-65° (Kelfkens et al., 1990). RAFs are summarized in Table 2.

Biological Amplification Factor (BAF)

Once the change in exposure to ambient UV has been established, a relation must be made with changes in skin cancer incidence. The biological amplification factor (BAF) gives the percent increase in skin cancer incidence (I) per percent increase in ambient UV exposure (de Gruijl and Van der Leun, 1994):

$$BAF = \frac{\frac{dI}{I}}{\frac{dE_{am}}{E_{am}}} \qquad (2)$$

BAFs for BCC and SCC were obtained by De Gruijl and Van der Leun (1994) based on epidemiolocal surveys by Scotto and Fears (1981) and experiments on mice (De Gruijl and Van der Leun, 1991). BAF values for the SCUP-h spectrum are listed in Table 2. It should be noted that effects of UVR are predominant for light-skinned persons and that the factors presented here were derived for light-skinned populations only.

Total Amplification Factor (AF)

The total amplification factor (AF) is the product of RAF and BAF. It gives the percent increase in skin cancer incidence per percent decrease in column O_3 [(de Gruijl and Van der Leun, 1994) and references within]:

$$AF = RAF \times BAF$$
$$AF = \frac{\%\text{ change skin cancer incidence}}{\%\text{ change column } O_3} \qquad (3)$$

Amplification factors for NMSC in light-skinned individuals are summarized in Table 2. A distinction between BCC and SCC has been made. Factors presented in Table 2 were also those presented in the UNEP 1994 Nonmelanoma Skin Cancer section (Longstreth et al., 1994).

Table 2: Amplification Factors NMSC. Source: de Gruijl & van der Leun, 1994.

$RAF_{0\text{-}65deg\ N}$	1.2	± 0.06	Radiation Amplification Factor (RAF)
BAF_{SCC}	2.5	± 0.7	Biological Amplification Factor for Squamous Cell Carcinoma (BAF_{SCC})
BAF_{BCC}	1.4	± 0.4	Biological Amplification Factor for Basic Cell Carcinoma (BAF_{BCC})
AF_{SCC}	3.0	± 0.8	Total Amplification Factor for SCC (AF_{SCC})
AF_{BCC}	1.7	± 0.5	Total Amplification Factor for BCC (AF_{BCC})
AF_{NMSC}	2.0	± 0.4	Total Amplification Factor for Nonmelanoma Skin Cancer (AF_{NMSC})

2.2.2.3 Baseline Incidence

Incidence rates for BCC and SCC depend on both latitude and age. In the case of SCC, lifetime exposure to UVR is a major factor (van der Leun et al., 1998) such that incidence rates are higher the older the age groups. In terms of latitude influence, the closer we are to the equator, the smaller the sun's zenith angle (angle between the sun and the vertical direction) and the stronger the UV exposure. Skin cancer incidence rates are therefore expected to decrease as we move away from the equator.

There are several data sources available from which one can derive baseline incidence rates. As mentioned previously, the American Cancer Society estimated the annual number of new BCC cases to be between 800,000 and 900,000 Americans and between 200,000 and 300,000 for SCC (ACS, 2008a). Historically, the reporting of skin cancer cases has not been consistent among U.S. states. As we are interested in changes in SCC and BCC incidence for three distinct latitude bands, we require baseline incidence rates specified for each band and subdivided by sex and by age group. The BCC and SCC incidence rates used in our analysis are the incidence rates compiled by Fears and Scotto and are based on a year-long U.S. EPA survey of nonmelanoma skin cancer incidence in the U.S. (Fears and Scotto, 1983). Though these incidence rates date from 1977-1978, they are used in the EPA's Atmospheric Health Effects Framework (AHEF) (ICF, 2006). Baseline incidence is obtained by applying the incidence rate to the baseline population.

2.2.2.4 NMSC Case-Fatality Rate and Mortality Rate

It is difficult to approximate NMSC mortality rates due to the under-reporting of NMSC as well as the mis-diagnosis of complications due to NMSC leading to death. While CMM incidence and mortality are rigorously monitored by the National Cancer Institute (NCI), limited recorded data exist for NMSC. NMSC is not fully reported in the NCI's Surveillance, Epidemiology, and End Results (SEER) data, which currently only has 26% of the U.S. population documented (Stang, 2007). Most available data sources on skin cancer specify that BCC and SCC are excluded. Even the NCI's *Annual Report to the Nation on the Status of Cancer* and the National Program of Cancer Registries (NPCR) administered by the U.S. Department of Health and Human Services Centers for Disease Control and Prevention both only report melanoma cases, omitting BCC and SCC in their skin cancer counts.

Despite the limited records of national NMSC mortality rates, a focused study yielded case-fatality rates based on Rhode Island residents between 1979 and 1987 (Weinstock et al., 1991). This study found case-fatality rates for BCC and SCC of 0.05% and 0.7%, respectively. The main limitation of using the Lewis and Weinstock case-fatality rates is the relatively small scale of the analysis. The authors of this study published follow-up studies in 2004 from 1988-2000 data and in 2007 from 1969-2000 data (Lewis and Weinstock, 2004, Lewis and Weinstock, 2007). Mortality rates from Lewis and Weinstock can be found in Appendix A. The follow-up studies show that over time, genital and nongenital NMSC mortality rates in the U.S. are decreasing. However, this may arguably be due to the lower level of awareness and detection of NMSC in the 1960's and 1970's. The updates provide mortality rates rather than case-fatality rates. It should be noted that the Lewis and Weinstock studies investigated both nongenital NMSC as well as genital NMSC. The correlation between UV exposure and genital NMSC is complex. UVR is known to activate HSV-1 and HPV, two sexually transmitted viruses (Norval et al., 2007). HPV can in turn cause NMSC. "UVR exposure and infection with certain cutaneous HPV types can act as co-factors in the development of not only SCCs but also of BCCs" (Norval et al., 2007). Considering that the presence or absence of HPV plays an important role in linking UVR to genital NMSC, we do not include genital NMSC effects in our assessment of aviation impacts on skin cancer. In the 2007 publication, the average mortality rate from nongenital NMSC between 1985-2000 for white males was 0.99 per 100,000 people, and 0.42 for white females. These rates are age-adjusted to 2000 U.S. standard population.

The AHEF model uses county-by-county mortality data for NMSC based on EPA/NCI data age-adjusted to the 1970 U.S. population (Scotto et al., 1991). Data from this source is presented on a cohort basis, i.e. rates depend on the year of birth. A last resource of mortality data is the National Cancer Institute's Cancer Mortality Maps and Graphs website[4], under the "Other (nonmelanoma) skin cancer" category. NCI nationally averaged NMSC mortality rates from 1990-1994, age-adjusted to 1970 U.S. population are 1.30 (95 % CI: 1.27 – 1.33) and 0.44 (95 % CI: 0.43 - 0.46) per 100,000 people for white males and white females, respectively. NMSC mortality rate maps are shown in Appendix B.

[4] NCI: Cancer Mortality Maps and Graphs website [online] URL: http://dceg.cancer.gov/cgi-bin/atlas/ca-type?site=osk. Web accessed March 2009.

2.2.2.5 Valuation

The valuation section of this thesis was done based on the value of a statistical life (VSL) recommended by the U.S. Department of Transportation (DOT) for all cost-benefit analyses and the mean cost per episode of NMSC measured by allowable charges as determined by Chen et al. (2006). The mean cost is estimated at $665 per episode, with a standard deviation of $1067, in year 2000 constant dollars. Such a large deviation comes from the variation in cost between treatment settings: hospital ($4939/episode), ambulatory surgical center ($935/episode), and physician's office ($500/episode) (Chen et al., 2006). Similar values were obtained from a previous study conducted in 2001 (Chen et al., 2001). The Chen et al. (2006) study is based on a compilation of total allowable costs per episode of NMSC from the Medicare Current Beneficiary Survey (MCBS) for 1999-2000. Mean cost per NMSC episode is shown in Table 3 based on the type of health-care practitioner. The weighted mean cost per episode is $663.

Table 3: Average cost per episode of NMSC depending on specialty of managing health-care practitioner. Source: Chen et al. (2006).

Type of specialist managing the episode	Percent of episodes treated by type of specialist	Average total treatment cost per episode of NMSC (U.S. Y2000 $)
Dermatologists alone	50.3%	$604
Surgeons	5.6%	$957
Multiple specialties	25.9%	$877
Primary care physicians	6.6%	$296
Other specialties	11.4%	$521

No distinction is made between treatment costs of BCC versus those of SCC. This can be justified by the nature of the treatment options for both types of skin cancer being almost identical, with the exception of photodynamic therapy (unique to BCC) and combined biologic therapy with retinoid treatment (unique to SCC). Treatment options common to both BCC and SCC are (NCI, 2009b):

- Mohs micrographic surgery;
- Simple excision;
- Electrodessication and curettage;
- Cryosurgery;
- Radiation therapy;
- Laser surgery;

- Topical chemotherapy with fluorouracil;
- Biologic therapy (trial).

The Environmental Protection Agency (EPA) is currently studying the cost of nonmelanoma skin cancer, which will be published in the "Cost of Illness Handbook," (EPA, 2009). A 1990 study estimated the willingness to pay (WTP) to avoid skin cancer to be $30,000 (1985 dollars) based on sunscreen expenditures (Murdoch and Thayer, 1990). ExternE approximates the value of lost welfare due to general non-fatal cancers at $450,000. Several reports caution however that this value is probably not applicable to skin cancer (Serup-Hansen et al., 2004, Pearce, 2000). Due to the scarcity of WTP studies for nonmelanoma skin cancers, the valuation in this report only includes direct costs associated with the treatment. Valuation for the number of nonmelanoma skin cancer cases averted by subsonic aviation emissions follow the discrete distribution from Table 3.

Monetization of the decrease in number of skin cancer mortalities is based on the DOT's *Revised Departmental Guidance: Treatment of the Value of Preventing Fatalities and Injuries in Preparing Economic Analyses* (DOT, 2008). The DOT guidance document recommends the use of a lognormal or Weibull distribution with a VSL mean of $5.8 million and a standard deviation of $2.6 million in 1997 dollars.

To facilitate cost comparisons with the air quality results presented in Chapter 3, we shall put all costs in year 2000 constant dollars. Following the 2008 DOT guidance document, we use the Consumer Price Index CPI-U given by U.S. Department of Labor, Bureau of Labor Statistics,[5] obtaining a mean VSL of $6.3 million with a standard deviation of $2.8 million (Y2000 $U.S.).

[5] U.S. Department of Labor Bureau of Labor Statistics [online], URL: http://www.bls.gov/cpi/#tables; accessed March 2009.

2.3 *Skin Cancer Impact Pathway in APMT*

The framework of the APMT skin cancer model is described in this section, from input to output. The skin cancer model will be integrated within the APMT Impacts module, contributing to the assessment of aviation impacts on the environment, as well as corresponding costs and benefits.

2.3.1 Model Architecture

The APMT skin cancer model takes average changes in ozone column from aviation emissions for three latitude bands and uses total amplification factors to estimate resulting changes in nonmelanoma skin cancer incidence and mortalities. The last step of the pathway consists of the valuation of computed changes in incidences and mortalities. Figure 3 presents a flowchart of the APMT skin cancer impact pathway.

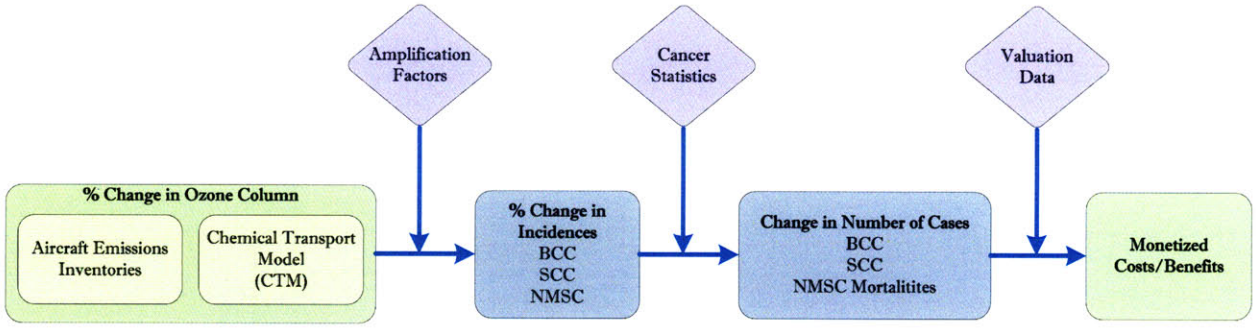

Figure 3: APMT Skin Cancer Benefits Valuation Framework

2.3.2 Percent Change in Ozone Column

Currently, changes in total ozone column due to aircraft emissions are obtained from published literature, as presented in section 2.2.1. However, for the future use of the skin cancer benefits model, any global emission inventory can be used and processed by a CTM to obtain percent changes in ozone column. The selection of a CTM to do this analysis must be based on the consideration that the model should have an adequate representation of stratospheric and tropospheric chemistry. While GEOS-Chem does not have a stratosphere, models such as the NASA GMI, the NCAR MOZART 3, or the combination of p-TOMCAT and SLIMCAT would potentially be adequate choices as they include stratospheric and tropospheric chemistry. Alternately,

a reduced order model mimicking CTM capabilities for estimating changes in ozone column due to aircraft NO_x emissions could be developed (more on this in Section 2.6, Future Work).

As the percent change in ozone and baseline incidence rates for skin cancer vary based on latitude, we have selected three distinct latitude bands on which to determine the impacts of changes in ozone column. The three bands are:

1) 20-30 °N
2) 30-40 °N
3) 40-50 °N

The uncertainty related to the input of percent change in column ozone is difficult to quantify accurately. There are uncertainties tied to the emissions inventories, as they are derived from simulations of aircraft emissions and therefore constitute an approximation of the amount of NO_x emitted by world-wide air traffic. Depending on the emissions inventories used by the CTM, the percent change in column ozone used by the APMT skin cancer model will have varying uncertainty. In addition to the inventory uncertainty, there is inherent uncertainty linked to the use of CTMs. In effect, the level of accuracy of an atmospheric model depends on both the completeness of the underlying chemical reactions on which the model is built and on the faithfulness with which it simulates atmospheric transport mechanisms. While inter-model comparisons can give a good idea of the range of results, the output uncertainty is usually difficult to quantify.

The combined uncertainty from the emissions inventories and from the CTM simulation will be approximated and applied to the percent change in O_3 by means of uncertainty coefficients with uniform distribution. Percent changes in column O_3 are reported with an "uncertainty factor of 2" by the IPCC 1999 report for year 1992 results. Therefore, we use uncertainty coefficients with a uniform distribution between 0.5 and 2.0.

2.3.3 Percent Change in Nonmelanoma Skin Cancer Incidence

The percent change in nonmelanoma skin cancer incidence is obtained by multiplication of the percent change in ozone column due to aviation by the SCC, BCC and NMSC amplification factors. The calculation is done per latitude band. Equation 4 represents the general calculation, where AF's for BCC, SCC and NMSC are given in Table 2:

$$\begin{aligned} \%\ \text{change incidence}_{\text{skin cancer type}} &= \%\ \text{change column } O_3 \times RAF \times BAF_{\text{skin cancer type}} \\ &= \%\ \text{change column } O_3 \times AF_{\text{skin cancer type}} \end{aligned} \quad (4)$$

Uncertainty on the BCC and SCC amplification factors are based on the published ranges by De Gruijl and van der Leun (1994), presented in Table 2. As argued by Allaire (2009) in his Ph.D. thesis, when a range around a mean value is given, a triangular distribution is the most suitable distribution to capture uncertainty considering maximum uncertainty conservation without losing information, such as the mean. Hence, we have selected triangular distributions of AFs with means and bounds specified in Table 2.

2.3.4 Change in Nonmelanoma Skin Cancer Incidence in the United States

To obtain the change in number of BCC, SCC, and NMSC mortalities, we apply the percent change in incidence to the baseline incidence for each latitude band. A baseline incidence of SCC and BCC cases for the given year of simulation is calculated by applying U.S. baseline incidence rates for each latitude band, as described in section 2.2.3, to the light-skinned population living in each band. Light-skinned population groups are most at risk of contracting skin cancer. Incidence rates vary by latitude, by sex and by age group.

The first step in determining the baseline incidence of nonmelanoma skin cancer is to grow the U.S. population data to the simulated year. For each latitude band, the APMT skin cancer model contains population data for year 1992, based on estimated population data from the U.S. Census Bureau (Bureau, 2000). State-by-State population data was compiled for light-skinned persons, which include Whites, Amerindians, Asians, Pacific Islanders, and "Other." Total population per latitude band is stored by sex, with 18 age groups each. Populations of the U.S. States were attributed to bands 1, 2 or 3 based on geography and follow the same attribution as that used in the EPA's AHEF model (ICF, 2006). As per this separation, the population of California was divided into two bands, with South California counties (Imperial, San Diego, Riverside, Ventura, Orange, Los Angeles, and San Bernardino) attributed to the 20-30°N band and all other counties attributed to the 30-40°N band. A copy of Appendix B of the AHEF model description document *Human Health Benefits of Stratospheric Ozone Protection* (ICF, 2006) can be found in Appendix C of this thesis. The population growth rates used to grow the population from year 1992 to the desired year were provided by the U.S. Census Bureau. The population data was taken as being deterministic.

Baseline incidence rates implemented in the model are the same as those used in the AHEF model, as this was the most up to date and complete compilation of BCC and SCC incidence rates available. The rates are for light-skinned populations for each latitude band and include distinctions of sex and age group. BCC and SCC baseline incidence rates are presented in Table 4 and Table 5.

Uncertainty on the baseline incidence rates comes from possible under-reporting of BCC and SCC cases, mainly due to the relative ease of NMSC treatment. This type of uncertainty would skew the incidence rates downwards. There is also added uncertainty on the incidence rates used in the model stemming from the fact that the survey data from which they were obtained was for June 1977 to May 1978 (Scotto and Fears, 1981, ICF, 2006). Based on the American Cancer Society (ACS, 2008a), "The number of [BCC and SCC] cancers has been increasing for many years. This is probably due to a combination of increased detection, more sun exposure, and aging of the population." Using baseline incidence rates from the late 1970's would effectively lead to a downward bias of the estimated baseline incidence. A study comparing BCC and SCC incidence rates in New Hampshire between 1979-1980 and 1993-1994 found the following increases in incidence rates: 80 % for BCC; 235 % for SCC in males; 350 % for SCC in females (Karagas et al., 1999). Calculating the equivalent percent increase per year over the 14 year period, we obtain an increase of 4.3 % per year for BCC incidence, 9.0 % for SCC in males and 11 % for SCC in females. These yearly increases can now be applied to the Scotto and Fears incidence rates from and Table 4 and Table 5. The use of these incidence growth rates defined for a New Hampshire study to all three latitude bands represents an added source of uncertainty. As NH is counted in the higher latitude band of 40-50°N, this could also be a downward source of uncertainty as NMSC incidences worldwide have increased over the last 20 years with decreasing latitude (Almahroos and Kurban, 2004).

Considering that the sources of uncertainty presented previously tend to lead to a downward bias, the uncertainty on baseline incidence rates (grown from 1977-1978 values) is approximated by uncertainty coefficients with a uniform distribution between 0.99 and 1.3. Table 6 summarizes the modifications applied to the baseline incidence rates listed in Table 4 and Table 5.

Table 4: Annual BCC incidence rate for males and females in the U.S., per age group and latitude band (cases per 100,000 people) for 1977-1978. Source: ICF, 2006.

	Male			Female		
Age	20 - 30°N	30 - 40°N	40 - 50°N	20 - 30°N	30 - 40°N	40 - 50°N
0-4	0.3	0.8	0.1	0.5	0.3	0.5
5-9	0.3	0.8	0.1	0.5	0.3	0.5
10-14	0.3	0.8	0.1	0.5	0.3	0.5
15-19	3.8	2.6	2.9	5.8	5	5.6
20-24	3.8	2.6	2.9	5.8	5	5.6
25-29	49.4	29.4	22.1	49.8	33.8	22.2
30-34	49.4	29.4	22.1	49.8	33.8	22.2
35-39	236	120	91.1	175	95.8	91
40-44	236	120	91.1	175	95.8	91
45-49	596	297	259	365	198	202
50-54	596	297	259	365	198	202
55-59	1080	557	466	561	310	287
60-64	1080	557	466	561	310	287
65-69	1790	872	761	815	454	466
70-74	1790	872	761	815	454	466
75-79	2330	1150	1160	1130	630	638
80-85	2330	1150	1160	1130	630	638
85+	2300	1140	1310	1190	608	754

Table 5: Annual SCC incidence rate for males and females in the U.S., per age group and latitude band (cases per 100,000 people) for 1977-1978. Source: ICF, 2006.

	Male			Female		
Age	20 - 30°N	30 - 40°N	40 - 50°N	20 - 30°N	30 - 40°N	40 - 50°N
0-4	0	0.1	0.2	0	0.1	0
5-9	0	0.1	0.2	0	0.1	0
10-14	0	0.1	0.2	0	0.1	0
15-19	0.3	0.8	0.3	0.1	0.1	0.1
20-24	0.3	0.8	0.3	0.4	0.1	0.1
25-29	11.2	3.3	1.6	4.3	2.4	1.4
30-34	11.2	3.3	1.6	4.3	2.4	1.4
35-39	43	22.2	7.4	15.3	7.1	4.1
40-44	43	22.2	7.4	15.3	7.1	4.1
45-49	169	67.7	32.6	55.7	19.5	10.5
50-54	169	67.7	32.6	55.7	19.5	10.5
55-59	377	170	87.4	121	48	27.5
60-64	377	170	87.4	121	48	27.5
65-69	640	295	147	254	91.6	54.8
70-74	640	295	147	254	91.6	54.8
75-79	966	490	350	383	173	113
80-85	966	490	350	383	173	113
85+	696	624	432	537	284	168

Table 6: Growth factors and uncertainty coefficients applied to baseline incidence rates.

	BCC Incidence Rate	SCC Incidence Rate Male	SCC Incidence Rate Female
Growth factor on baseline incidence rate (Table 4, Table 5) (% growth rate/year)	4 %	9 %	11 %
Uncertainty coefficient	Uniform (0.99 – 1.3)	Uniform (0.99 – 1.3)	Uniform (0.99 – 1.3)

For analyses based on future projections of aviation scenarios, the user may decide to set the growth factors on baseline incidence rate to zero, thereby using 1977-1978 incidence rates. In effect, for scenarios many years into the future (e.g. 2025 or 2050) applying the growth factors presented in Table 6 would be speculative. Alternately, the user may define an acceptable growth factor between the future year and 1977-1978 and compute the equivalent yearly growth rate. For a multi-year future projection, key years would be simulated individually then results would be interpolated. For example, if projected impacts were to be assessed between years 2000 and 2050, three distinct simulations could be done for years 2000, 2025, and 2050. Estimated impacts for years in between would be interpolated. In this example, the user would specify separate incidence growth rates:

1) Year 2000 simulation: baseline incidence growth rate based on Table 6, applied on 8 years;
2) Year 2025 simulation: baseline incidence growth rate from 1978 to 2025 based on user;
3) Year 2050 simulation: baseline incidence growth rate from 1978 to 2025 based on user.

The lack of epidemiological studies on baseline incidence rates for NMSC makes the choice of growth rate difficult.

2.3.5 Change in Nonmelanoma Skin Cancer Mortalities

As presented in Section 2.2.2.4, NMSC mortality rates and case-fatality rates are still being studied by the scientific community as a comprehensive and complete data registry of NMSC cases throughout the U.S. still has not been created. Thus, before selecting the method by which to approximate the effect of changes in ozone on the number of NMSC premature mortalities, a comparative analysis of 1992 aviation impacts was done with the available case-fatality rates and mortality rates. Results are shown in Table 7.

Table 7: Comparative analysis of 1992 aviation impacts on NMSC mortality using mortality rates from different sources.

	Data Range (Years)	Rates	Applied Uncertainty Coefficients	1992[6] Aviation Impacts on NMSC Mortalities (5% - 95 % CI)
Case-fatality rate (% fatality per case) (Weinstock et al., 1991)	1979 - 1987	BCC: 0.05 % SCC: 0.7 %	Uniform (0.90 – 1.10)	11 (5.7 – 17)
Mortality rate (per 10^5 people) (Lewis and Weinstock, 2004)	1985-2000 (age-adjusted, Y2000)	White Males: 0.99 White Females: 0.42	Uniform (0.90 – 1.10)	11 (7.1 – 16)
Mortality rate (per 10^5 people) (NCI, 2009a)	1990-1994 (age-adjusted, Y1970)	White Males: 1.30 (95 % CI: 1.27 – 1.33) White Females: 0.44 (95 % CI: 0.43 - 0.46)	Triangular (1.27/1.30 – 1.33/1.30) (0.43/0.44 – 0.46/0.44)	14 (7.8 – 23)

Considering that the applicability of the APMT skin cancer model lies on its ability to analyze baseline and policy scenarios, we select the mortality rates supplied by Lewis & Weinstock (2004) because they are obtained from a nation-wide study and they have the advantage of being age-adjusted to year 2000 U.S. population. The NCI data, age-adjusted to year 1970 population ratios, may not be as appropriate when analyzing future aviation scenarios. Mortality rates are decreasing (Section 2.2.2.4), which explains the lower number of mortalities for the 1985-2000 rates compared to the 1990-1994 rates. The range of estimated NMSC mortalities will depend greatly on the choice of uncertainty distribution applied by the user. Skewing the uncertainty distribution upwards will lead to results in the range of those obtained using the NCI mortality rates.

2.3.6 Valuation

Following the skin cancer impact pathway outlined in section 2.3.1, once the total changes in BCC and SCC cases, as well as NMSC mortalities due to aircraft emissions have been estimated, dollar

[6] 1992 Changes in O_3 column from IPCC (1999) report.

amounts are attributed to each of these changes in endpoints. The valuation of health impacts in APMT is an important feature for use by policymakers in the context of cost-benefit analyses.

The valuation of each new BCC and SCC case is based on the cost of treatment per NMSC episode as published in Chen et al. (2006) and discussed in section 2.2.2.5. To account for variability in treatment cost depending on the specialty of the managing health-care practitioner, we use a discrete distribution. As shown in Table 3, the distribution of costs (in Y2000 $U.S.) is as follows: episodes treated by dermatologists (50.3 % of cases) cost on average $604, episodes treated by surgeons (5.6 % of cases) cost an average $957, episodes treated by multiple specialties (25.9 % of cases) cost an average $877, episodes treated by primary care physicians (6.6 % of cases) cost an average $296, and episodes treated by other specialties (11.4 % of cases) cost an average $521. Since no information was available with regards to uncertainty on the average cost per episode for each specialty, we apply the deterministic values of the above discrete distribution.

For each NMSC death, the value of a statistical life is used in the monetization step. As recommended by the Department of Transportation, we use a lognormal distribution with a mean of $6.3M (Y2000 $U.S.) and a standard deviation of $2.8M (DOT, 2008). The distribution is shown in Figure 4. The 90 % confidence interval of this distribution is between $2.9M and $12M.

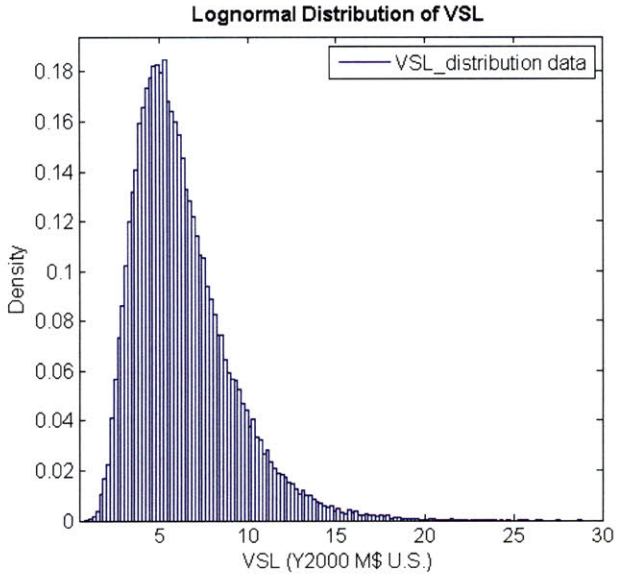

Figure 4: Lognormal distribution of the value of a statistical life (VSL) (in Million U.S. Y2000 $).

2.3.7 Uncertainty Analysis

By definition, a model simulates and estimates the effects of a series of inputs, given a set of parameters. The accuracy of the model outputs depends on the accuracy with which the model's algorithms and parameters represent reality. The employment of Monte Carlo simulations consists of a common method used to propagate uncertainty within a model. The APMT skin cancer model applies Monte Carlo simulations to account for uncertainty throughout the impact pathway. Parameters of the uncertainty distributions used in each step of the pathway have been discussed in section 2.3 where applicable. These uncertainty parameters can be modified as desired by the user of the model. Depending on the uncertainties specified, confidence intervals on the outputs will be more or less broad. The ability to specify confidence intervals on the number of cases of NMSC and mortalities averted, along with their valuations, is especially useful to policymakers.

When analyzing more than one scenario, for example a baseline case and different policies, we use paired Monte Carlo simulations to account for cases where the variables and their distributions are the same for both the policy and baseline cases. Uncertainty distributions for the different variables within the model are taken to be common to all scenarios. As such, Monte Carlo simulations are generated once for the first scenario and reused for subsequent scenarios in the scope of the same analysis. More information on the use of paired Monte Carlo simulations can be found in MIT S.M. thesis by Rojo (Rojo, 2007).

2.4 *Impacts of Subsonic Aviation on Nonmelanoma Skin Cancer Incidence and Mortality in the United States, Years 1992 and 2002*

The results of two analyses using the APMT Impacts Skin Cancer module are presented in this section. Scenarios are of baseline aviation for years 1992 and 2002. We offer estimates of the total change in new BCC and SCC cases in the United States, along with the associated change in NMSC mortalities. Valuations for each of the changes in endpoints are also given. Monte Carlo simulations done in this study had 3,750 runs, a sufficient amount for convergence of results.

2.4.1 Year 1992 Baseline Aviation Scenario

2.4.1.1 Scenario Description

We use the results of the IPCC (1999) report as inputs to the skin cancer model for simulating baseline aviation in 1992. Changes in ozone column for the three latitude bands are read off figure 5-5 (pg. 177) of the report (Penner et al., 1999). A replica of this figure is shown below in Figure 5. The APMT skin cancer model takes average percent changes of O_3 for July and October and computes a yearly average. Percent changes in O_3 column for year 1992 are summarized in Table 8.

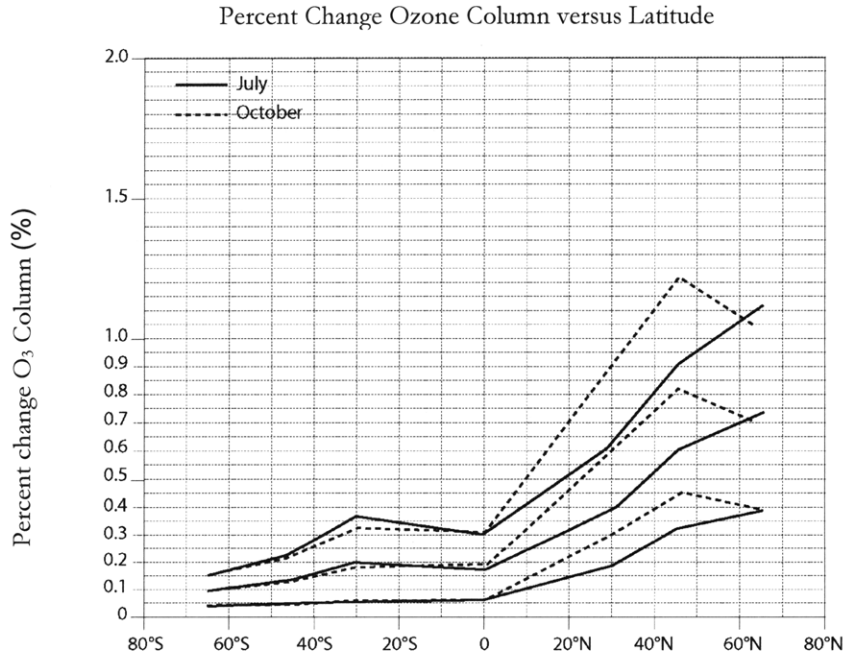

Figure 5: Percent change in ozone column due to subsonic aviation for years 1992 (lower set of curves), 2015 (center), and 2050 (top) depending on latitude. The results for 2015 are said to be "fair" while those for 2050 are "poor." Source: IPCC, 1999.

Table 8: Percent change in ozone column for year 1992 due to subsonic aviation. Values read from Figure 5.

Latitude Band	July (% Change O_3 Column)	October (% Change O_3 Column)
20-30 °N	0.17	0.26
30-40 °N	0.23	0.35
40-50 °N	0.31	0.43

2.4.1.2 Impacts of 1992 subsonic aviation on NMSC incidence and mortality

In year 1992, subsonic aircraft NO_x emissions contributed to an estimated increase in ozone column of 0.27 % (90 % CI : 0.12 – 0.41 %) for the 20-30 °N latitude band, an increase of 0.36 % (90 % CI: 0.17 – 0.56%) for the 30-40 °N band, and an increase of 0.46 % (90 % CI: 0.21 – 0.71 %) for the 40-50 °N band. These increases in ozone column resulted in augmented absorption of UV-A and UV-B radiation by the ozone layer in each of these bands. The decrease in UVR reaching the ground had the benefits of reducing the number of new BCC and SCC cases. Estimated percent reductions in BCC and SCC cases by latitude band are shown in Table 9.

Table 9: U.S. percent reduction in BCC and SCC incidence by latitude due to subsonic aviation in 1992.

Latitude Band	BCC % reduction in incidence (5% - 95% CI)	SCC % reduction in incidence (5% - 95% CI)
20-30 °N	0.45 (0.21 – 0.74)	0.80 (0.36 – 1.3)
30-40 °N	0.61 (0.28 – 0.99)	1.1 (0.50 – 1.7)
40-50 °N	0.78 (0.35 – 1.3)	1.4 (0.62 – 2.2)

Table 10 presents the estimated reductions in terms of numbers of new BCC and SCC cases, as well as NMSC mortalities per latitude band. Monetized impacts are also shown. This table demonstrates that BCC benefits are most important in the mid-latitude band with 1,300 fewer new cases, followed

by the southern latitude band (20 - 30 °N) with 1,200 and the northern band (40 - 50 °N) with 870. For SCC, the benefits are most important in the southernmost latitude band with 630 fewer cases in 1992 compared to 600 and 250 in the middle and northern bands, respectively. This geographic distribution of impacts depends on two main factors: the percent change in ozone and the baseline incidence rate in each band. Changes in percent ozone column are most important towards the North, mainly due to aircraft flight routes. Conversely, NMSC incidence rates increase towards the South due to higher UV exposure throughout the year. For SCC, the effects are most notable in the South as the higher incidence rates supplant the geographic gradient of changes in ozone column. For BCC, we find again that the baseline incidence plays a larger impact on the geographic distribution of benefits than the percent change in ozone. In the case of potential NMSC mortalities averted due to aviation, results are influenced both by the percent change in ozone pattern (highest towards the North) as well as the total population living in each band. The northern band has a decrease of about 3.6 mortalities, compared to 5.0 in the middle band and 2.8 in the southern band. The higher number of reduced mortalities in the 30-40 °N band is due to the fact that the population in the middle band is the highest and that the same NMSC mortality rate (per 100,000 people) was applied to all three bands. The higher benefit in the North is due to the higher change in ozone column in the North. When looking at the sum of monetized benefits from NMSC incidences and mortalities averted, we find that the highest benefit is seen in the middle latitude band, followed by the northern and the southern bands in decreasing order of impacts (Figure 6).

Table 10: U.S. decrease in BCC and SCC incidences and mortalities by latitude due to subsonic aviation in 1992 (number of new cases). Monetized impacts (benefits) per latitude are also shown.

Latitude Band	BCC Decrease in incidence (5% - 95% CI)	SCC Decrease in incidence (5% - 95% CI)	NMSC Mortality Decrease in mortalities (5% - 95% CI)	Monetized Total Impacts Million U.S. Y2000 $ (5% - 95% CI)
20-30 °N	1,200 (530 – 1,900)	630 (280 – 1,000)	2.8 (1.1 – 4.0)	17 (5.7 – 35)
30-40 °N	1,300 (570 – 2,100)	600 (270 – 980)	5.0 (2.3 – 8.0)	33 (11 – 69)
40-50 °N	870 (390 – 1,400)	250 (110 – 410)	3.6 (1.7 – 5.8)	23 (7.8 – 49)

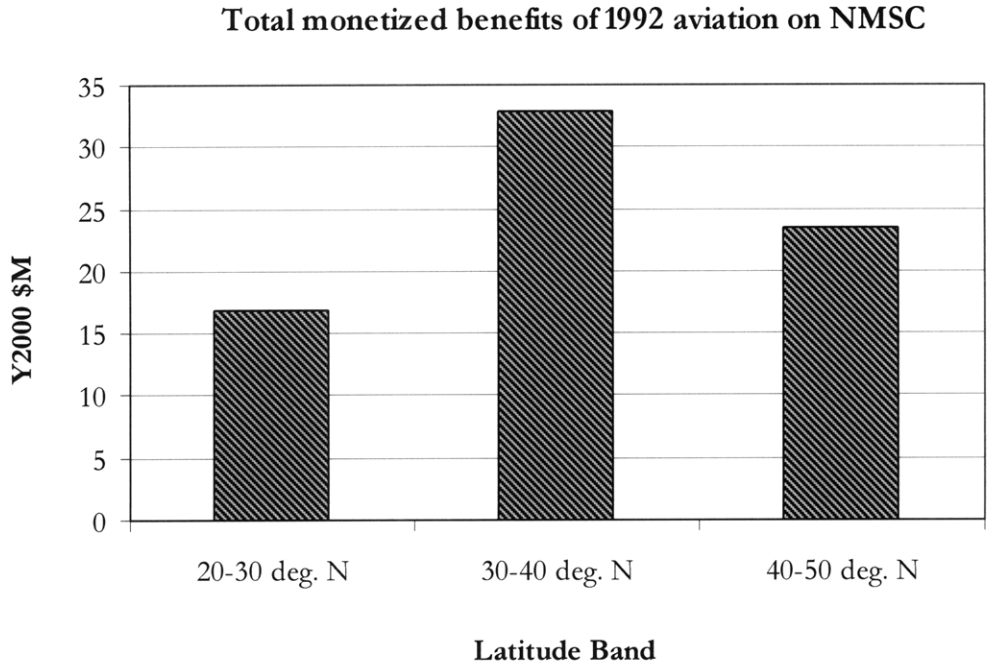

Figure 6: Total monetized benefits of 1992 aviation on NMSC incidence and mortality by latitude band.

The net benefit from subsonic aircraft NO_x on nonmelanoma skin cancer incidence and associated mortality in the U.S. in 1992 is estimated at \$73 M (90 % CI : \$38 – \$120 M) in 2000 dollars. This corresponds to the prevention of approximately 3,300 new BCC cases (90 % CI : 2,000 – 4.800), 1,500 new SCC cases (90 % CI : 910 – 2,100), and 11 NMSC premature mortalities (90 % CI : 7.1 – 16). Table 11 presents the total impacts of aircraft NO_x on nonmelanoma skin cancer incidence and mortality due to changes in the ozone column. The cost breakdown by endpoint is shown in Figure 7 where 96% of total cost benefits are due to the prevention of 11 cases of premature mortality.

Table 11: U.S. decrease in NMSC health impacts to subsonic aviation in 1992.

NMSC Endpoint	Decrease in Incidence New Cases in 1992 (5% - 95% CI)	Monetized Impacts Million U.S. Y2000 $ (5% - 95% CI)
BCC	3,300 (2,000 – 4,800)	2.2 (1.3 – 3.4)
SCC	1,500 (910 – 2,100)	0.99 (0.56 – 1.5)
NMSC Premature Mortality	11 (7.1 – 16)	70 (36 - 120)

The cost per tonne of aircraft NO_x can be approximated knowing that the IPCC inventory accounted for approximately 0.5 Tg of NO_x in 1992. The benefit from aircraft NO_x in 1992 is about 150 $/tonne NO_x (90 % CI : 75 – 250 $/tonne).

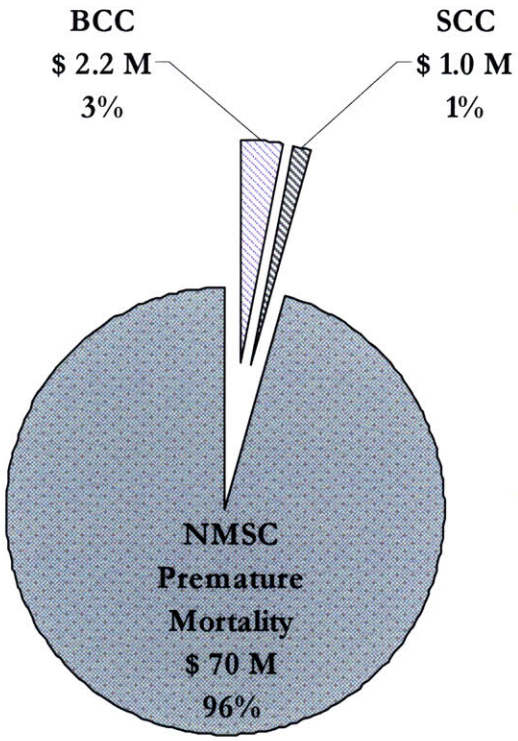

Figure 7: Monetized impacts of subsonic aviation on nonmelanoma skin cancer incidence and mortality, year 1992 (Million U.S. Y2000 $).

2.4.2 Year 2002 Baseline Aviation Scenario

2.4.2.1 Scenario Description

We use the results from Köhler et al. (2008) as inputs to the skin cancer model for simulating baseline aviation in 2002. Changes due to subsonic aviation are presented by Köhler et al. in Dobson Units (DU) in their figures 9 and 10 (reproduced in Appendix D). Percent changes in ozone column for the three latitude bands are computed from the changes in DU assuming standard ozone of 290 DU in the 20-30 °N band, 300 DU in the 30-40 °N band, and 320 DU in the 40-50 °N band (NOAA, 2006). A NOAA map of standard ozone column (in DU) can be see in Appendix E. Percent changes in O_3 column for year 2002 are summarized in Table 12.

Table 12: Percent change in ozone column for year 2002 due to subsonic aviation. Values read from (Köhler et al., 2008).

Latitude Band	Y2002 Change O_3 Column (DU)	Standard O_3 Column (DU)	Y2002 Change O_3 Column (%)
20-30 °N	1.35	290	0.47
30-40 °N	1.60	300	0.53
40-50 °N	1.60	320	0.50

2.4.2.2 Impacts of 2002 subsonic aviation on NMSC incidence and mortality

The same uncertainty distribution as that for the IPCC inventory was applied to the Kohler et al. percent changes in O_3, with uncertainty coefficients from 0.5 to 2.0. In the year 2002, subsonic aircraft NO_x emissions contributed to an estimated increase in ozone column of 0.58 % (90 % CI: 0.27 – 0.90 %) for the 20-30 °N latitude band, an increase of 0.66 % (90 % CI: 0.31 – 1.0 %) for the 30-40 °N band, and an increase of 0.63 % (90 % CI: 0.29 – 0.98 %) for the 40-50 °N band. These increases in ozone column resulted in augmented absorption of UV-A and UV-B radiation by the ozone, decreasing the UVR reaching the ground and reducing the number of new BCC and SCC cases. Estimated percent reductions in BCC and SCC cases by latitude band are shown in Table 13.

Table 13: U.S. percent decrease in BCC and SCC incidence by latitude due to subsonic aviation in 2002.

Latitude Band	BCC % decrease in incidence (5% - 95% CI)	SCC % decrease in incidence (5% - 95% CI)
20-30 °N	0.99 (0.45 – 1.6)	1.8 (0.79 – 2.8)
30-40 °N	1.1 (0.51 – 1.8)	2.0 (0.91 – 3.2)
40-50 °N	1.1 (0.49 – 1.8)	1.9 (0.85 – 3.1)

The net benefit from subsonic aircraft NO_x on nonmelanoma skin cancer incidence and associated mortality in the U.S. is estimated at $130 M (90 % CI : $68 – $220 M) in 2000 dollars. This corresponds to the prevention of approximately 6,200 new BCC cases (90 % CI : 3,800 – 9,100),

2,900 new SCC cases (90 % CI : 1,700 – 4,200), and 20 NMSC premature mortalities (90 % CI : 13 – 28). Cost breakdown by endpoint is shown in Figure 9 with 96% of total cost benefits due to the prevention of 20 cases of premature mortality. Table 14 presents the total impacts of aircraft NO_x on nonmelanoma skin cancer incidence and mortality due to changes in the ozone column.

Table 14: U.S. decrease in NMSC health impacts to subsonic aviation in 2002.

NMSC Endpoint	Decrease in Incidence New Cases in 2002 (5% - 95% CI)	Monetized Impacts Million U.S. Y2000 $ (5% - 95% CI)
BCC	6,200 (3,800 – 9,100)	4,2 (2.3 – 6,5)
SCC	2,900 (1,700 – 4,200)	1.9 (1.1 – 3.0)
NMSC Premature Mortality	20 (13 – 28)	130 (64 - 210)

Table 15 presents the estimated reductions in terms of numbers of new BCC and SCC cases, as well as NMSC mortalities per latitude band. Monetized impacts are also shown. This table demonstrates that BCC benefits are most important in the southern latitude band with 2,600 fewer new cases, followed by the mid-latitude band with 2,400 and the northern band with 1,200. Similarly for SCC, the benefits are most important in the southernmost latitude band with 1,400 fewer cases in 2002 compared to 1,100 and 350 in the middle and northern bands, respectively. As was seen in the 1992 case, the geographic distribution of impacts depends on two main factors: the percent change in ozone and the baseline incidence rate in each band. The difference here is that the 2002 inventory of percent change in ozone is slightly higher in the mid-latitude band, followed closely by the northern band. Changes in O_3 are smallest for the southernmost band. As was the case in 1992, latitudinal patterns of NMSC mortalities follow the spatial distribution of the U.S. population (Figure 8). Total impacts are highest in the middle latitude band, followed by the southern band and the northern band in decreasing order. With very similar changes in ozone column for the North and South bands, both have very close monetized impacts ($ 33 M versus $ 38 M). The South has higher incidence rates which appear to supplant the geographic gradient of changes in ozone column.

Table 15: U.S. decrease in BCC and SCC incidences and mortalities by latitude due to subsonic aviation in 2002 (number of new cases). Monetized impacts (benefits) per latitude are also shown.

Latitude Band	BCC Decrease in incidence (5% - 95% CI)	SCC Decrease in incidence (5% - 95% CI)	NMSC Mortality Decrease in mortalities (5% - 95% CI)	Monetized Total Impacts Million U.S. Y2000 $ (5% - 95% CI)
20-30 °N	2,600 (1,200 – 4,300)	1,400 (630 – 2,300)	5.6 (2.5 – 8.9)	38 (13 – 78)
30-40 °N	2,400 (1,100 – 3,900)	1,100 (510 – 1,800)	9.4 (4.3 – 15)	61 (20 – 130)
40-50 °N	1,200 (540 – 2,000)	350 (160 – 580)	5.1 (2.3 – 8.1)	33 (11 – 69)

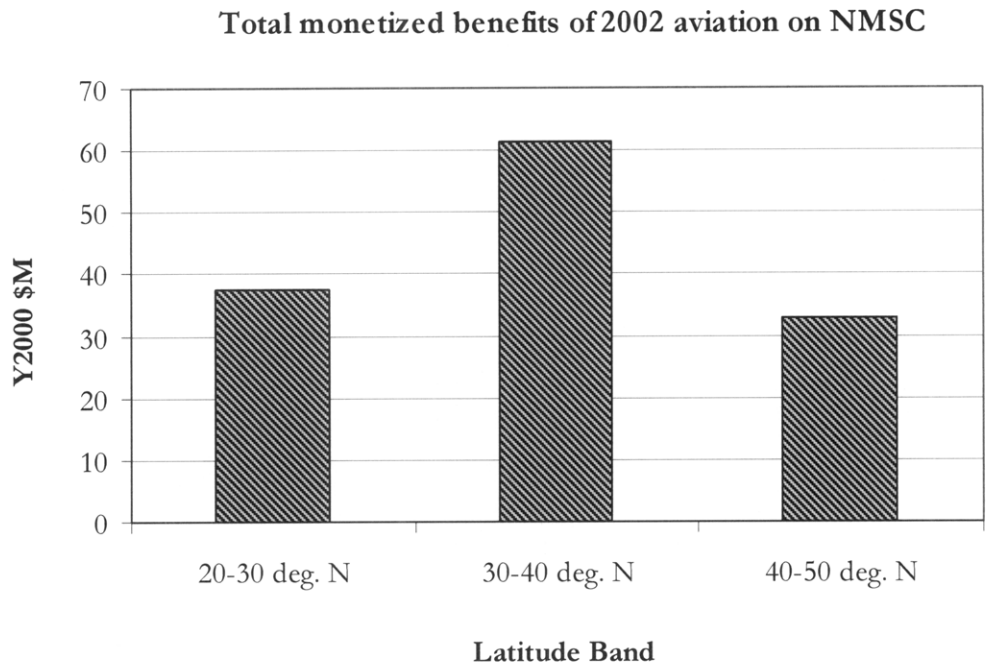

Figure 8: Total monetized benefits of 2002 aviation on NMSC incidence and mortality by latitude band.

The cost per tonne of aircraft NO_x can be approximated knowing that the AERO2K inventory accounted for approximately 0.68 Tg of NO_x in 2002. The benefit from aircraft NO_x in 2002 is about 190 $/tonne NO_x (90 % CI : 99 – 330 $/tonne).

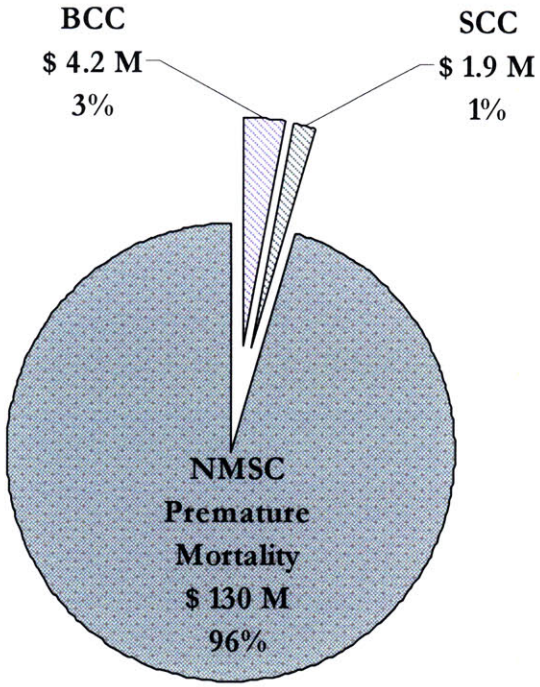

Figure 9: Monetized impacts of subsonic aviation on nonmelanoma skin cancer incidence and mortality, year 2002 (Million U.S. Y2000 $).

2.4.3 Discussion

From the results of the 1992 and 2002 studies, we find that the changes in NMSC cases and associated mortalities due to aircraft NO_x emissions are larger in 2002 than in 1992. There are several factors contributing to the larger impacts seen in 2002. The increase in air traffic was translated into an increase in global NO_x emissions, leading to higher percent changes in ozone column for each of the three latitude bands. As well, the population of the U.S. was grown from year 1992 census data to 2002 levels using U.S. census forecasts. In other words, not only was the change in ozone column more important in 2002, the number of people on the ground being affected by UVR was higher. Additionally, the baseline incidence rate was increased by 4% annually for BCC, by 9% annually for male SCC, and by 11 % annually for female SCC, as described in section 2.3.4. Therefore, a change in incidence of 1% in 2002 translates to higher change in the number of cases of SCC and BCC than a change of 1% in 1992. This also explains the higher monetized benefit per tonne of NO_x for the 2002 scenario (190 $/tonne) versus that of the 1992 scenario (150 $/tonne). Another contributing factor is the ageing population, whereby the number of people increases in the older, most susceptible age groups. It can be expected that benefits from

aircraft emissions in terms of skin cancer will increase in future years, as air traffic increases, and population increases. The use of changes in ozone column from two different sources also contributes to differences between 1992 and 2002 results. The IPCC simulation and the Köhler simulation used different CTMs, meaning that different chemical mechanisms are modeled. In addition, different background atmospheres were used.

The benefits from aircraft emissions on skin cancer incidence and mortality arise from the fact that the ozone layer is being depleted by long-lived anthropogenic compounds (BAS, 2008). The increase in ozone attributed to world-wide air transportation merely replaces a portion of the ozone being otherwise depleted. In short, without the contribution of aircraft NO_x, the equivalent number of new cases of BCC, SCC and NMSC mortalities would be observed.

In the 1992 scenario, percent changes in incidences were highest in the 40 - 50 °N latitude band and decreased towards the equator. In the 2002 scenario, percent changes in incidences were highest in the 30 – 40 °N latitude band, followed by the 40 – 50 °N band, and the 20 – 30 °N band in decreasing order. This spatial pattern of impacts is due to the higher percent change in O_3 column in the middle latitude band compared to the other two. Although both the 30 – 40 °N and the 40 – 50 °N bands saw an approximate change of O_3 column of 1.6 DU, their standard ozone column differed, with mean annual values of 300 DU and 320 DU, respectively.

2.5 Atmospheric and Health Effects Framework (AHEF)

The Atmospheric and Health Effects Framework is a model created by ICF International for the EPA (ICF, 2006). Its role is to assess the health impacts related to changes in the ozone layer. Initially intended to evaluate the impacts of ozone depletion and policies aimed at mitigating the depletion, the model can also be used to evaluate the impacts of aircraft emissions. A recent NASA/EPA collaborative study assessed the impacts on human health of supersonic aircraft flying in the stratosphere (EPA, 2001). No work has been done to this date to assess the impacts of subsonic aviation on human health in terms of skin cancer endpoints. The AHEF model is the most up-to-date model used by the EPA for analyzing impacts of changes in ozone. It was used in the 2008 analysis of the U.S. Sunwise program aimed at educating youths about the dangers of UVR (Kyle et al., 2008).

The AHEF model was peer-reviewed in August and September 2003 by an expert in the field of biological UV impacts assessment and by another expert in the field of atmospheric sciences. Their findings are summarized in the AHEF Peer Reviewed Report (ICF, 2006):

> *"(...) the reviewers stated that the methodology used in this model represents a sound, state-of-the-art approach to assessing ozone-related health effects. A number of comments identified areas for clarification of specific technical items, all of which have been considered by the authors. The reviewers stated that the report provides solid analysis and discussion of results, given the scope of the work and the uncertainties that currently exist in the areas of ozone depletion and UV radiation health impacts estimation."*

In this section, we compare results obtained with the APMT skin cancer model to those obtained with the EPA's AHEF model. The Köhler et al. (2008) changes in ozone are used as inputs to assess the impacts of subsonic aircraft NO_x on NMSC incidence and mortality in the U.S..

2.5.1 Overview of the AHEF impact pathway

The impact pathway used by the AHEF model is in large part very similar to the APMT skin cancer model impact pathway outlined in section 2.3 with the exception that it accounts for carcinoma malignant melanoma (CMM) and does not evaluate the monetary value of calculated impacts. A full description of differences between models will be given in Section 2.5.3.

The impact pathway outlined in the supersonic aircraft study, and shown in Figure 10, illustrates the general interaction of the model's components. The main varying element when using the AHEF surrounds the choice of CTM used to derive the changes in ozone column, upstream of the TUV model.

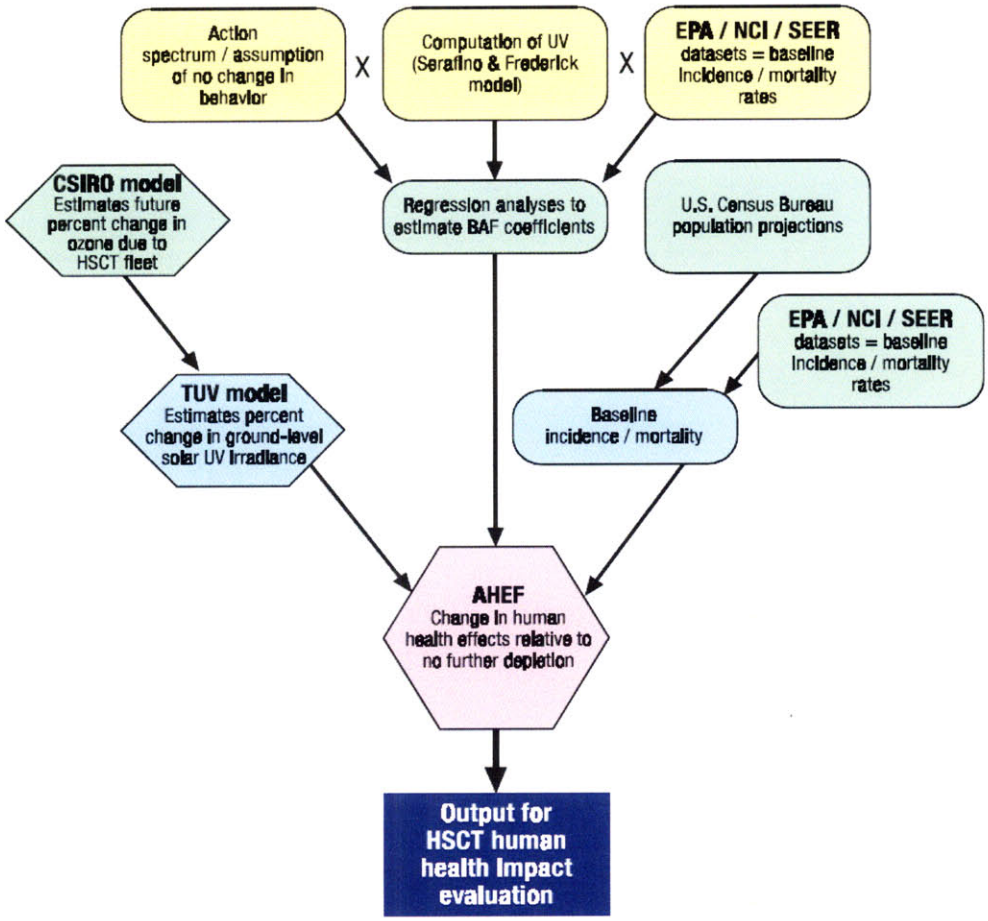

Figure 10: AHEF impact pathway as used in the NASA/EPA 2001 study of supersonic aircraft. Acronyms: BAF - biological amplification factor, NCI - National Cancer Institute, SEER - Surveillance, Epidemiology, and End Results Program. Source: U.S. EPA (2001) *Human Health Effects of Ozone Depletion From Stratospheric Aircraft*, Figure 2-1.

2.5.1.1 Changes in ozone column

In Figure 10, the CTM shown for the NASA/EPA study was the CSIRO model. While ICF uses CSIRO, the choice of CTM is left to the user. As discussed previously, the selection of a CTM must be done considering the fidelity of reproducing tropospheric and stratospheric chemistry.

The framework is limited to impacts in the United States alone. The geographical domain is divided into three latitude bands: 20-30 °N, 30-40 °N, and 40-50 °N.

2.5.1.2 Changes in UV exposure at the ground

Where the APMT skin cancer model used total amplification factors (AFs) which included radiation amplification factors (RAFs) and biological amplification factors (BAFs), the AHEF impact pathway employs the Tropospheric Ultraviolet and Visible (TUV) Radiation Model [(Madronich, 1992, Madronich, 1993), (Madronich and de Gruijl, 1993, Madronich et al., 1996, Madronich et al., 1998)] to first determine the change in UV exposure at the ground associated with a given change in ozone column. Then, changes in UV irradiance are multiplied with BAFs. The TUV model uses lookup tables derived from the spectral irradiance of the sun at ground level for varying times, latitudes, longitudes, wavelengths and other atmospheric transmission parameters, combined with the concept of biologically weighted radiation based on different action spectrums (EPA, 2001) This procedure can be summarized by the usage of spatially defined RAFs to determine changes in biologically weighted irradiance at the ground level, including consideration of the altitude of the ozone changes.

The AHEF requires that the TUV outputs be weighted as per specific action spectra relevant to SCC, BCC, and CMM. In the three cases, the SCUP-h action spectrum was selected as the most up to date and appropriate, although it is noted in the model documentation that SCUP-h was chosen for CMM because an action spectrum for CMM does not exist at present. This is commented in the AHEF peer review section (ICF, 2006):

> *"[The expert reviewer on UV biological assessment] highlighted the fact that one of the greatest sources of uncertainty in estimating UV radiation-induced health impacts is the lack of adequate experimental data from which a biological action spectrum fro cutaneous malignant melanoma (CMM) can be developed. Due to this lack of information, the AHEF predicts cases of malignant melanoma based on the SCUP-h action spectrum for squamous cell carcinoma (SCC). [The expert] agreed that the SCUP-h spectrum is the most appropriate action spectrum available to model CMM at this time. He noted that the action spectrum for CMM still remains to be determined, and that use of the SCUP-h in modeling CMM should be reconsidered if future research reveals that the shape of the action spectrum for CMM is not congruent with the SCUP-h action spectrum. EPA acknowledges that further scientific research in these and other areas could complement and significantly enhance the information presented in [the AHEF] report."*

2.5.1.3 Percent changes in skin cancer incidence and mortality

The changes in UV radiation reaching the ground, as computed by the TUV model, are input into the AHEF health impacts model where they are multiplied with a set of biological amplification factors to obtain changes in SCC, BCC, and CMM incidence along with changes in NMSC and CMM mortality. As seen in Section 2.2.2.2, a BAF relates percent changes in skin cancer incidence with percent changes in ambient UV exposure. As with the RAFs, the BAFs used by the AHEF model also hinge on the SCUP-h action spectrum. SCC and BCC BAFs are taken from (de Gruijl and Forbes, 1995), while those for CMM and NMSC mortality are derived from statistical analyses of SEER and EPA/NCI data (ICF, 2006). A table of BAFs used in the AHEF model is reproduced in Appendix F. Different BAFs are assigned to male and female populations. For all endpoints except for SCC incidence, the male BAFs used are higher than the female ones.

2.5.1.4 Changes in number of new skin cancer cases and mortalities

The AFEF model applies the percent changes in BCC, SCC, and CMM incidence and mortalities to the number of baseline incidence cases to determine the change in skin cancer cases and mortalities per county. For all endpoints, BAFs apply only to light-skinned populations.

The CMM incidence rates were obtained from 1973-1994 data originating from the National Cancer Institute's (NCI) SEER Program [(ICF, 2006), and referenced within]. They are classified by age, by sex, and by latitude band. The CMM BAFs have also been sorted by cohort group, as it was found that CMM incidence follows a cohort trend, i.e. depending on the date of birth (ICF, 2006). CMM mortality rates were taken from the analyses of 1950-1984 data from the EPA/National Cancer Institute (EPA/NCI) (Scotto et al., 1991, Pitcher and Longstreth, 1991). CMM mortality rates are also classified by cohort group.

The NMSC incidence rates used in the AHEF model have been described in detail in section 2.3.4. The NMSC mortality rates used are obtained from EPA/NCI data and are classified by age, by sex and by cohort. These NMSC mortality rates were derived from 1950-1984 data. Mortality rates for all other years were obtained by projecting the existing data (ICF, 2006). As was discussed previously, the completeness of the NCI data is questionable due to under-reporting of NMSC incidences and mortalities, and is said to only include a small portion of the U.S. population (Stang, 2007).

The numbers of baseline incidences and mortalities are computed by applying the incidence and mortality rates to the U.S. population of the year in question. Population data in the AHEF is obtained from the National Center for Health Statistics (NCHS) for the simulated year and is aggregated by age, sex, and race. The population included is usually Caucasian males and females, although for this study the U.S. Census race group "other" (includes Asians, Pacific Islanders, etc. – all but Black) was also included for better comparison with the APMT estimates.

The outputs of the model are changes in BCC, SCC, CMM incidences, along with NMSC and CMM mortalities. Results can be aggregated by state and by latitude band. The AHEF model does not attempt to do a valuation of these changes in endpoints.

2.5.2 Similarities and differences between the APMT skin cancer model and the AHEF model

In this section we present a comparative study highlighting the similarities and differences between the APMT skin cancer model and the AHEF.

2.5.2.1 Model structure

As its name suggests, the AHEF is a framework comprised of two different models: the TUV and the AHEF health impacts model. Changes in ozone input into the framework have come from the CISRO atmospheric chemistry model in past studies, although other CTMs may be used. Conversely, the APMT skin cancer model acts as a stand-alone model where inputs, i.e. percent changes in O_3 column, come from any CTM.

The APMT skin cancer model has the advantage of being a simplified model where the user can easily modify its parameters. To name a few examples, the user can modify the AFs used, the incidence rates used, and the population growth rate. While the AHEF is owned by the EPA, it is managed and run by ICF International, making it difficult to use for policymaking analyses by outside groups. In terms of its adaptability, it is claimed that the modular structure of the AHEF "enables new action spectra or new information on other UV-mediated human health endpoints to be easily incorporated into the modeling framework." (ICF, 2006)

A particularity of the AHEF is that health effects due to ozone perturbations are calculated as changes in endpoints with respect to effects observable at 1979-1980 ozone levels. In addition, the AHEF assumes that the Montreal Adjustments to the Montreal Protocol are respected over time. The practical consequences of these particularities is best illustrated by the NASA/EPA study (EPA, 2001) on high-speed civil transport (HSCT), or supersonic aircraft. To obtain an estimate of the changes in health endpoints due to HSCT, two scenarios had to be run to compute the incremental health effects over time with respect to 1979-1980 ozone: 1) the Montreal Adjustments to the Montreal Protocol without HSCT contributions; 2) the Montreal Adjustments to the Montreal Protocol with HSCT contributions. The health effects due solely to HSCT are then obtained by taking the difference between health effects from both scenarios.

2.5.2.2 Changes in ozone column

The APMT skin cancer model and the AHEF use different data sources to obtain changes in ozone column. The APMT model's inputs are percent change in ozone column for three latitude bands, where the changes in ozone can come from any CTM, but with specified assumptions. The AHEF uses total ozone column values from 1979-1980 (for baseline), future ozone column data following the Montreal Adjustments of the Montreal Protocol, plus ozone column changes due to the given scenario relative to the Montreal Adjustments.

2.5.2.3 Changes in biologically weighted UV irradiance

For both models, changes in cancer-causing UV irradiance are weighted as per the SCUP-h action spectrum. The methodology used by the APMT model and the AHEF to relate changes in ozone column to changes in UV irradiance both rely on the concept of radiation amplification factor. In the case of the APMT model, an overall RAF of 1.2 ± 0.06 is included in the total amplification factor (AF) used to relate percent change in ozone column to percent change in skin cancer incidence (de Gruijl and Van der Leun, 1994). This single RAF is applied for all latitudes between 0 – 65 °N (refer to Section 2.2.2.2 for justification). Conversely, the AHEF uses the TUV model to obtain temporal irradiance. As we have discussed, the TUV provides lookup tables of "weighted solar UV irradiance at sea level as a function of solar zenith angle and projected total column ozone based on the following assumptions: obstruction-free and cloud-free skies; standard profiles of air density, temperature, and tropospheric ozone (USSA 1976); typical continental aerosols (Elterman 1968); and 10 percent isotropic ground reflectivity." (ICF, 2006)

2.5.2.4 Percent change in skin cancer incidence

While both models utilize BAFs to estimate percent changes in skin cancer incidence, they are used differently, as was the case for the RAFs. The APMT skin cancer model, as we know, uses total AFs for BCC and SCC, which include BAFs for each of these endpoints. From Section 2.2.2.2, the AFs taken from de Gruijl and Van der Leun (1994) were based on BAFs of 2.5 ± 0.7 and of 1.4 ± 0.4 for SCC and BCC, respectively. The AFs, and by definition these BAFs, are applied to both female and male light-skinned populations. It should be noted however that the choice of AFs and by extension BAFs is left to the user. The AHEF uses the BAFs directly on the UV irradiance inputs coming from the TUV. The AHEF uses many more BAFs than the two in the APMT model, with BAFs for CMM, CMM mortality, BCC, SCC, and NMSC, all of which are specified by sex (refer to Appendix F for full list.) In the case of BCC and SCC incidence, BAFs differ slightly from those mentioned above and used in the APMT analyses presented in Section 2.4 as they come from a different study, that of de Gruijl and Forbes.

2.5.2.5 Change in skin cancer incidence and mortality

The baseline incidence rates for BCC and SCC by sex and by latitude which have been implemented into the APMT model were taken to be the same as those used in the AHEF model. However, in the APMT skin cancer model, growth factors are applied to the male and female baseline incidence rates to account for the increasing NMSC incidence trend (refer to Section 2.3.4). Therefore, for years above 1977-1978 for which the data was taken, baseline incidence rates are higher in the APMT model. For both models, baseline incidence rates are given by latitude band. In the AHEF, the baseline incidence rate of each county is determined by the location of the county centroid with respect to the three latitude bands.

Another difference between the models consists of the baseline population used. In APMT, U.S. Census data from 1992 is grown to the desired year based on population growth rates specified per year by the U.S. Census Bureau. In AHEF, the stored population data has been compiled from the National Center for Health Statistics, for each simulated year. The AHEF therefore has more accurate population data compared to the grown population data used in APMT. However, the compilation time and storage resources required for the AHEF's more accurate data are a tradeoff.

The method used by the APMT skin cancer model and the AHEF model to evaluate changes in NMSC mortalities constitutes an important difference between models. The AHEF uses a BAF for NMSC mortality, along with cohort-based NMSC mortality rates obtained from 1950-1984 EPA/NCI data and projections (refer to Section 2.5.1.4). While the AHEF documentation notes that NMSC mortality "does not display a cohort trend" it would appear that the data used is indeed classified by cohort (ICF, 2006). The APMT model on the other hand estimates the percent change in NMSC cases based on the NMSC AF, and applies this percent change to the baseline mortality. The baseline mortality is derived from Lewis and Weinstock (2004) NMSC mortality rates (see Section 2.3.5).

The resolution of the APMT model and the AHEF differ in that the APMT model computes aggregated impacts for three latitude bands while the latest version of the AHEF computes county-level impacts. The AHEF's resolution change from the three latitude bands to a county-level resolution is recent. While this new finer-resolution model was used to obtain results presented in Section 2.5.3, it has not yet been documented in AHEF literature.

2.5.2.6 Valuation of impacts

The AHEF does not have the capability of monetizing the computed health impacts. The APMT skin cancer model includes monetization of all health effects for use in policy-making.

2.5.2.7 Treatment of uncertainty

The treatment of uncertainty in the APMT model and in the AHEF differs significantly. As the propagation of uncertainty is an important feature of the APMT suite of tools, careful consideration is given to adequately capture and propagate all sources of uncertainty in the skin cancer model. As was described in Section 2.3, Monte Carlo simulations are used throughout the APMT skin cancer impact pathway, allowing for statistical analysis of the model's outputs. As a result, estimated health impacts and valuations can be specified with confidence intervals based on the user-defined uncertainty distributions used in the simulation.

The AHEF model adopts an entirely different approach to uncertainty (ICF, 2006):

"Although some might attempt to combine these different sources using statistical techniques, it is best to consider each source separately for two reasons. First, the quantitative estimates of the levels of uncertainty of the AHEF's many inputs and modeling components were derived using different techniques of varying levels of precision. Second, and perhaps more important, is that uncertainties concerning some of the inputs and computations might be inversely related. (...) the AHEF embodies the best inputs, assumptions, and computational procedures that are known."

In other words, when the AHEF model is run, additional analyses are required to assess lower and upper bounds on the health effects outputs. This is done for each source of quantifiable uncertainty individually (EPA, 2001, ICF, 2006), which could be a time-consuming effort. A quantification of theses sources of uncertainty as found in the AHEF documentation is shown in Table 16. As for the unquantifiable sources of uncertainty, they are not included in the uncertainty assessment.

Unquantifiable sources of uncertainty identified for the AHEF model are (ICF, 2006):

- *Composition of the future atmosphere;*
- *Future conditions of the ozone layer;*
- *Effect of climate change on ozone depletion;*
- *Global compliance with modeled policy scenarios;*
- *Laboratory techniques and instrumentation for deriving action spectra;*
- *Demographic and human behavioral changes;*
- *Baseline information.*

The same is true for the AMPT model, however an uncertainty distribution was applied to the baseline incidence rate and baseline case-fatality rate, based on reason.

Table 16: Major sources of quantifiable uncertainty for the AHEF model. Source: ICF report (2006), pg. 42.

Source of Uncertainty	Quantified Uncertainty
Translating column ozone to ground-level UV	
TUV Model	≈ 5%
Translating UV exposure to human health effects	
Uncertainty in the BAFs	≤ 30%
• CMM mortality (6%)	
• NMSC mortality (5%)	
• NMSC incidence (30%)	
Uncertainty with choice of action spectrum	≈ 50%
Early life exposure vs. whole life exposure	≈ 10%
Total $\sqrt{(5^2 + 30^2 + 50^2 + 10^2)}$	**≈ 60%**

2.5.3 Comparison of results between APMT skin cancer model and AHEF

In this section, we present results of a comparative study done with the AHEF model based on detailed changes in ozone column obtained from the Köhler et al. study for year 2002 aviation (Köhler et al., 2008). The AHEF model's county-level resolution allowed for health impacts to be calculated based on changes in ozone column with finer resolution. The changes in ozone (in DU) caused by aircraft NO_x were obtained from Köhler with a latitude-longitude resolution of approximately 5.6 degrees by 5.6 degrees and were applied to each U.S. county based on the location of the county's centroid.

AHEF estimates are based on NCHS population data for year 2002 including all light skinned race groups, i.e. "Whites," "American Indians and Alaskan Natives," as well as "Asians and Pacific Islanders." Results of the AHEF analysis for NMSC incidences and mortalities are shown in Table 17, and have been aggregated by latitude band to allow for comparisons to be made with APMT estimates. The lower and upper bounds are based on quantified model uncertainty ranges given in Table 16. For the lower bound case, the AHEF was run with uncertainty parameters in Table 16 set to their low case (e.g. action spectrum 50% lower). The same was done for the upper bound with parameters set to the high case (e.g. action spectrum 50% higher).

Table 17: U.S. decrease in BCC and SCC incidence by latitude due to subsonic aviation in 2002 as calculated by the AHEF model. Decrease in NMSC mortalities are also shown.

Latitude Band	BCC decrease in incidence (lower and upper bounds)	SCC decrease in incidence (lower and upper bounds)	NMSC decrease in mortalities (lower and upper bounds)
20-30 °N	1,400 (950 – 1,900)	740 (530 – 940)	2.5 (2.3 – 2.7)
30-40 °N	1,800 (1,200 – 2,400)	960 (680 – 1,200)	11 (10 – 12)
40-50 °N	950 (640 – 1,300)	320 (230 – 410)	2.0 (1.8 – 2.2)
Total U.S.	4,100 (2,800 – 5,500)	2,000 (1,400 – 2,600)	16 (14 – 17)

Latitudinal patterns observed in Table 17 can be compared directly with APMT results presented in Table 15. Differences may be attributed to the higher geographic resolution of the AHEF model and of the input data. The AHEF used monthly changes in ozone from the Köhler study with a 5.6

degree by 5.6 degree resolution. Calculations were made on a county-level basis. Changes in UV irradiance took into account seasonal variability. In the case of the APMT analysis, yearly averaged changes in ozone were applied to three latitude bands, a coarser approach. A standard O_3 column DU was also assumed to obtain % changes in ozone column (refer to Section 2.4.2.1).

Table 18: Comparison of U.S. decrease in NMSC incidences and mortalities obtained with the APMT model and with the AHEF model. Numbers shown are for 2002 baseline aviation. Changes in ozone column from Köhler et al..

Endpoint	APMT Impacts Skin Cancer Model (5% - 95% CI)	AHEF Model (Lower and Upper Bounds)
BCC Incidences	6,200 (3,800 – 9,100)	4,100 (2,800 – 5,500)
SCC Incidences	2,900 (1,700 – 4,200)	2,000 (1,400 – 2,600)
NMSC Mortalities	20 (13 – 28)	16 (14 – 17)

Comparing the APMT results with those obtained with the more complex AHEF model, we find that the percent difference between BCC and SCC incidences estimated by both models is about 50 % in both cases. APMT estimates tend to be higher than AHEF estimates. This may be explained in large part by the incidence growth factor and the upward biased uncertainty distribution applied to the BCC and SCC baseline incidence rates to account for increasing skin cancer rates and under-reporting (refer to Table 6). To illustrate, a test case was done using the APMT skin cancer model with the incidence growth factor set to zero and without the uncertainty distribution on the baseline incidence rate. Results differed from the AHEF model by about 34 % for the BCC endpoint and by about 25 % for the SCC incidence.

Estimated impacts changes of melanoma skin cancer incidence and mortality due to aircraft NO_x in 2002 are shown in Table 19. Changes in UV irradiance due to aircraft NO_x in 2002 is estimated to have led to a decrease of approximately 200 CMM cases and 29 fewer CMM mortalities. The number of CMM mortalities prevented are approximately twice as numerous as the number of NMSC mortalities. Knowing that premature mortality valuations dominate health impact assessments, we can easily see that monetized CMM benefits would be double those of NMSC benefits.

Table 19: U.S. decrease in CMM incidence and mortality by latitude due to subsonic aviation in 2002 as calculated by the AHEF model.

Latitude Band	CMM decrease in incidence (lower and upper bounds)	CMM decrease in mortalities (lower and upper bounds)
20-30 °N	59 (55 – 64)	6.5 (6.0 – 6.9)
30-40 °N	87 (81 – 94)	17 (16 – 18)
40-50 °N	48 (45 – 52)	5.6 (5.2 – 6.0)
Total U.S.	200 (180 – 210)	29 (27 – 31)

2.6 APMT model limitations and future work

In this section we discuss the limitations of the APMT skin cancer model and propose areas for future work.

The source of inputs to the model constitutes a limitation with respect to its applicability in policy assessment. In effect, the reliance on a complex CTM to obtain changes in ozone column due to aircraft NO_x makes the model ill-suited for the rapid analyses of different policy scenarios. The findings of Köhler et al. reveal that changes in global ozone column are a linear function of changes in aircraft NO_x for perturbations up to 20 % (Köhler et al., 2008). Based on this study, one may hypothesize that changes in ozone column over the U.S. may also be linear with aircraft NO_x inventories. If this hypothesis of linearity is proven to be true, results from the Köhler study could be used in APMT as a baseline. Different aviation scenarios could hence be analyzed by scaling the baseline changes in ozone column by the ratio of NO_x emissions inventories. However, this hypothesis of regional linearity remains to be verified using full CTM simulations. If the change in ozone column is shown to be non-linear for regional perturbations, future efforts may involve the development of a reduced-order model. The objective of such a model would be to estimate percent changes in ozone column at the three Northern latitude bands of interest using global aviation emissions inventories as input. An approach similar to that used to develop the Air Quality Response Surface Model (RSM) could be employed [(Masek, 2008), and the subject of Chapter 3].

The limited data available on U.S. NMSC incidence rates, case-fatality rates, and mortality rates represents another limitation of the skin cancer model. NMSC is not fully reported in SEER therefore incidence rates and mortality rates are not well documented; more studies are required (Stang, 2007). Any data available is also subjected to under-reporting due to the relative ease of treatment and misdiagnosed cause of death (for example if the skin cancer weakened the person and they contracted another disease/illness). Future work will include regular updating of the incidence and mortality rates per age, sex, and latitude band as new surveys and studies are made public.

The exclusion of melanoma (CMM) incidence and mortality endpoints also limits the complete assessment of aircraft NO_x on human health effects. However, considering that the AHEF has been peer reviewed and that the SCUP-h action spectrum was found to be the "most appropriate action

spectrum available to model CMM" (ICF, 2006), future work may be geared towards including CMM into the APMT model. One simple way of doing this would be to do a linear scaling of the NMSC results, since both CMM and NMSC would use the same action spectrum. The CMM scaling factor could be derived from the AHEF results from Section 2.5.3. It was shown that aviation-related changes in CMM incidences represent approximately 3 % of NMSC incidences. Conversely, CMM mortalities represent approximately twice the number of NMSC mortalities. Besides CMM, other endpoints of changes in UV irradiance which could be included in future work as action spectra become available and more reliable are: cataract, cornea damage, generalized DNA damage, and immune effects, to name a few. UVR has also been linked to the activation of HPV and HSV-1 viruses. Also, a positive change in UVR negatively affects the production of vitamin D, a known cancer preventing agent (Norval et al., 2007).

The valuation currently implemented in the model only accounts for the direct costs of treatment. The cost of illness (COI) for skin cancer which is forthcoming as part of the "Cost of Illness Handbook" (EPA, 2009) may be used in the future to better approximate the health benefits from subsonic aviation. COI as defined by the EPA includes direct costs, welfare loss, and production loss. Using the COI would therefore portray more accurately the full costs and benefits.

Another limitation of the model is that health impacts are only computed for light-skinned populations. This is entirely due to the state of the research in the field. In the future, when an action spectrum for skin cancer in dark-skinned humans and derived amplification factors are published, the model should be updated such that effects on the full population are captured thereafter. Similarly, when nonmelanoma incidence and mortality rates are made available, along with data for other countries, it could be used to expand the breadth of the model from U.S. only to world-wide.

Future work on the APMT skin cancer model could also include the disaggregation of total amplification factors into RAFs specified by latitude and BAFs specified by age and sex. In terms of RAFs, perhaps the functionality of the TUV could be reproduced in a reduced-order model. Finally, future efforts can be invested in better defining the uncertainty distributions which were set by reason but are not quantified as of yet. This would improve the accuracy with which skin cancer impacts of subsonic aviation are estimated.

3 Impact of LTO Aircraft Emissions on Air Quality and Associated Health Impacts

Aircraft emissions released into the air contain particles and gases which contribute to increasing the ambient concentration of pollution. Of the various components of air pollution, particulate matter is typically the greatest concern. Unlike the benefit gained from NO_x emissions relative to skin cancer incidences, when it comes to air quality, emissions have a net cost on health. Chapter 3 addresses the impacts of LTO aircraft emissions on air quality through two reduced order models and presents the health costs associated with different scenarios.

We begin Chapter 3 with a background review of particulate matter stemming from aircraft emissions. Section 3.2 follows with an overview of best practices for conducting a health impact assessment, referred to as the health impact pathway, as defined by the U.S. EPA and the European Union CAFE program. The need for reduced order models in policymaking is put into the context of air quality assessment in Section 3.3. The impact pathway implemented in APMT is reviewed in 3.4. We introduce the intake fraction model (Rojo, 2007) and the response surface model (Masek, 2008). Section 3.5 presents the newly developed RSM v2 and highlights the changes made from the first RSM by Masek. Comparisons between the RSM v2 reduced-order approximations and the high-fidelity CMAQ air quality model simulation results are also given. In Section 3.6, a comparison of the iF model and the RSM v2 model is made, with a focus on applicability and resolution. Section 3.7 presents a full impact analysis for year 2005 aviation using both the iF model and the RSM v2 model. Three illustrative policy scenarios are also presented. An uncertainty assessment of the new RSM v2 can be found in Section 3.8, including a global sensitivity analysis and a distributional sensitivity analysis highlighting the factors on which to focus future research to reduce output uncertainty. Model limitations and future work conclude the chapter.

3.1 Background

The United Nations' International Civil Aviation Organization (ICAO) has projected an international air transportation growth rate of approximately 4.6 % per year up to 2025 and a freight traffic grow rate of 6.6 % per year (ICAO, 2007). This increase in traffic is expected to increase the amount of aircraft emissions being released into the atmosphere. When found at ground level, several of the resulting pollutants contribute to a worsening of ambient air quality and hence negatively impact human health. Regulatory bodies world-wide are looking to mitigate these negative health impacts by means of regulations and policies addressing the composition of jet fuel, the development and implementation of new aircraft engine technology, and the use of fuel-saving taxi, landing, and takeoff procedures. When assessing policy options, decision-makers rely on models to simulate the effects of these policies and to compare the costs and benefits of one policy versus another.

In this Background section, we begin with a review of the criteria pollutants that the EPA and the FAA regulate, and we define what constitutes PM_{25}. We then address the need for reduced order models in policymaking and present the two APMT air quality models, which will be the topic of the remainder of this chapter.

3.1.1 LTO emissions: criteria pollutants

The U.S. Environmental Protection Agency lists six common air pollutants posing a threat to health, to the environment, and to structures as "criteria pollutants." Criteria pollutants include: particulate matter, ground-level ozone, carbon monoxide, sulfur oxides, nitrogen oxides, and lead. For each of these, the EPA has set standards, known as the National Ambient Air Quality Standards, as mandated by the Clean Air Act (Code, 1955 with Amendments in 1990). Since the removal of lead from gasoline had significant impacts on decreasing lead concentrations in the air, particulate matter and ozone are now considered to be the predominant air pollutants causing health damages.

3.1.2 $PM_{2.5}$ - Fine PM

Defined by the EPA as fine particles of 2.5 micrometers or less, $PM_{2.5}$ includes solid, liquid, and heterogeneous (mixed solid and liquid) particles (EPA, 2004a). These fine particles get inhaled by

humans and become trapped within the lung tissues, potentially causing serious medical harm. The major health endpoints caused by $PM_{2.5}$ are (Rojo, 2007):

- Premature mortality in adults and infants;
- Chronic bronchitis;
- Hospital admissions due to respiratory as well as cardiovascular ailments;
- Emergency room visits due to asthma;
- Minor restricted activity days.

$PM_{2.5}$ is subdivided into two categories based on its formation:

- Primary PM: particles emitted directly in exhaust, such as soot and non-volatiles;
- Secondary PM: particles formed in the atmosphere as a result of chemical reactions between the emitted gases and other elements in the air.

The combustion occurring in aircraft engines leads to the formation of both primary and secondary particulate matter. Primary components of $PM_{2.5}$ that are emitted from aircraft are non-volatile PM (nvPM), volatile PM from sulfur and volatile PM from organics. Emitted precursors of secondary PM include nitrogen oxides (NO_x), sulfur dioxide (SO_2) and volatile organic compounds (VOC). Particulate matter originating from aircraft emissions are usually categorized as $PM_{2.5}$ due to the size distribution of the components (Holve and Chapman, 2005).

Considering that measurements for aircraft emissions worldwide or even nationwide are not yet fully available, approximations are typically made using the First Order Approximation (FOA 3) method elaborated by the ICAO Committee on Aviation and Environmental Protection (CAEP) and presented in Appendix D of the *Airport Air Quality* report (CAEP, 2006). The FOA 3 approximations for nvPM are based on engine smoke number, determined with engine soot being collected in a filter at the exhaust of the engine during its certification. Volatile PM is approximated using available measurements of condensable sulfur and hydrocarbons. Due to the current limited understanding of their role in PM formation, lubrication emissions are not included in the FOA 3 method (Masek, 2008).

Equations 5 – 7 constitute the FOA 3 equations used to approximate aircraft emissions, where K's are constants. Equations 8 – 10 are identities.

$$\text{nvPM} = K1 \times \text{fuel burn} \times \text{nvPM EI} \quad (5)$$

$$\text{volPM}_{\text{sulfur}} = K2 \times \text{fuel burn} \times \text{fuel sulfur content} \times \text{sulfur conversion efficiency} \quad (6)$$

$$\text{volPM}_{\text{organics}} = K3 \times \text{fuel burn} \times \text{HC EI} \times \text{HC conversion efficiency} \quad (7)$$

$$NO_x = K4 \times \text{fuel burn} \times \text{NOx EI} \quad (8)$$

$$SO_2 = K5 \times \text{fuel burn} \times \text{fuel sulfur content} \quad (9)$$

$$\text{V OC} = K6 \times \text{fuel burn} \times \text{HC EI} \quad (10)$$

3.2 Health impact pathway

Emissions from aircraft engines contain components of primary $PM_{2.5}$, as well as particulate matter precursors. When found at ground level, $PM_{2.5}$ contributes to a decrease in ambient air quality which negatively impacts human health.

Section 3.2.1 reviews the current procedure used by the US Environmental Protection Agency (EPA) and Section 3.4 briefly reviews the impact pathway used by the Partnership for AiR Transportation Noise and Emissions Reduction (PARTNER) in the APMT model to evaluate the local air quality impacts of aviation. This methodology was recently used to determine the health impacts of commercial aviation in the United States as mandated by Section 753 of the Energy Policy Act of 2005 (U.S. Public Law 109-58) (Ratliff et al., 2009). An overview of current practices used by the European Union's Clean Air for Europe (CAFE) program and examples of recent applications of AQ health impact analyses worldwide can be found in Section 3.2.1.1.

3.2.1 Overview of U.S. EPA best practices for air quality health impact assessment

Taken from Rojo (2007), Figure 11 presents the air quality health impact pathway at a broad level. The emissions resulting from the baseline or policy scenario being studied are modeled using an air quality modeling tool. The outputs of the air quality model, changes in ambient PM concentrations, are then used in combination with dose-response functions which relate changes in health endpoints to changes in pollutant concentrations. The calculated changes in health endpoints are then given dollar amounts by applying a set of valuations for all endpoints. The total cost of the scenario in terms of air quality health impacts can then be compared to other costs and benefits, such as those related to climate and noise impacts, and to the policy's implementation costs.

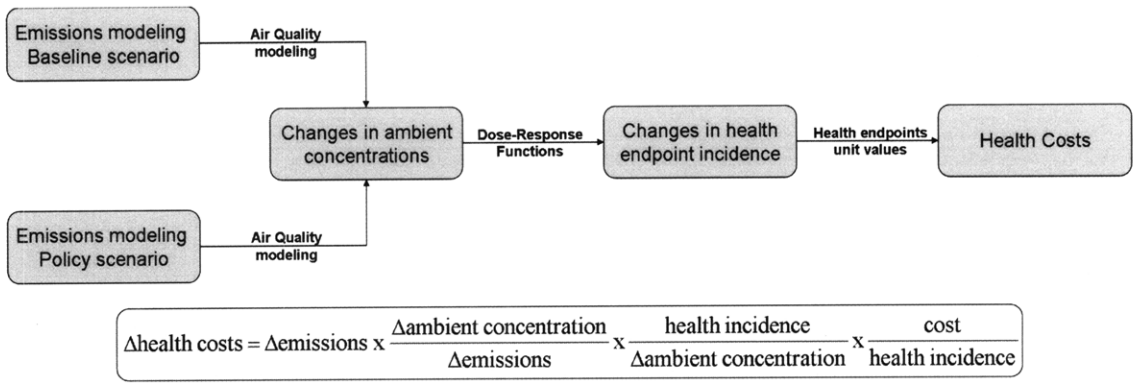

Figure 11: Health impact pathway for air quality assessment. Source: Rojo (2007), fig. 3.

Three primary steps compose the EPA's analysis of a policy's impact on local air quality. First, candidate airports are selected for study. The FAA Emissions and Dispersion Modeling System (EDMS) (CSSI, 2007) estimates an emissions inventory for aircraft landing and take-off (LTO) cycles around the given airports for a given time frame. EDMS accounts for emissions from both aircraft main engines and auxiliary power units (APUs).

Next, EDMS emissions inventories are related to changes in ambient concentrations of pollutants using the CMAQ modeling system, a 3-D grid-based air quality model. Resultant concentrations depend on location from the airport, chemical reactions in the atmosphere, meteorology, and other factors. As will be discussed in Section 0, reduced order models used to estimate changes in ambient concentration include the intake fraction (iF) method based on the source-receptor matrix developed by Jonathan Levy (Greco et al., 2007) and recently used to study the impacts of the Clean Air Interstate Rule (EPA, 2005a) or the response surface model (RSM), used by PARTNER's Aviation Environmental Portfolio Management Tool (APMT). As per EPA practice, concentrations of PM are then "SMATed." The Speciated Modeled Attainment Test (SMAT) seeks to reconcile modeled concentrations with measured concentrations from monitors (EPA, 2006a). It should be noted that the current APMT RSM does not SMAT air quality concentrations (more on this in Section 3.9.1).

Finally, the Environmental Benefits Mapping and Analysis Program (BenMAP) developed for the EPA (Abt, 2005) combines pollutant concentration changes with population data to estimate changes in health incidences, such as chronic bronchitis and premature death, using concentration

response functions (CRFs) from health studies. EPA has used BenMAP to estimate the health effects of PM and ozone.

Health effects valuation was not done for the Energy Policy Act 2005 aviation study, but EPA has computed valuations of health effects in the past. A valuation capability is implemented in APMT. The valuation results depend on the given population's willingness to pay, as well as the value of a statistical life (VSL), assigned by policymakers.

3.2.1.1 Past applications

3.2.1.1.1 European Union CAFE Practices

The EU CAFE program uses a methodology very similar to EPA's procedure to assess the health impacts of $PM_{2.5}$ and ozone. Emissions are evaluated by the Cooperative Programme for Monitoring and Evaluation of the Long-range Transmission of Air Pollutants in Europe (EMEP) and converted to concentrations using the Regional Air Pollution Information and Simulation (RAINS) model (Amann et al., 2004). The Health Impact Assessment (HIA) block (Hurley et al., 2005) within the CAFE Cost-Benefit Analysis (CBA) model (Holland et al., 2005, CAFE, 2006) quantifies health endpoint changes using CRFs. CAFE CBA then computes the monetary valuation of health impacts.

3.2.1.1.2 Applications of US EPA and EU CAFE Local Air Quality Impact Assessment Practices

Policy-makers worldwide have used local air quality health impact analyses. Following are a few examples of applications by the U.S. EPA, the EU CAFE and by other international bodies.

EPA Rulemakings

EPA practices for health impact analyses have been used in several US rulemakings: 1) Tier 2/Gasoline Sulfur Rule (EPA, 1999); 2) Clean Diesel Trucks, Buses, and Fuel: Heavy-Duty Engine and Vehicle Standards Highway Diesel Fuel Sulfur Control Requirements (EPA, 2000); 3) Control of Emissions from Nonroad Diesel Engines (EPA, 2004c); 4) Clean Air Interstate Rule (EPA, 2005a). BenMAP has also been used for the Clean Air Visibility Rule (EPA, 2005b), PM National Ambient Air Quality Standard (EPA, 2006b), Mobile Source Air Toxics (EPA, 2007a), Ozone National Ambient Air Quality Standard (EPA, 2007b), and Locomotive and Marine Engines Rule

(EPA, 2008). EPA and PARTNER recently studied the local air quality and health impacts of aviation for the US Congress as mandated by the Energy Policy Act of 2005 (Ratliff et al., 2009).

EU CAFE Applications

Recent applications of the EU CAFE health impact practices include the Thematic Strategy on Air Pollution (CEC, 2005b) as well as the Impact Assessment documents for the Thematic Strategy on Air Pollution and the Directive on Ambient Air Quality and Cleaner Air for Europe (CEC, 2005a). These assessments looked at the health impacts of $PM_{2.5}$ and ozone for 25 EU countries.

International Applications

BenMAP has been used to conduct health impact analyses in Korea (Environment Institute), India (Indian Institute of Technology, National Environmental Engineering Research Institute, Maharashtra Pollution Control Board), China (State Environmental Protection Agency, Peking University, and Tsinghua University), Mexico (Universidad Nacional Autonoma), and Taiwan (National Taiwan University).

The World Bank recently published a study on local quality health impacts in China (2007) for PM_{10} using the Chinese Environmental Cost Model (CECM) (World_Bank, 2007). CECM's cost-benefit analysis employs methods in accordance with those used by in the USA and the EU, such as CRFs.

3.3 Need for reduced order models in policymaking applications

In an iterative policy assessment process, multiple policy scenarios need to be analyzed over long timeframes, often spanning several decades. To estimate the impacts of aircraft emissions on air quality and hence on human health, changes in pollutant concentrations at ground level are computed by atmospheric chemistry transport models (CTMs). These highly complex models simulate the chemical reactions and transport mechanisms of the atmosphere. Briefly, the typical methodology used by these models consists of subdividing the Earth's atmosphere into grid boxes, where specified horizontal and vertical resolutions are observed. Each grid box is governed by a set of equations meant to simulate chemical and physical phenomena such as convection, deposition, condensation, and chemical reactions of all sorts. For each specified time-step (e.g. one hour), the model calculates the concentration of each species of atmospheric components. Exchanges between cells are also reproduced as the boundary conditions of each cell depends on the conditions simulated in neighboring cells. Simulating an entire year's atmospheric conditions on an hour-by-hour basis is computationally intensive. In the case of the Community Multiscale Air Quality (CMAQ) model (Byun and Ching, 1999, Byun and Schere, 2006), the simulation runtime for twelve months of data on an hourly basis is three days. In light of this, it is apparent that the analysis of several multi-year scenarios becomes extremely computation- and resource- intensive.

Analyzing scenarios for policymaking often involves conflicting requirements: accuracy, timeliness, transparency, and cost-consciousness (NRC, 2007). Despite the high level of accuracy seen in today's CTMs, their high resource demands and long runtimes often make them unsuited for rapid policy assessments. In this context, a reduce order model has the advantage of producing results in a timely fashion, having limited complexity and hence higher transparency.

From the EPA's health impact pathway outlined in Section 3.2, we find that the functionality of CMAQ and BenMAP in this framework could be reduced to a single reduced order model. This idea is the basis of the APMT Impacts Air Quality reduced order model (APMT Impacts - AQ).

3.4 APMT Impact Pathway

A comprehensive description of the air quality health impact pathway used in the APMT AQ framework can be found in Rojo's S.M. thesis (2007). Therefore, only a brief overview of the framework used in the health impacts reduced order model is presented in this section. Again, the model replaces the use of a complex CTM to calculate changes in ambient $PM_{2.5}$ concentration and the use of BenMAP to calculate changes in health endpoints, thus accelerating the impact assessment process.

3.4.1 Emissions Inventories: AEDT/EDMS

The emissions inventories utilized in APMT analyses follow the EPA's *Procedures for Emission Inventory Preparation - Vol IV: Mobile Sources* (EPA, 1992), whereby only aircraft emissions below 3,000 feet of altitude are considered in health impact analyses. The EPA considers that emissions above this level do not pose a significant threat. It should be noted however that a current study is putting this assumption into question by investigating the impacts of cruise emissions on human health (Barrett et al., 2009).

Emissions inventories are generated using the FAA Aviation Environmental Design Tool Emissions Dispersion Modeling System (AEDT/EDMS) (CSSI, 2007). Landing, takeoff, and taxi emissions are simulated on an aircraft-by-aircraft basis and are aggregated at the airport level for the purpose of our air quality studies. $PM_{2.5}$ emissions are estimated by the AEDT model via the FOA 3 approximations described in Section 3.1.2. The 325 airport EPAct inventory served as a basis for the development of the RSM. This means that the RSM model can account for 325 U.S. airports, representing 95% of commercial aviation activity in the U.S. (Ratliff et al., 2009).

Assumptions on uncertainty for AEDT/EDMS inventories are taken to be the same as for AEDT/SAGE, as described in Rojo (2007). Specifically, it was assumed that real emissions could be estimated by applying mean shifts to the deterministic AEDT/EDMS inventories derived from landing and takeoff times-in-mode (LTO TIM) based on aircraft performance. Mean shifts were expressed as uncertainty coefficients having uniform distributions between 0.92 and 1.12 for LTO fuelburn and LTO SO_x, 0.83 and 1.23 for LTO NOx, and 0.52 and 2.06 for LTO non-volatile PM, or primary PM. For SO_x emissions, the inventory is created with assumed fuel sulfur content (FSC).

An additional uncertainty coefficient following a Weibull distribution was applied to capture the FSC distribution based on PQIS data for U.S. JP8 FSC in years 2002 to 2007 (DESC, 2002-2007). The distribution is shown in Figure 12. Weibull fit parameters are λ = 0.0627 (scale) and k = 1.2683 (shape). The mean FSC is 0.0574 % mass or 574 ppm.

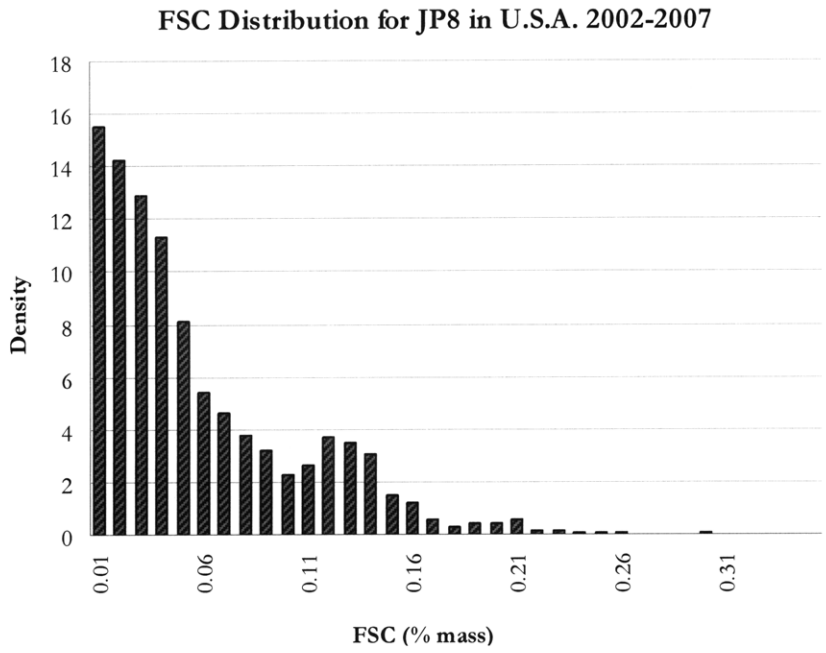

Figure 12: PQIS data for U.S. JP8 FSC in years 2002 to 2007 (DESC, 2002-2007).

3.4.2 Exposure analysis: from the intake fraction model to the speciated RSM

Air quality modeling is required to relate aircraft emissions inventories to changes in ambient pollutant concentrations across the country. As this work was developed in support of the APMT Impacts Air Quality block (Impacts - AQ) for direct application in policymaking, two different types of reduced order models were designed with the aim of obtaining approximations of results obtained by CTMs. The two types of air quality models used in APMT to calculate the health impacts of aircraft emissions are: the intake fraction (iF) model derived from a source-receptor matrix and the response surface model (RSM) derived from CMAQ simulations.

The key difference between the iF model and the RSM model hinges on the methodology used to approximate changes in $PM_{2.5}$ resulting from a given aviation scenario. The approximation of health

impacts associated with these changes in concentration and their valuation essentially follows the same impact pathway.

3.4.2.1 Intake fraction model

The concept of the intake fraction refers to a non-dimensional measure of population weighted changes in concentration times the nominal breathing rate and divided by the amount of emissions of a pollutant or its precursor responsible for the change in concentration (Greco et al., 2007, Bennett et al., 2002). Greco et al. developed a set of intake fractions for particulate matter originating from mobile sources based on source-receptor matrices. Greco et al. (2007) presents the intake fraction for emissions Q_j in county j having an impact on county i as:

$$iF_j = \frac{\sum_i P_i \Delta C_{ij} \cdot BR}{Q_j} \qquad (11)$$

Where i is the receptor county, j is the emitter county, P is the affected population, ΔC_{ij} is the change in concentration of $PM_{2.5}$ in county i due to a specific pollutant in county j, and BR is the breathing rate. By multiplication of the emissions emitted by county j (Q_j) by the intake fraction of county j (iF_j) over the breathing rate (BR), the population weighted change in concentration over all counties in the U.S. is obtained ($\Sigma_i P_i \Delta C_{ij}$).

The four types of intake fractions used in assessing the health impacts of aviation emissions are: primary PM, secondary sulfates, secondary nitrates, and the bounce-back effect. The bounce-back effect captures the reactive preference of ammonia with sulfates, leading to the decrease of secondary nitrates in the presence of SO_2. The Greco et al. intake fractions are on a county-by-county basis.

Based on the most relevant Greco et al. intake fractions, the APMT intake fraction model (APMT iF) simulates the impacts of a single county's emissions on nationwide health effects. Therefore, this model is suitable for analyses looking to isolate contributions of a single airport and determining the contributions of the different primary and secondary pollutants at the source (Rojo, 2007). This reduced order model based on source-receptor matrices is limited by the scope of the matrices and their level of complexity in terms of atmospheric chemistry and transport. Because the matrices were derived for ground-level mobile sources, the model cannot capture the full effect of the vertical profiles over which aircraft emissions are emitted. In other words, the APMT iF model assumes that

all emissions are released at the ground level, and spread from there. The APMT RSM was designed to specifically eliminate this limitation.

3.4.2.2 Response Surface Model

The APMT's response surface model, or RSM, consists of a reduced order model built from statistical analyses of CTM simulations. The basis of the RSM lies on a set of 27 simulations which were done using CMAQ. The number of CTM simulations used to build the RSM was determined by both the time and resource constraints, as well as the level of accuracy desired and the number of independent parameters selected. To limit the dimensionality of the model, four independent parameters were chosen and varied nationally through a design of experiments (Masek, 2008). The four independent parameters are:

- Fuelburn,
- Fuel sulfur content,
- Inventory nvPM EI,
- Inventory NO_x EI.

From the outputs of the 27 CTM simulations, i.e. the approximate changes in $PM_{2.5}$ concentrations at ground level, statistical linear regressions over the four independent parameters were derived for implementation in the RSM. The cell-by-cell linear regressions are effectively the cornerstone of the RSM's capability of extrapolating changes in $PM_{2.5}$ concentration at any other setting of the four parameters.

Changes in population exposure are computed directly from the RSM extrapolated changes in $PM_{2.5}$ concentration multiplied by the affected population. The RSM model's resolution corresponds to CMAQ's 36 km by 36 km Lambert Conformal grid resolution over the U.S.. Population exposure and associated health impacts are calculated on a cell-by-cell basis. Nationwide impacts are simply obtained by summing impacts for all cells over the domain.

The strength of the RSM rests on its consideration of the vertical distribution of aircraft emissions and of complex atmospheric chemistry found in CTMs. Due to the constraints limiting the number of CTM simulations on which to build the RSM, the model is limited by the number of independent parameters being varied. Similarly, as emissions from airports were varied uniformly across the U.S., the RSM is best suited for national level policies compared to regional policies.

Of note, the concept of a response surface model has been used in the past by the U.S. EPA to assess the health impacts of the National Ambient Air Quality Standards (NAAQS) (EPA, 2006c). Their RSM was based on ten times more CMAQ simulations and was designed for a broad range of emission sources (Masek, 2008).

The first version of the APMT RSM model was engineered to optimize the accuracy of replicating the estimated change in total $PM_{2.5}$ for a given set of aircraft emissions below 3,000 feet and to compute associated health impacts (Masek, 2008). Studies done by the author of this thesis (in collaboration with S. Kuhn) revealed that optimizing for the total $PM_{2.5}$ concentration led to an inaccurate apportionment of impacts among the different $PM_{2.5}$ species. To address this, improvements have been made to the model such that regressions are made for each PM species separately rather than for their total. The development of this improved "speciated RSM" is the topic of Section 3.5.

3.4.3 Health impact analysis: CRFs

Once the changes in population exposure due to aircraft emissions have been approximated, either at the national level (iF) or at the grid-cell level (RSM), we relate these changes to changes in health endpoints. This is done by means of concentration response functions (CRFs), or dose response functions, which are derived from epidemiological studies. The full justification behind the selection of each concentration function and uncertainty used in the APMT air quality health impacts framework can be found in the Supplementary Information section of *The magnitude and distribution of fine particle-related public health impacts of aircraft emissions in the United States* (Brunelle-Yeung et al., In preparation) and in Rojo (2007). Table 20 reviews the most recent CRFs used for each air quality endpoint and the valuation used.

3.4.4 Valuation of impacts

The valuation scheme used in the APMT health impacts model is explained in detail in Rojo (2007), with updated values per incidence presented in Table 20. Refer to Section 2.3.6 for more information regarding the origin of the distribution used for a value of a statistical life in the APMT skin cancer and air quality health impacts models.

Table 20: Concentration - response functions and valuations for air quality health impact analysis. Source: Brunelle-Yeung et al. (in preparation).

$PM_{2.5}$ – related endpoints	Risk increase (% per $\mu g.m^{-3}$ $PM_{2.5}$)	Value of a Statistical Incidence (U.S. Y2000 $)
Premature mortality: Long-term exposure (adults age 30+) Long-term exposure (infants age < 1 yr)	Triangular 1.0 (0.6 – 1.7) Triangular 0.7 (0.4 – 1)	Lognormal distribution with mean $6.3 M and standard deviation $2.8 M (5% - 95% CI : $2.9 - $12 M)
Chronic bronchitis	Triangular 1.5 (1.3 – 2.0)	Mean $0.34 M Distribution described in Supporting Information
Hospital admissions - respiratory	Triangular 0.2 (0.14 – 0.29)	Discrete distribution $15,647 (75%) $31,294 (25%)
Hospital admissions - cardiovascular	Triangular 0.16 (0.14 – 0.19)	Discrete distribution $18,387 (75%) $36,774 (25%)
Emergency room visits for asthma	Triangular 0.8 (0.6 – 1.1)	Discrete distribution $286 (75%) $572 (25%)
Minor Restricted Activity Days	Triangular 0.7 (0.6 – 0.9)	Discrete distribution $25 (25%) $52 (50%) $75 (25%)

3.4.5 Uncertainty analysis

The APMT air quality models use Monte Carlo simulations to account for uncertainty throughout the impact pathway. Parameters of the uncertainty distributions used in each step of the pathway have been discussed in Section 3.4 where applicable. These uncertainty parameters can be modified as desired by the user of the model. Depending on the uncertainties specified, confidence intervals on the outputs will be more or less broad. The ability to specify confidence intervals on the number of mortalities and other endpoints, along with their valuations, is especially useful to policymakers.

As discussed previously, when analyzing more than one scenario, we use paired Monte Carlo simulations. Monte Carlo distributions are generated once for the first scenario and reused for

subsequent scenarios in the scope of the same analysis. For more information on the use of paired Monte Carlo simulations, refer to the MIT S.M. thesis by Rojo (Rojo, 2007).

In Section 3.8, we present the uncertainty assessment of the speciated RSM model. Results of a global sensitivity analysis and a distributional sensitivity analysis reveal the factors which contribute most to the models' output uncertainty and which should be the focus of further research.

3.5 RSM- Speciated Model (RSM v2)

3.5.1 Overview of RSM v1 - Unspeciated

As an introduction to the improvements done to the RSM, we begin with some additional technical details on the unspeciated response surface model (RSM v1). The information presented here is meant to complement the overview given in 3.4.2.2. Full details on the RSM v1 can be found in Masek's MIT S.M. thesis (Masek, 2008). Key elements are reviewed here as they are also relevant to the RSM v2. Section 3.5.1 in its entirety references Masek (2008).

The idea behind the RSM's air quality modeling capabilities rests on linear regressions which are extracted from the statistical analysis of a more complex model, CMAQ. This high-fidelity model was sampled repeatedly for varying input settings. Through linear regressions, approximations of outputs otherwise obtained by CMAQ can be estimated by the RSM for any combination of inputs not sampled.

The 27 samplings of CMAQ done to develop the RSM v1 were meant to encompass the most likely aviation scenarios for the next 20 years. This was accomplished by first selecting a range over which the four independent parameters were most likely to fall, given possible aviation policy scenarios likely to be the subject of future health impact analyses. Second, a Halton low-discrepancy sequence (Halton, 1960) was used to uniformly sample the inputs for 27 representative high-fidelity simulations. This sampling method was selected for its ability to accept larger amounts of sample points without becoming unbalanced. In other words, more CMAQ runs can be made for additional sample points to complement the design space without having to redo the previous 27 runs. Table 21 presents the range of values for the four independent parameters. A list of input settings for the 27 CMAQ simulations, as defined by the design of experiments, is given in Appendix A of Masek (2008).

Table 21: Range of input settings for the four independent variables. A fuelburn multiplier setting of zero corresponds to a no-aviation case. Source: Masek (2008), Table 2.4.

Independent variable	Minimum	Maximum
Fuelburn multiplier	0.0	2.5
FSC multiplier	0.025	5.0
NO_x EI multiplier	0.7	1.1
nvPM EI multiplier	0.25	3.6

Notable particularities of the 27 CMAQ simulations are:

- Instead of a year-long simulation, four representative months were simulated: February, April, July and October 2001 with spin-up period of 5 days per month;
- CMAQ changes in concentration attributed to aircraft emissions were computed on an hourly cell-by-cell basis, then post-processed into a yearly average change in PM concentration;
- Background and meteorological data came from the U.S. EPAct study where NEI 2001 data with no aviation was used as background and meteorology was obtained from MM5 2001;
- Vertical profiles for each of the 325 airports followed one of three representative airport profiles: Atlanta (ATL), Chicago (ORD), and Providence (PVD).

The species retained in the measure of total $PM_{2.5}$ concentration in the RSM v1 were: ammonia, sulfates, nitrates, elemental carbon, organic carbon, and crustal material. Table 22 relates the PM components to the CMAQ species:

Table 22: PM components related to CMAQ species. Source: Masek (2008), Table 2.3.

PM component	CMAQ name	Component CMAQ species
Ammonia (NH4)	PM_AMM	ANH4I + ANH4J
Sulfates (SO4)	PM_SULF	ASO4I + ASO4J
Nitrates (NO3)	PM_NITR	ANO3I + ANO3J
Elemental carbon (EC)	PM_EC	AECI + AECJ
Organic carbon (ORG)	PM_ORG_TOT	AORGAI + AORGAJ + AORGBI + AORGBJ + 1.167×(AORGPAI + AORGPAJ)
Crustal material	PM_OTH	A25I + A25J

In RSM v1, a linear regression model unique to each grid-cell takes inventory multipliers and approximates changes in PM2.5 concentration due to aircraft emissions as per equation 12:

$$[PM_{2.5}] = \beta_1 \cdot FB\ multiplier + \beta_2 \cdot SO_x\ multiplier + \beta_3 \cdot NO_x\ multiplier + \beta_4 \cdot nvPM\ multiplier \qquad (12)$$

This first version of the RSM model yields a fit of approximate changes in $PM_{2.5}$ with R^2 values above 0.95 for 95% of cells (Masek, 2008). It should be noted however that two of the runs (RSM012 and RSM019) used in the development of the RSM v1 were flawed and yielded abnormal results. The two simulations were redone for RSM v2, however their results remained questionable and it is suspected that the emissions inventories used in these two CMAQ simulations are flawed. These two runs have been dropped for RSM v2, leading to much lower errors on all remaining runs.

3.5.2 Moving to a speciated RSM

Despite the close fit obtained with RSM v1 for total $PM_{2.5}$ changes in concentration, analysis of contributions per PM species revealed that the contribution from each species could not be obtained accurately with the single-equation structure. In effect, interactions between ammonium, NO_x, SO_x, and nvPM were not being well captured. To illustrate, we present a comparison of population weighted changes in concentration per PM species as estimated by the RSM v1 and by CMAQ:

Table 23: Relative contribution to total population weighted changes in concentration, per emission species, for baseline aviation, year 2005 inventory. Results obtained from the unspeciated RSM v1.

PM - Component	Percent contribution of nationwide yearly average ($\Sigma P \cdot \Delta C$)
Fuelburn: volPM-org and VOC	29 %
Sox: SO_2 and volPM-sulf	29 %
NOx	27 %
NvPM	14 %

Table 24: Relative contribution to total population weighted changes in concentration, per emission species, for baseline aviation, year 2005 inventory. Results obtained from CMAQ run "RSM 999."

PM - Component	Percent contribution of nationwide yearly average ($\Sigma P \cdot \Delta C$)
Organic particulate matter	3.4 %
Ammonium (NH4)	16 %
PM Nitrates	44 %
PM Sulfates	12 %
Elemental Carbon (EC)	24 %

It should be noted that ammonium (NH_4) is not a product of aircraft emissions. However, available ammonium in the atmosphere reacts with aircraft SO_x and NO_x to form secondary particulate matter, specifically ammonium-sulfates ($(NH_4)_2SO_4$) and ammonium-nitrates (NH_4NO_3). The CMAQ output of NH_4 ions included here is the amount which has reacted with nitrates and sulfates to form $PM_{2.5}$.

Without even considering the apportionment of ammonium to sulfates and nitrates, it is clear from the organics contributions shown in Table 23 and Table 24 that there is an inconsistency between the RSM approximation and CMAQ results. The RSM estimates that 29 % of health impacts are due

to organics (volatile PM organics and volatile organic compounds (VOC)), while the CMAQ simulation yielded a 3.4 % contribution from organics. A similar disagreement is observed for the other species, with a 14 % contribution from non-volatile PM (analogous to EC) with the RSM v1 model compared to a 24 % contribution from EC in CMAQ. The apportionment of health impacts to different PM constituents is useful to policymakers when analyzing impacts of a policy targeting a specific component. Therefore, a new RSM was developed such that each PM component was approximated independently. We now explain the choice of regression type used for the speciated model.

3.5.3 New speciated linear regression model – RSM v2

The air quality modeling in the RSM v2 consists of a set of five linear regression equations (equations 13-17) for each grid-cell in the U.S. domain. From the inputs of airport-by-airport emissions, a spatial interpolation scheme is used to determine the overall grid-cell multipliers for the four independent variables. The multipliers are determined by calculating the ratio of emissions for the given scenario over the emissions in the baseline aviation scenario, "RSM999" (Masek, 2008). The approximated NH_4 change in concentration is apportioned to sulfates and nitrates to form secondary PM. With computed changes in concentration of primary and secondary $PM_{2.5}$, changes in population exposure and associated health impacts are computed. This section presents the mechanics behind the speciated reduced order air quality model introduced in RSM v2 and highlights changes implemented in the APMT AQ model since RSM v1.

3.5.3.1 Linear behavior of change in concentration due to aviation

As was demonstrated by Masek (2008), changes in total $PM_{2.5}$ concentrations were approximately linear with aircraft contributions. This has been explained by the relatively small contribution of aircraft emissions compared to the background. Now, as a speciated RSM model is sought, we investigate whether linear regressions can be used to approximate the five CMAQ outputs: Organic particulate matter, Ammonium (NH_4), PM Nitrates, PM Sulfates, and Elemental Carbon (EC). An analysis was done on the relationship between each output and the four emissions multipliers. It was found through a series of patch plots that the relationship between EC and the nvPM multiplier is linear and that the response of PM Sulfates is almost linear with the SO_x multiplier but has a small dependence on the NO_x multiplier as well. The CMAQ results also revealed that the AMM and PM Nitrates changes in concentration were also linear with respect to the NO_x and SO_x multipliers. As a

result, the sum of secondary nitrates and secondary sulfates (AMM + PM Sulfates + PM Nitrates) was also linear. The change in concentration of PM Organics appears to be approximately linear with fuelburn and NO_x. The following patch plots (Figure 13) demonstrate this observed linearity. A linear function of two variables will be a planar surface. The plots shown are cross-sectional cuts of the surface, at a view that shows the most linearity possible. Non-linearities are shown as jagged edges protruding from the main surface.

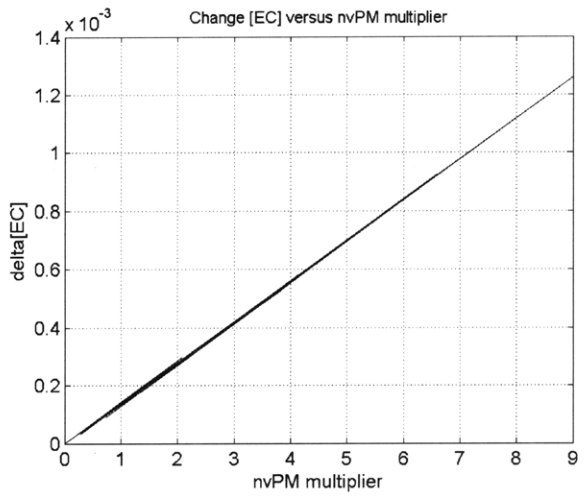

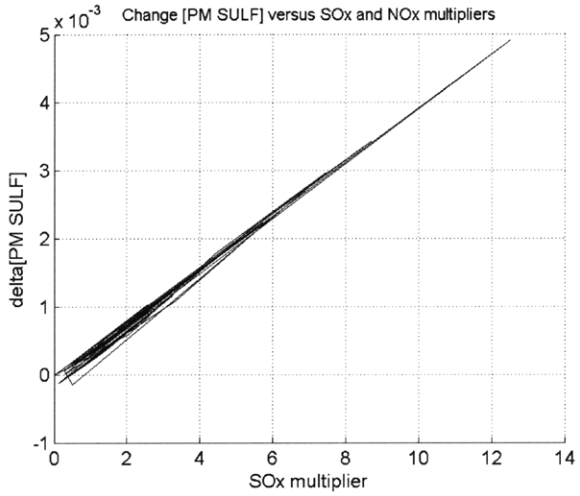

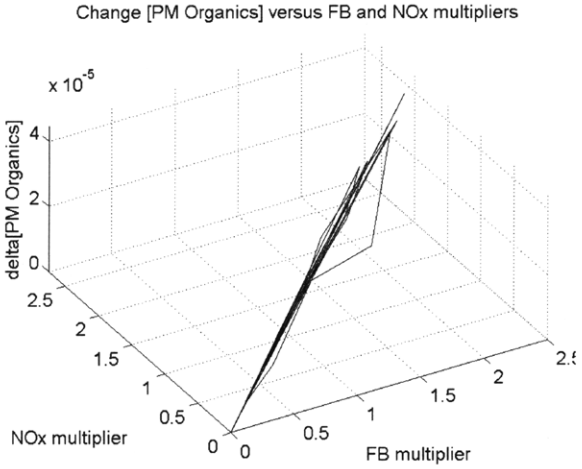

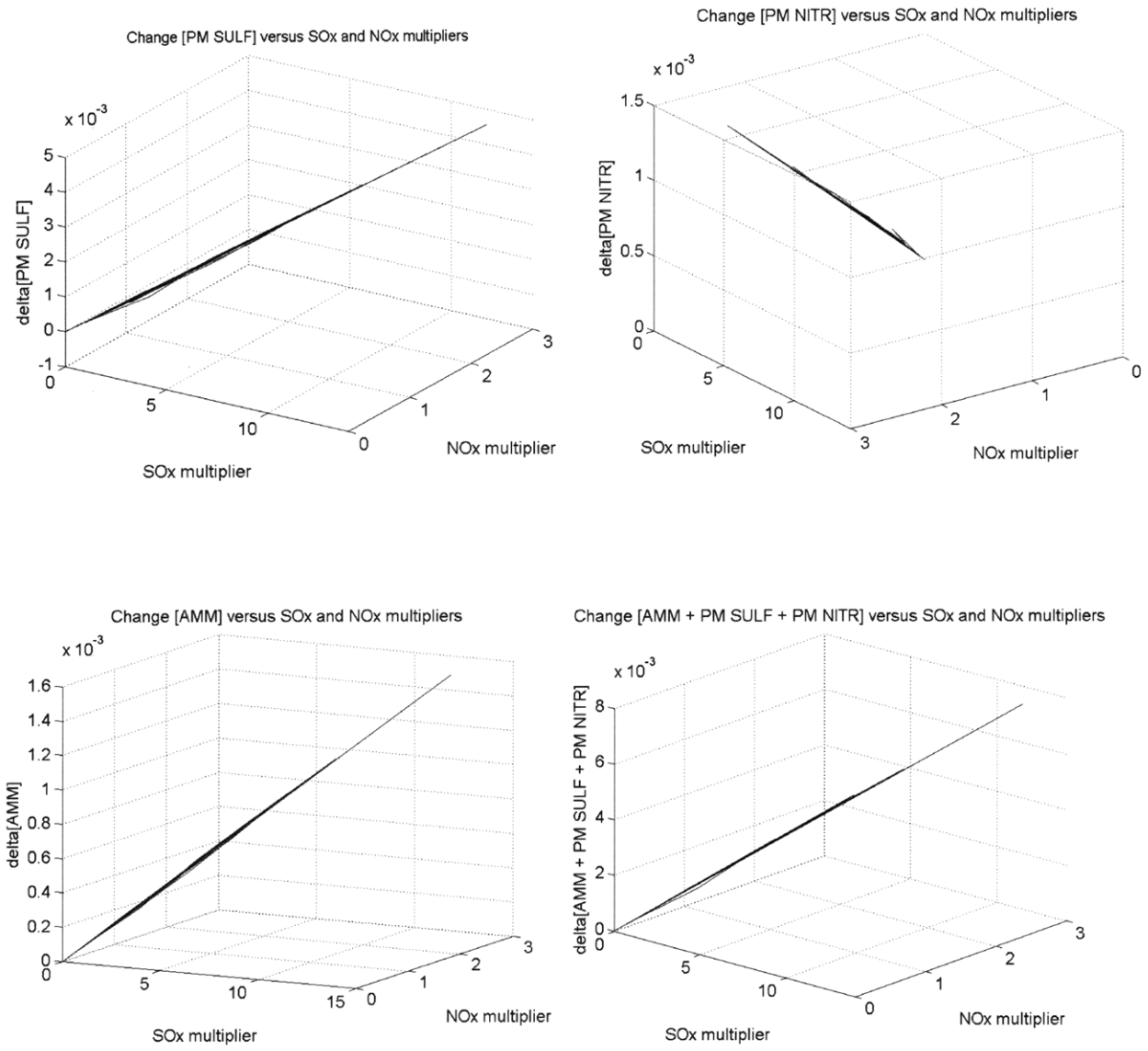

Figure 13: Patch plots of CMAQ results over all 27 simulations. Changes in PM concentration per species versus emissions multipliers. A linear function over one variable is a line; a linear function over two variables is a plane. Linearity is demonstrated for all species.

The plots in Figure 13 demonstrate that the five CMAQ outputs can effectively be approximated by linear regressions over the four independent emissions multipliers, as follows:

$$[PM\ org] = \beta_1 \cdot FB\ multiplier + \beta_2 \cdot SO_x\ multiplier + \beta_3 \cdot NO_x\ multiplier + \beta_4 \cdot nvPM\ multiplier \quad (13)$$

$$[AMM] = \beta_1 \cdot FB\ multiplier + \beta_2 \cdot SO_x\ multiplier + \beta_3 \cdot NO_x\ multiplier + \beta_4 \cdot nvPM\ multiplier \quad (14)$$

$$[PM\ nitrates] = \beta_1 \cdot FB\ multiplier + \beta_2 \cdot SO_x\ multiplier + \beta_3 \cdot NO_x\ multiplier + \beta_4 \cdot nvPM\ multiplier \quad (15)$$

$$[PM\ sulfates] = \beta_1 \cdot FB\ multiplier + \beta_2 \cdot SO_x\ multiplier + \beta_3 \cdot NO_x\ multiplier + \beta_4 \cdot nvPM\ multiplier \quad (16)$$

$$[EC] = \beta_1 \cdot FB\ multiplier + \beta_2 \cdot SO_x\ multiplier + \beta_3 \cdot NO_x\ multiplier + \beta_4 \cdot nvPM\ multiplier \quad (17)$$

Chemically speaking, the known interactions and dependencies between PM components and the four independent variables are shown in Table 25:

Table 25: Known dependencies between CMAQ outputs, i.e. $PM_{2.5}$ components and the four independent variables. NO_x and nvPM are used in lieu of inventory NO_x EI, and inventory nvPM EI, respectively. SO_x refers to inventory fuel sulfur content, due to the direct proportionality.

PM - Component	Known interactions/dependencies with:	Description of interaction/dependency
Organic particulate matter	Fuelburn NO_x	Amounts of unburnt and partially-burnt hydrocarbons (HC) (volatile organic compounds, soot) increases with increasing fuelburn. NO_x EI has an impact on primary (POA) and secondary organic aerosols (SOA) (Woody, 2009, Lane et al., 2008).
Ammonium (NH_4)	SO_x NO_x	NH4 in the atmosphere reacts with SO_4 and NO_3 to form ammonium-sulfate and ammonium-nitrate
PM Nitrates	NO_x SO_x nvPM	The amount of NO_3 ions in aerosol form (given by ANO3I + ANO3J) in CMAQ corresponds to fully reacted nitrates with NH_4. There is a dependency with the amount of NH_4 left over after it has reacted with sulfates. Also, EC (i.e. nvPM) can have small effects on nitrate formation due to its alteration of aerosol optical depth.
PM Sulfates	SO_x NO_x	The amount of SO_4 ions in aerosol form (given by ASO4I + ASO4J) in CMAQ corresponds to fully reacted sulfates with NH_4. There is a dependency with the amount of NH_4 available in the environment at a specific geographic location, which depends on NO_x in certain areas. The amount of PM Sulfates depends on the amount of SO_x emissions produced, i.e. fuel sulfur content.
Elemental Carbon (EC)	nvPM	Non-volatile PM consists of EC, dust and metals. It is not chemically reactive and comes directly out of the engine.

In theory, if the interdependencies summarized in Table 25 are complete, the linear regressions for each PM2.5 species would be of the form:

$$[PM\ org] = \beta_1 \cdot FB\ multiplier + \beta_2 \cdot NO_x\ multiplier \quad (18)$$

$$[AMM] = \beta_1 \cdot SO_x\ multiplier + \beta_2 \cdot NO_x\ multiplier \quad (19)$$

$$[PM\ nitrates] = \beta_1 \cdot NO_x\ multiplier + \beta_2 \cdot SO_x\ multiplier + \beta_3 \cdot nvPM\ multiplier \quad (20)$$

$$[PM\ sulfates] = \beta_1 \cdot SO_x\ multiplier + \beta_2 \cdot NO_x\ multiplier \quad (21)$$

$$[EC] = \beta_1 \cdot nvPM\ multiplier \quad (22)$$

In practice, by doing regressions on a cell-by-cell basis for each of the five species over the four independent variables, the regression parameters (β's) for variables not shown in equations 18-22 did not exactly go to zero. Indeed, fits with regressions over all four parameters (equations 13-17) yielded better approximations than regressions over limited variables (equations 18-22). This can be explained by the presence of other complex interactions within CMAQ as well as statistical noise. Nonetheless, the choice of limiting the number of variables to those with physical significance or using the full regression over all four parameters is left to the user. Results presented in the following sections use equations 18 – 22 where we have limited the variables to those with known interactions.

3.5.3.2 Apportionment of ammonium to secondary sulfates and nitrates

Once approximated changes in concentration of AMM, EC, PM SULF, PM NITR and PM ORG due to aircraft emissions are calculated, an apportionment of the AMM to secondary nitrates and secondary sulfates is necessary in order to determine which proportion of health impacts is due to which type of secondary PM. The apportionment is done based on the mechanics of the ISORROPIA model, used in CMAQ (Nenes et al., 1998).

SO_4^{-2} and NO_3^{-1} ions produced from aircraft emissions contribute to $PM_{2.5}$ in the form of secondary PM when they are neutralized by NH_4, becoming $(NH_4)_2SO_4$ and NH_4NO_3, respectively. The available ammonium in the atmosphere depends on many factors such as geographic location and humidity. The reactive preference of ammonium for sulfates over nitrates depends on ambient relative humidity, temperature, sulfate ratio, and sodium ratio. Only if there is ammonium left over after having reacted with sulfates, then NH_4NO_3 will form (EPA, 2004b). This preference has been captured by the ISORROPIA model (Nenes et al., 1998). The CMAQ species PM_NITR (ANO3I + ANO3J) represents nitrate ions which have been neutralized by NH_4. In the case where NH_4NO_3 forms, the ISORROPIA "aerosol type" is considered to be "sulfate poor" (Nenes et al., 1998). As per the model, on an hour-by-hour basis, there should be full neutralization of ANO3 and ASO4 by AMM. Following stoichiomety, equation 23 is true on an hourly basis (concentrations in $\mu g/m^3$):

$$[AMM] = 2 \cdot [SO_4] \cdot \frac{\text{Mol Mass}_{NH_4}}{\text{Mol Mass}_{SO_4}} + [NO_3] \cdot \frac{\text{Mol Mass}_{NH_4}}{\text{Mol Mass}_{NO_3}} \qquad (23)$$

However, because we are interested in yearly averaged changes in concentration, we find that the yearly changes do not exactly correspond to full neutralization as seen in equation 23. Therefore, an apportionment of the yearly averaged AMM concentration is done as follows:

- If there is NO_3 present, attribute enough of the AMM to fully neutralize it;
- Give the remaining AMM to SO_4;
- Compute the exceeding SO_4 concentration and assume that it also contributes to $PM_{2.5}$ in the form of H_2SO_4;
- Add H_2 ions to the remaining SO_4 ions.

The result is a yearly averaged change in $PM_{2.5}$ concentration, broken down in four categories:

1) Elemental carbon (non-volatile primary PM),
2) Organic PM (from volatile organic PM or VOCs),
3) Ammonium-nitrate (NH_4NO_3),
4) Ammonium-sulfate ($(NH_4)_2SO_4$) and sulfuric acid (H_2SO_4).

For the baseline aviation case (RSM Run999), the domain-averaged concentration of AMM missing for a full neutralization of SO_4 and NO_3 ions represents approximately 13 % of the total $PM_{2.5}$ concentration using the above apportionment scheme. However, the population-weighted change in concentration (dC·P) between the full neutralization and the APMT apportionment scheme differs by only 1 %. One can conclude that the difference in terms of health impacts is negligible.

The jagged edges in the PM Organics patch plot shown in Figure 13 were entirely due to CMAQ RSM012 and RSM019 runs. The results of these two runs were clear outliers in terms of the PM Organics species. It was found that the inventories of RSM012 and RSM019 were flawed for one month out of four representative months. Considering that the multipliers for these two runs were not at the limits of the range described by the DOE, results consistent with the general linear trends shown by the other 25 simulations were be expected. Patch plots of all species as shown in Figure 13, but without runs RSM012 and RSM019 can be found in Appendix G. The omission of these two runs significantly reduces the error between RSM results and CMAQ results. Therefore, RSM v2 regressions are done over 25 CMAQ simulations with the omission of RSM012 and RSM019. From this point forward, we shall use "RSM v2a" to refer to the preliminary and less accurate version of the speciated RSM based on all 27 CMAQ runs and a full regression over all 4 variables. "RSM v2" refers to the current model with 25 CMAQ runs and a regression on a limited set of variables.

Figure 14 presents the four components' population-weighted change in concentration (dCP) summed over the entire domain. dCP is directly proportional to health impacts. Error analyses between the RSM v2 approximations and the CMAQ results are presented in the right hand column for each species, per run. The RSM v2 prediction errors for EC dCP do not exceed 3.4 % in magnitude for any of the 25 runs. For secondary nitrates, the percent error does not exceed 8.2 % in magnitude. For secondary sulfates, the magnitude of the error does not exceed 15 % for any of the runs. The magnitude of the error attributed to PM Organics does not exceed 11.4 %. When looking at total $PM_{2.5}$, RSM v2 results for all runs are within the ± 3.5 % error range from CMAQ results.

The R^2 values of a linear model provide a measure of linearity. The R^2 values for the RSM v2a, in order of linearity, were: $R^2_{PM\ SULF} = 0.981$, $R^2_{EC} = 0.969$, $R^2_{AMM} = 0.946$, $R^2_{PM\ ORG} = 0.820$, $R^2_{PM\ NITR} = 0.782$. PM Nitrates displayed the least linearity, followed by PM Organics. The R^2 values for the current RSM v2, in order of linearity, are: $R^2_{EC} = 0.997$, $R^2_{PM\ SULF} = 0.997$, $R^2_{AMM} = 0.969$, $R^2_{PM\ NITR} = 0.811$, $R^2_{PM\ ORG} = 0.750$. PM Organics displayed the least linearity, followed by PM Nitrates. The non-linearities associated with PM Nitrates are due to the complex equilibrium equations within the ISORROPIA model. These equations determine the formation of secondary nitrates based on available ambient ammonium, reactions with sulfates (which also depend on sodium availability), humidity, and other factors. In the case of organics, as was mentioned, the non-linearities are due to HC EI variable not being represented.

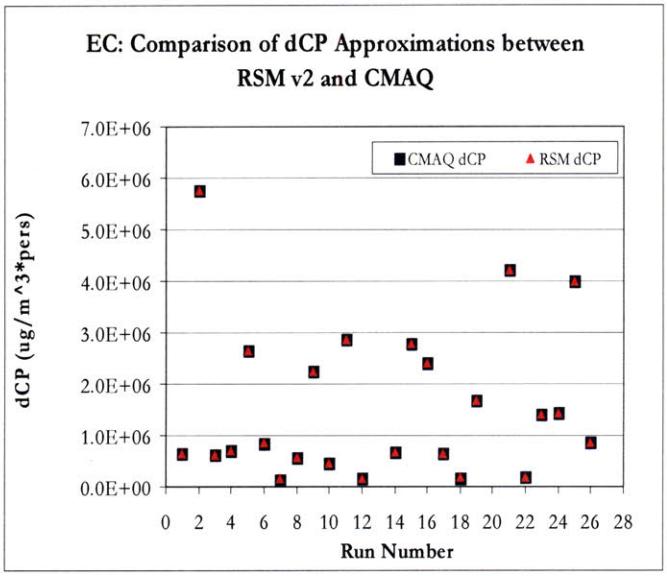
EC: Comparison of dCP Approximations between RSM v2 and CMAQ
CMAQ dCP
RSM dCP
dCP (ug/m^3*pers)
7.0E+06
6.0E+06
5.0E+06
4.0E+06
3.0E+06
2.0E+06
1.0E+06
0.0E+00
0 2 4 6 8 10 12 14 16 18 20 22 24 26 28
Run Number

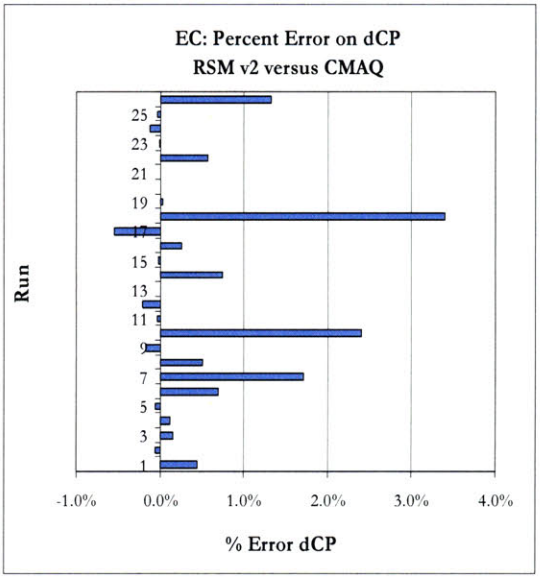
EC: Percent Error on dCP RSM v2 versus CMAQ
Run
25
23
21
19
17
15
13
11
9
7
5
3
1
-1.0% 0.0% 1.0% 2.0% 3.0% 4.0%
% Error dCP

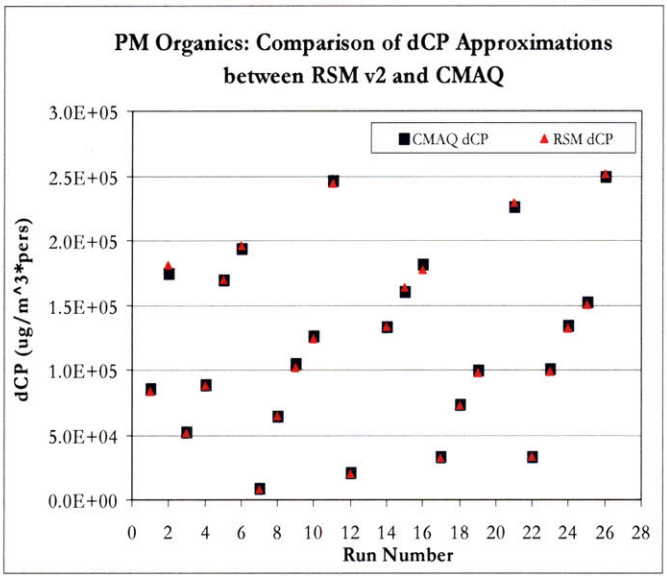
PM Organics: Comparison of dCP Approximations between RSM v2 and CMAQ
CMAQ dCP
RSM dCP
dCP (ug/m^3*pers)
3.0E+05
2.5E+05
2.0E+05
1.5E+05
1.0E+05
5.0E+04
0.0E+00
0 2 4 6 8 10 12 14 16 18 20 22 24 26 28
Run Number

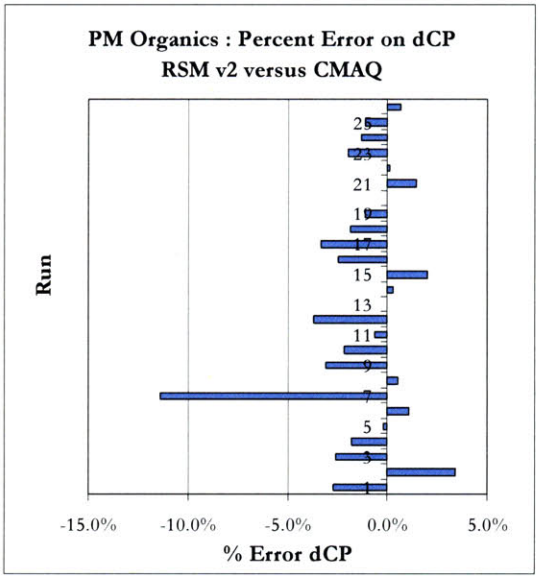
PM Organics : Percent Error on dCP RSM v2 versus CMAQ
Run
25
23
21
19
17
15
13
11
9
7
5
3
1
-15.0% -10.0% -5.0% 0.0% 5.0%
% Error dCP

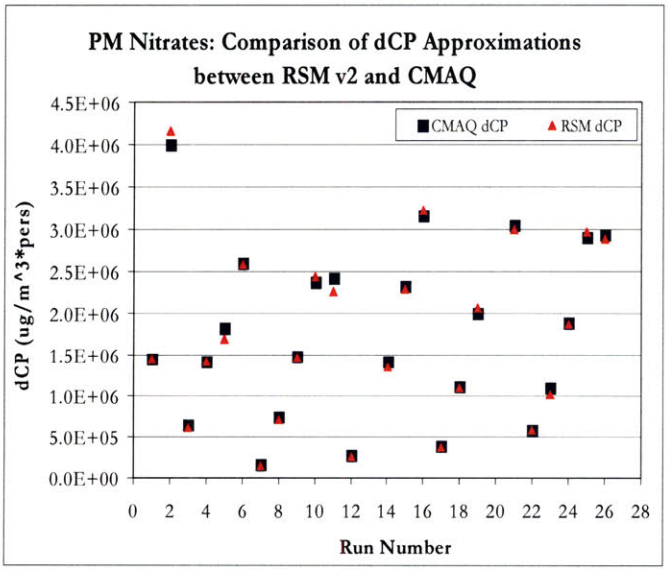
PM Nitrates: Comparison of dCP Approximations between RSM v2 and CMAQ
CMAQ dCP
RSM dCP
dCP (ug/m^3*pers)
4.5E+06
4.0E+06
3.5E+06
3.0E+06
2.5E+06
2.0E+06
1.5E+06
1.0E+06
5.0E+05
0.0E+00
0 2 4 6 8 10 12 14 16 18 20 22 24 26 28
Run Number

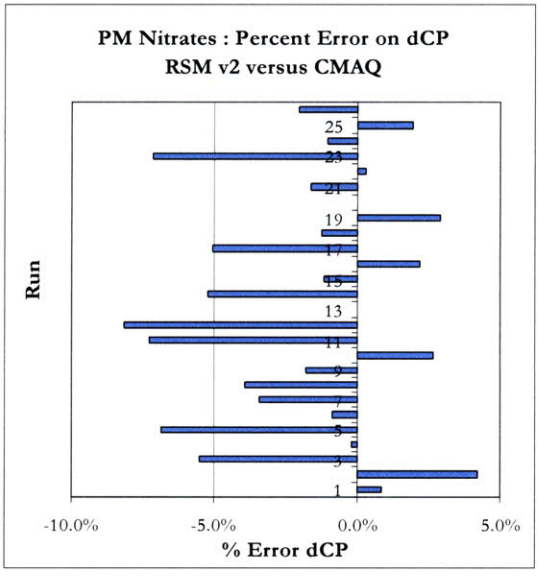
PM Nitrates : Percent Error on dCP RSM v2 versus CMAQ
Run
25
23
21
19
17
15
13
11
9
7
5
3
1
-10.0% -5.0% 0.0% 5.0%
% Error dCP

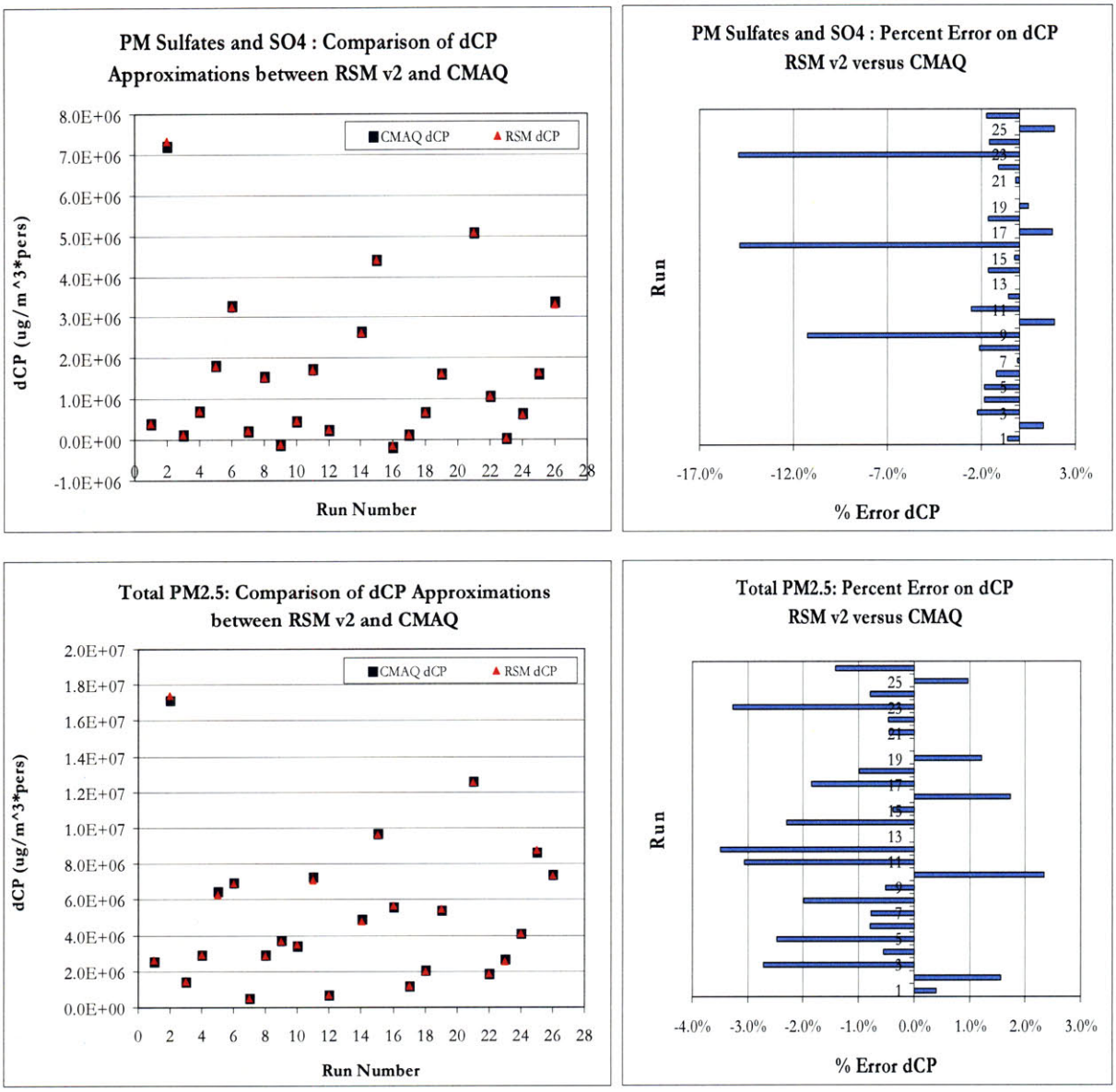

Figure 14: Left hand column: Population-weighted changes in concentration (dCP) per species obtained by CMAQ and RSM v2. Right hand column: Error analysis on RSM v2 dCP per run versus CMAQ dCP. Results are shown for 25 CMAQ runs.

3.5.3.3 Other changes from RSM v1

Besides the implementation of a speciated linear regression model, a few updates were introduced into the RSM v2. An overview of these changes is given in this section.

In RSM v2, fractional impacts from each $PM_{2.5}$ species are obtained from actual approximated changes in population weighted concentrations. In RSM v1, fractional impacts were approximated using the ratio of β's in the total $PM_{2.5}$ equation (equation 12).

New in the RSM v2 is the application of a fuel sulfur content distribution based on new PQIS data, as presented in Section 3.4.1. This variability distribution is applied to the FSC value assumed in the emission inventory of the given scenario. The user specifies the FSC content assumed and has the option of applying the distribution or not. This distribution arises from natural sulfur content variability between crude oil sources, and the processing of jet fuel between refineries worldwide. In scenarios such as an ultra-low sulfur jet fuel standard (ULS), the type of FSC distribution to be expected is unknown.

Another modification made to the RSM consists of the removal of Monte Carlo simulations for the parameters of the spatial interpolation. The spatial interpolation derives emission grid-cell multipliers when a grid-cell includes more than one airport (Masek, 2008). In RSM v1, parameters α and β were sampled independently and each Monte Carlo simulation used a combination of these parameters. Parameters α and β followed discrete distributions where α had 0.5 probability of being 0 or 1, and β had 0.25 probability of being 1, 2, 3, or 9. As explained by Masek (2008), different combinations of α and β represent different interpolation methods. For example, a combination of $\alpha = 1$ and $\beta = 0$ corresponds to using a weighted average method, a combination of $\alpha = 0$ and $\beta = 1$ corresponds to using an inverse distance method, and a combination of $\alpha = 0$ and $\beta = \infty$ corresponds to using a nearest neighbor method. Rather than sampling combinations of α's and β's, the code has been modified such that the spatial interpolation method is set by the user. The results presented in the following sections were obtained with a setting of $\alpha = 1$ and $\beta = 1$.

Finally, the distribution of the value of a statistical life (VSL) was updated as described in Section 3.4.4. The distribution is now lognormal instead of normal.

3.6 Comparison of the iF model and the RSM v2 model

3.6.1 Applicability for air transportation assessments

The iF model was derived from source-receptor matrices which were developed for ground-level mobile sources using outputs from the Climatological Regional Dispersion Model (CRDM) (Greco et al., 2007). An advantage of the RSM is its consideration of the vertical profile of aircraft emissions. Similarly, because the RSM's foundation consists of CMAQ simulations, more complex chemical interactions are considered. For example, the RSM approximates the ISORROPIA model's NH_4 apportionment in the formation of ammonium-sulfate and ammonium-nitrate; the iF model uses separate intake fractions for nitrates, sulfates, and bounce-back to approximate the preferential neutralization of sulfates over nitrates by NH_4.

As we have discussed, the linear response of $PM_{2.5}$ to aircraft emissions is due to the relatively small contribution of aviation compared to the background which includes all other anthropogenic pollution. Linearity is observed in both models.

3.6.2 Regionality and resolution

The resolution offered by the iF model is at the county-level. The resolution of the RSM is at a 36 km × 36 km grid-cell-level. There are areas where the RSM has a finer resolution than that of the iF and vice versa. It should also be considered that the RSM is best suited for national level policies. From Section 3.4.2.2, the training runs on which the RSM is built had nation-wide changes in emission multipliers. Therefore, for regional-level policies, uncertainty is being introduced when using the RSM (Masek, 2008).

3.7 Results – Air quality health impacts of aviation

3.7.1 Impacts of aviation in the U.S., year 2005

In this section we present the results of an analysis looking at the air quality health impacts of aviation in the U.S. for year 2005 inventories. Our analysis is based on landing, take-off and taxi (LTO) aircraft emissions below an assumed mixing height of 3000 feet above ground level.

3.7.1.1 Emissions Inventory

The emissions inventory used in this study was generated with the FAA Aviation Environmental Design Tool Emissions Dispersion Modeling System (AEDT/EDMS) (refer to Section 3.4.1). EDMS was used to calculate the non-volatile PM (nvPM), volatile PM derived from sulfur ($nvPM_{sulfur}$) and from organics ($nvPM_{organics}$), NO_x, SO_x, and volatile organic compounds (VOC) produced during the LTO cycle for 325 airports in the continental U.S. using FOA 3 approximations. The operations at these airports account for 95% of commercial aviation activity in the U.S.. Fifteen of the airports had zero inventories, leaving the total number of airports included in this study at 310. The inventory used for this section is the same as the 2005 baseline aviation scenario used for the RSM development ("RSM999"), but with a correction to the nvPM emissions species due to an error in the assumed bypass ratio for the initial inventory used by Masek (Masek, 2008). The emissions inventory pre-bypass ratio correction had approximately 3.1 times more nvPM emitted per year than the post-bypass ratio corrected inventory. All other species remained unchanged.

Table 26: Estimated national aircraft emissions in kT per year, including characterization of uncertainty for baseline aviation, Y2005.

	NO_x	SO_x	Primary $PM_{2.5}$
AEDT/EDMS deterministic inventories (in kT per year)	75	10	0.47
Corrected inventories accounting for modeling uncertainties (2.5% - 97.5% percentile range)	77 (63 – 91)	8.7 (0.52 – 27)	0.60 (0.26 – 0.94)

In total, aircraft from the 310 selected airports in the continental U.S. emitted approximately 600 tonnes of primary $PM_{2.5}$, 10,000 tonnes of SO_2 and 77,000 tonnes of NO_x in 2005 below 3,000 feet

altitude. Table 26 presents estimated national aircraft emissions, both deterministically and following the application of emission inventory uncertainties based on ICAO times-in-mode (Rojo, 2007).

3.7.1.2 RSM v2 Results

Using the RSM v2, the population-weighted change in $PM_{2.5}$ concentration across the U.S. domain due to subsonic aviation in 2005 was approximately 2.2 x 10^6 μg-people/m^3. The increase in adult premature mortalities due to this change in concentration is estimated at 210 deaths per year (90% confidence interval: 130 - 340) (Table 27). The monetized value of the mortality and morbidity effects using RSM v2 outputs is estimated at $1.4 billion in year 2000 US dollars (90% confidence interval: $550 million, $2.8 billion). Of these total impacts, 4 % are found to stem from emissions of volatile organic compounds and volatile particulate matter from organics, another 12 % from emissions of sulfur dioxide and volatile particulate matter from sulfur, 70 % from nitrogen oxide emissions, and 14% from non-volatile particulate matter emissions (Table 28).

Table 27: US nationwide health impact of aviation-related PM2.5

PM – related endpoints	**Health impacts In cases per year (5% – 95% CI)**		**Monetized impacts In Millions U.S. Y2000 $ (5% – 95% CI)**	
Model	**iF**	**RSM v2**	**iF**	**RSM v2**
Premature mortality: Long-term exposure (adults age 30+)	470 (190 – 930)	210 (130 – 340)	3,000 (790 – 7,800)	1,400 (510 – 2,700)
Long-term exposure (infants age < 1 yr)	3.1 (1.3 – 6.1)	1.4 (0.89 – 2.1)	20 (5.3 – 51)	9.0 (3.5 – 18)
Chronic bronchitis	190 (84 – 350)	86 (60 – 120)	65 (5.7 – 290)	30 (4.3 – 94)
Hospital admissions - respiratory	140 (58 – 260)	62 (40 –92)	2.7 (0.95 – 6.5)	1.2 (0.66 – 2.3)
Hospital admissions - cardiovascular	140 (61 – 250)	63 (44– 89)	3.2 (1.2 – 7.4)	1.4 (0.84 – 2.7)
Emergency room visits for asthma	270 (120 – 500)	120 (82 – 180)	0.096 (0.034– 0.23)	0.04 (0.02– 0.08)
Minor Restricted Activity Days	180,000 (81,000 – 340,000)	83,000 (59,000 – 120,000)	9.3 (2.7 – 21)	4.2 (1.7 – 7.4)
TOTAL DAMAGES			**3,100 M U.S. Y2000$ (1,000 – 6,700)**	**1,400 M U.S. Y2000$ (550 – 2,800)**

Table 28: Apportionment of impacts to EC, PM Sulfates, PM Nitrates, PM Organics from aviation, computed using the RSM model. Note that PM Sulfates represents changes in $(NH4)_2SO_4$ and H_2SO_4 and PM Nitrates represents changes in NH_4NO_3.

	EC	PM Sulfates	PM Nitrates	PM Organics
Contribution to health damages in Million U.S. Y2000 $ per year	200 (14%)	170 (12%)	980 (70%)	57 (4.0%)

The geographic distribution of changes in PM from the different species can be seen in Figure 15 where changes in concentration (dC) are shown over the U.S. domain. Secondary nitrates from aviation are located mostly in the Eastern U.S. and in California. Contributions from PM Sulfates are mostly observed in the South and in the Southern California. Elemental carbon impacts are mostly located in the North-East. PM organics are localized in the vicinity of airports, with highest contributions around large airports. Similar maps of EC and PM organics on a finer scale can be found in Appendix H.

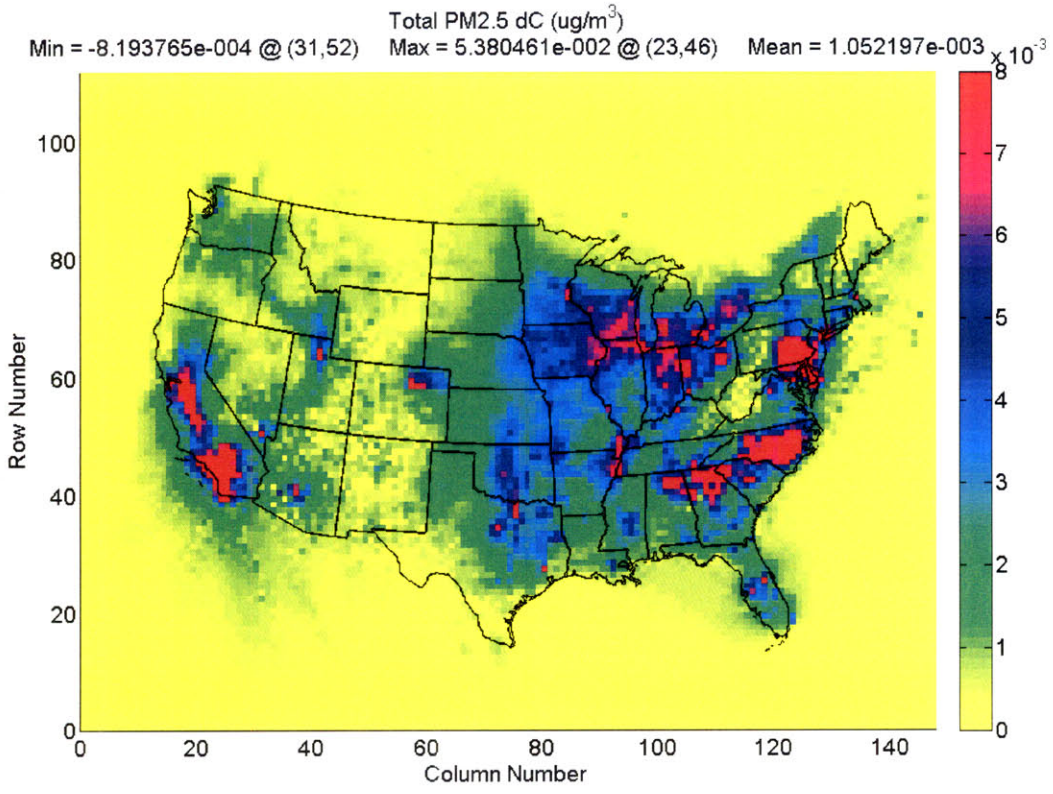

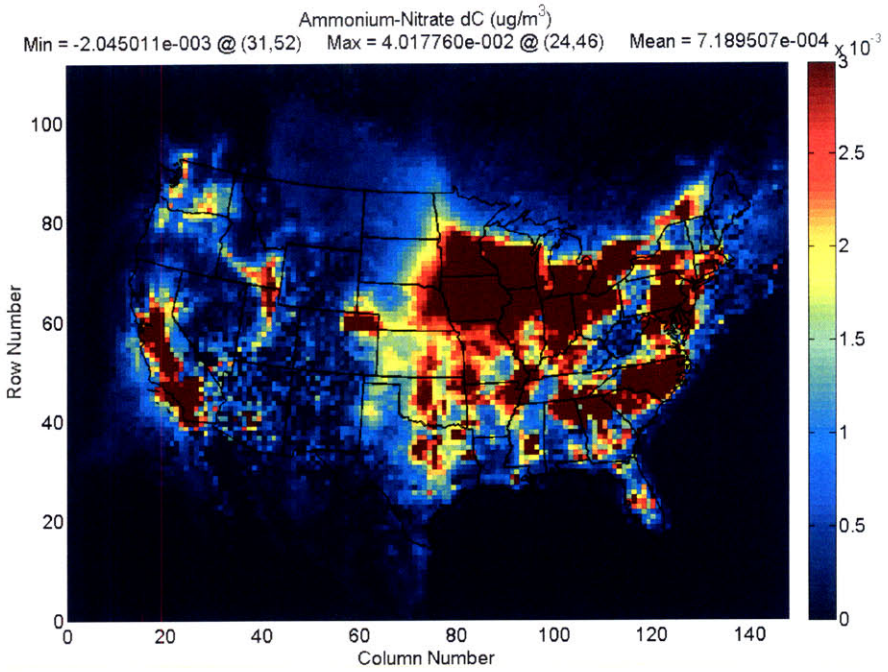
Ammonium-Nitrate dC (ug/m3)
Min = -2.045011e-003 @ (31,52) Max = 4.017760e-002 @ (24,46) Mean = 7.189507e-004
x 10-3
Row Number
Column Number
0
20
40
60
80
100
120
140
0
0.5
1
1.5
2
2.5
3

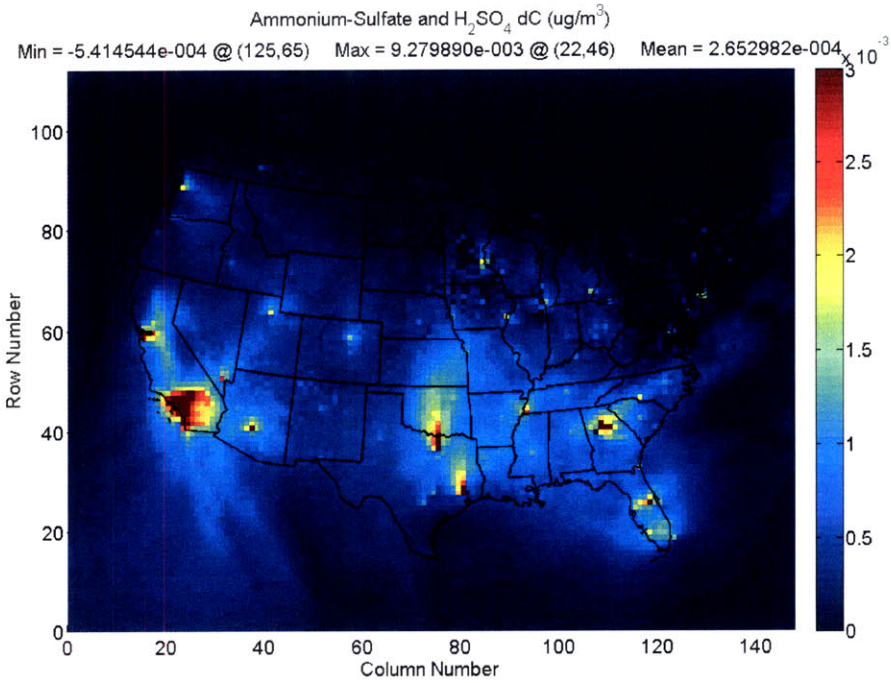
Ammonium-Sulfate and H2SO4 dC (ug/m3)
Min = -5.414544e-004 @ (125,65) Max = 9.279890e-003 @ (22,46) Mean = 2.652982e-004
x 10-3
Row Number
Column Number
0
20
40
60
80
100
120
140
0
0.5
1
1.5
2
2.5
3

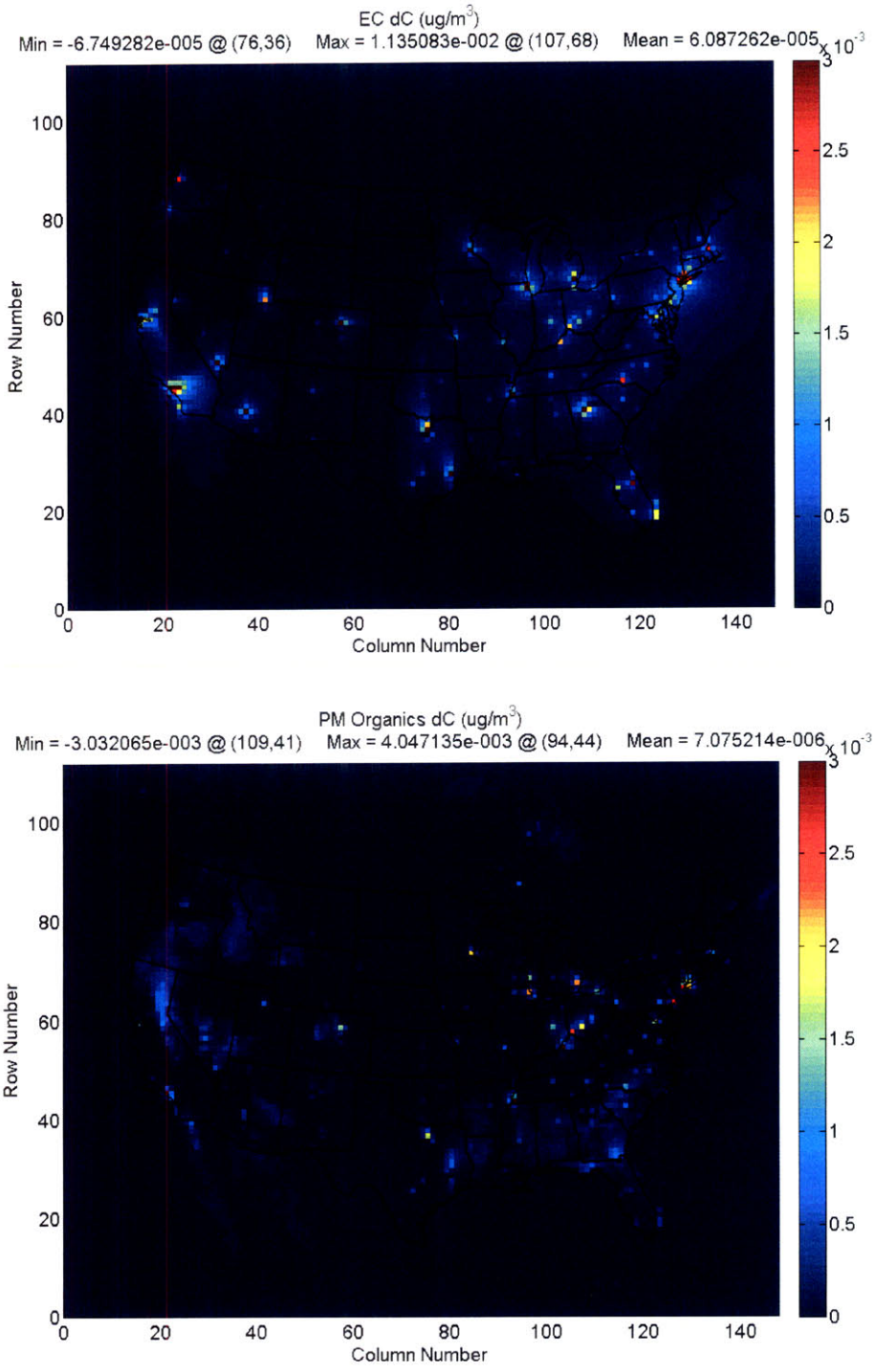

Figure 15: Maps of change in concentration (dC, μg/m^3) with respect to the background for baseline aviation, year 2005. From top to bottom, species shown are: total $PM_{2.5}$, ammonium-nitrate, ammonium-sulfate and H_2SO_4, elemental carbon, and organic particulate matter. Note that the total $PM_{2.5}$ plot (top) uses a different colormap scale.

3.7.1.3 iF Results

In comparison, using the iF values derived from the S-R matrix, the product of population and marginal change in pollutant concentration is 5.1 x 10^6 μg-people/m^3, approximately a factor of two higher than the value obtained using the RSM. Consequently, health impacts estimates from the iF model are approximately a factor of two higher than those from the RSM, as demonstrated in Table 27.

Marginal damages per ton of emissions can be calculated for each individual airport using the iF results. By understanding which pollutants dominate at an airport-level and which have the highest marginal cost, policymakers can better evaluate future policies aimed at controlling these pollutants. The emissions-weighted average intake fractions across U.S. airports are 7.0 x 10^{-6} for primary $PM_{2.5}$, 1.5 x 10^{-6} for secondary sulfate from SO_2, 2.8 x 10^{-7} for secondary nitrate from NO_x, and -3.4 x 10^{-7} for secondary nitrate from SO_2 (related to the "bounce-back" effect, in which emissions of SO_2 may result in a decrease in secondary nitrate formation, given the preferential reaction of ammonium with sulfate over nitrate). The unweighted average intake fractions are 3.7 x 10^{-6} for primary $PM_{2.5}$, 8.3 x 10^{-7} for secondary sulfate from SO_2, 1.6 x 10^{-7} for secondary nitrates from NO_x and -1.9 x 10^{-7} for the bounce-back effect (secondary nitrate from SO_2). The somewhat greater values given emissions weighting reflects the fact that emissions are higher at larger airports, which are proximate to larger downwind populations and therefore have higher intake fractions (Brunelle-Yeung et al., In preparation).

Table 29 presents the relative contribution of each type of particulate matter to total damages using the iF values, along with national average marginal damage functions for the three emitted species. As in the RSM outputs, secondary particulate matter contributes a majority of the health effects, with secondary nitrate contributing to 54% of the total damages on average and secondary sulfate contributing to 33% of the total damages on average.

Table 29: Relative importance of primary fine particulate matter, ammonium-sulfate, and ammonium-nitrate, computed using the iF model[7]

	Primary $PM_{2.5}$	**Ammonium-Sulfate (SO_x Emissions)**	**Ammonium-Nitrate (NO_x Emissions + Nitrate Bounce-back)**
Contribution to health damages in U.S. Y2000 M $	360 (13 %)	1,100 (33 %)	1,600 (54 %)
	Primary $PM_{2.5}$	**SO_x Emissions (Amm-Sulfate + Nitrate Bounce-back)**	**NO_x Emissions (Secondary Nitrate)**
Marginal damages in $ per tonne emitted (5%-95% CI)	600,000 (200,000 – 1,400,000)	96,000 (26,000 – 240,000)	24,000 (6,000 – 65,000)

3.7.1.4 Spatial Patterns

The intake fraction values can be used to study regional variations, identifying pollutants from any individual airport contributing most to impacts at the national level. Figure 16 presents on a county basis the type of pollutant having the largest impact on total national aggregate health impacts, as emitted by that county. Out of the 310 airports considered, 59 % of them had health effects dominated by secondary nitrates, with 39 % dominated by secondary sulfates and 2 % by primary $PM_{2.5}$. For certain Northeastern airports in this region and a few coastal counties elsewhere, primary $PM_{2.5}$ and ammonium sulfate impacts dominate. The few airports dominated by primary $PM_{2.5}$ were in coastal regions. As can be seen, secondary nitrate intake fractions are lower in the Northeastern U.S. (Greco et al., 2007). This is explained by low ambient concentrations of ammonia (NH_4) and high ambient sulfate concentrations, combined with the natural transport of aircraft plumes towards the Atlantic Ocean. Consequently, secondary sulfates were most significant in non-urban areas of the Northeastern U.S..

[7] Values represent mean health damages and mean proportion of total damages, which will not be directly proportional due to non-linear uncertainty propagation. Note that the "nitrate bounce-back" effect is attributed to secondary nitrate concentrations in the first row but SO_2 emissions in the second row.

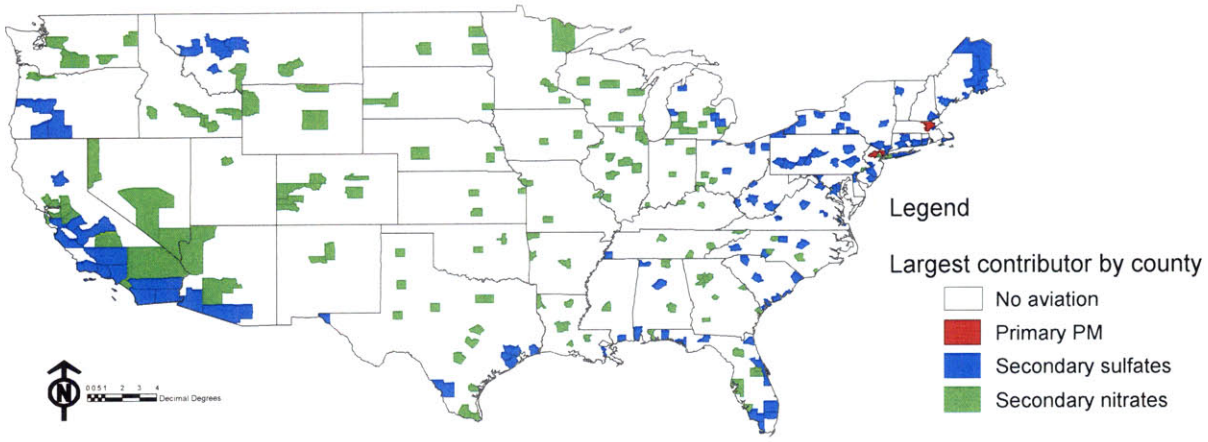

Figure 16: Largest contributor to total national aggregate health impacts of aviation by source county. The shaded counties represent the 310 airports evaluated within the intake fraction analysis.

The speciated RSM v2 model outputs can also be used to glean information on the spatial patterns by pollutant species. While the intake fraction by definition gives pollutant contributions to total national aggregated health impacts, the RSM can be used to determine which pollutant contributes to the largest change in $PM_{2.5}$ concentration on a grid-cell basis. We recall that the contribution by species on total nationwide health impacts also depends on the population in the given cell, a quantity included in the intake fraction (dC·P). If we are interested in looking spatial patterns of concentrations, Figure 17 provides insight on a cell-by-cell level of the type of pollutant contributing the most to changes in $PM_{2.5}$ concentrations in that cell. In certain regions such as over the oceans and in the Rocky Mountains, aviation causes only very minute changes in concentrations, as seen in the top panel in Figure 15. These regions with very small changes are showing as ammonium-sulfate and H_2SO_4 dominated in Figure 17. The largest surface area of the country is dominated by ammonium-nitrate. A small number of North-East cells are dominated by elemental carbon (nvPM) and a few areas in the Rocky Mountains are dominated by PM organics, although this is probably due to low concentrations. The observed dominance of secondary nitrates in the North-East is due to the higher traffic and hence the higher amounts of aircraft emissions being released. Compared to results from the iF model, the use of vertically distributed inventories combined with the modeling of complex CMAQ atmospheric chemistry has led to different spatial patterns, for secondary sulfates especially. Of note, the iF contributions map ranked pollutants as per total national health impacts while the RSM map was strictly a comparison of pollutant concentrations per cell.

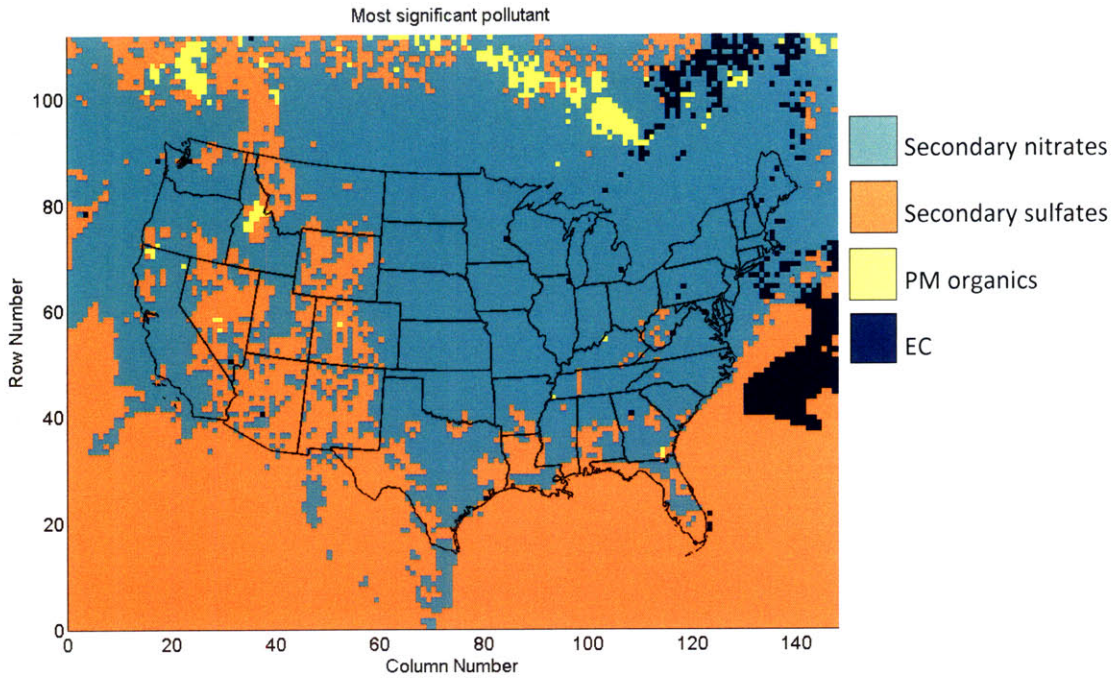

Figure 17: Map of most significant pollutant as given by the RSM. Legend: blue is for EC, turquoise for secondary nitrates, yellow for organics, and orange for secondary sulfates.

3.7.1.5 Aviation scenario analysis

To better characterize the similarities and differences between the two reduced-form models within a policy context, we analyze three plausible proposals for reducing environmental impacts of aviation. The first proposed policy is a NO_x stringency policy consisting of a 10% reduction in NO_x emissions. The second policy is aimed at reducing the sulfur content of jet fuel by 90% (which we approximate in the S-R matrix by solely focusing on the SO_2 emissions implications). The third policy is a combination of the same NO_x and fuel sulfur stringencies. While these policies are considered feasible and consistent with recent policy discussions, they are simply used here for illustrative purposes. A 10% NOx reduction was chosen due to the limited impacts of possible stringent engine standards and long fleet-wide implementation times. The low sulfur scenario is consistent with reductions in fuel sulfur content that have been pursued in other transportation sectors.

The air quality and health impacts of the policies are presented in Table 30. For consistency between scenarios, the fuel sulfur content variability was not applied considering that the sulfur distribution following an aviation low-sulfur fuel standard is undetermined. For a 10% NO_x stringency policy,

the mean number of adult premature mortalities is reduced by 11 per year with the RSM and by 29 per year using iF values. A 90% reduction in fuel sulfur leads to a mean estimate of 58 fewer deaths per year with the RSM and 150 per year using iF values. The combined policies yield a reduction of approximately 69 mortalities with the RSM and 160 with the iF model. These findings reinforce the value of these reduced order methods for rapidly assessing policy-relevant aviation scenarios.

Table 30: Scenario analysis of U.S. nationwide health impact of aviation-related PM (Y2005) for a 10 % NO_x reduction policy, a 90 % FSC reduction policy, and a joint 10 % reduced NOx and 90 % FSC reduction policy.

Scenario	Product of population and marginal $PM_{2.5}$ concentration change (μg-people/m^3) from baseline aviation case (5% – 95% CI)	Variation of adult premature mortality from baseline aviation case (5% – 95% CI)	
	RSM v2	RSM v2	iF
10% NO_x decrease policy applied to baseline aviation	1.1×10^5 (0.92×10^5 – 1.3×10^5)	11 (7.1 – 16)	29 (11 – 55)
90% fuel sulfur content decrease policy applied to baseline aviation	5.9×10^5 (5.4×10^5 – 6.5×10^5)	58 (40 – 80)	150 (68 – 250)
10% NO_x decrease and 90% fuel sulfur content decrease policy applied to baseline aviation	7.1×10^5 (6.5×10^5 – 7.6×10^5)	69 (47 – 95)	160 (84 – 260)

The analysis of low fuel sulfur scenarios revealed that population-weighted changes in concentration (dC·P) from PM Sulfates were negative for low SO_x emissions. In other words, PM Sulfates contribute to a negative number of mortalities. This response is also seen in CMAQ results for low FSC scenarios. For example, in the case of Masek's "RSM008" simulation where the FSC multiplier was set at its lowest sampled DOE value[8], i.e. 0.12653 (representing a 86 ppm case), CMAQ results demonstrated a population-weighted change in concentration of -1.3 % with respect to the background (RSM000). The negative contribution of PM Sulfates explains why the 90 % FSC

[8] The 0.025 lower bound (17 ppm) was assigned to RSM000, therefore was never actually sampled since the fuelburn multiplier was zero, meaning zero SOx emissions.

reduction benefit amounts to 58 saved lives, a number greater than the contribution of PM Sulfates in the baseline case (about 18 %, or 40 mortalities). Physically, this would mean that at low SOx levels, the sulfates produced by aircraft emissions are reducing ambient PM concentrations compared to the background. Such a phenomenon cannot be explained by atmospheric chemistry, and is most likely due to modeling noise. More specifically, when using CMAQ with very low aircraft SOx emissions, the SO_4 concentrations due to aviation are very close to the ambient levels, such that the difference falls within in the noisy region of the model. Because ambient SO_4 is highest in densely populated regions, the noise becomes amplified with the calculation of population-weighted changes in concentration. Moreover, the 90% reduction in FSC scenario may fall within a region of the sample space which may be under-sampled, even though an FSC multiplier of 0.1 is well within the DOE range of 0.025 to 5.0 (refer to Table 21). FSC multipliers below 1 which were sampled in the DOE are {0.127; 0.228; 0.330; 0.736; 0.837; 0.939}. It should be noted that NO_x, nvPM, and fuelburn multipliers were also varied simultaneously. From a series of tests where only FSC was varied, simulation results using the RSM v2 showed that estimated sulfate contributions were negative for FSC reductions of roughly 65 % and more (multiplier less than or equal to 0.35), corresponding to FSC content of approximately 240 ppm based on a 680 ppm standard. In light of this, the negative PM Sulfate contributions are most likely due to CMAQ noise and the under-sampling of the low FSC region in the RSM.

Beyond the negative PM Sulfates contribution, the PM Nitrates dC·P also decreased in the FSC reduction scenario, contributing to a further decrease in mortality with respect to the baseline. As seen in Section 3.5.3.1, PM Nitrates concentrations are dependent on the SO_x multiplier. The negative influence of SO_x on concentrations of PM Nitrates observed in the low FSC scenario is of opposite sign than that of the bounce-back iFs used in the intake fraction model. One would expect that with lower SO_4 concentrations, more ammonium would be available for neutralizing NO_3, leading to higher PM Nitrates given an FSC decrease. However, this is not the response obtained in our case. The decrease in PM Nitrates observed for low-SO_x conditions can be explained by both the complex chemical mechanisms modeled within CMAQ and again, the possible under-sampling of the low FSC multiplier region.

Two other aviation scenarios were analyzed, this time within the bounds of physical interpretability. The first scenario consists of a 60 % FSC reduction (272 ppm equivalent), and the second is a joint

60 % FSC reduction and a 10 % NO_x reduction. Results are shown in Table 31. For the 60 % FSC reduction case, PM Sulfates contributed to 2.0 % of health impacts, representing 3.9 premature mortalities, a positive contribution with physical meaning. The PM Sulfates contribution in the baseline case was approximately 40 mortalities. In total, compared to the 2005 baseline, this low FSC policy reduced the number of premature mortalities due to aircraft emissions by 39 cases (90% CI: 26 – 54). The joint FSC and NO_x stringency policies yielded a benefit of 50 fewer premature mortalities (90% CI: 34 – 69).

Table 31: Scenario analysis of U.S. nationwide health impact of aviation-related PM (Y2005) for a 60 % FSC reduction policy and a joint 10 % reduced NOx and 60 % FSC reduction policy.

Scenario	Product of population and marginal $PM_{2.5}$ concentration change (μg-people/m^3) from baseline aviation case (5% – 95% CI)	Variation of adult premature mortality from baseline aviation case (5% – 95% CI)
	RSM v2	RSM v2
10% NO_x decrease policy applied to baseline aviation	1.1×10^5 (0.92×10^5 – 1.3×10^5)	11 (7.1 – 16)
60% fuel sulfur content decrease policy applied to baseline aviation	4.0×10^5 (3.6×10^5 – 4.3×10^5)	39 (26 – 54)
10% NO_x decrease and 60% fuel sulfur content decrease policy applied to baseline aviation	5.1×10^5 (4.7×10^5 – 5.5×10^5)	50 (34 – 69)

Although the RSM does not allow for the same level of regional analysis as is possible with the iF model, some regional distinctions can be observed when comparing a baseline aviation case to a policy scenario. Figure 18 presents changes of $PM_{2.5}$ concentrations (μg/m^3) throughout the United States for the three scenarios compared to baseline aviation. It can be seen that the effects of the FSC reduction policy are four times greater than those of the NO_x stringency policy, with dC·P changes of 4.0×10^5 μg-people/m^3 and 1.1×10^5 μg-people/m^3 with respect to the baseline case, respectively. As expected, areas in the vicinity of larger airports, such as Los Angeles International Airport, experience the largest reductions of $PM_{2.5}$.

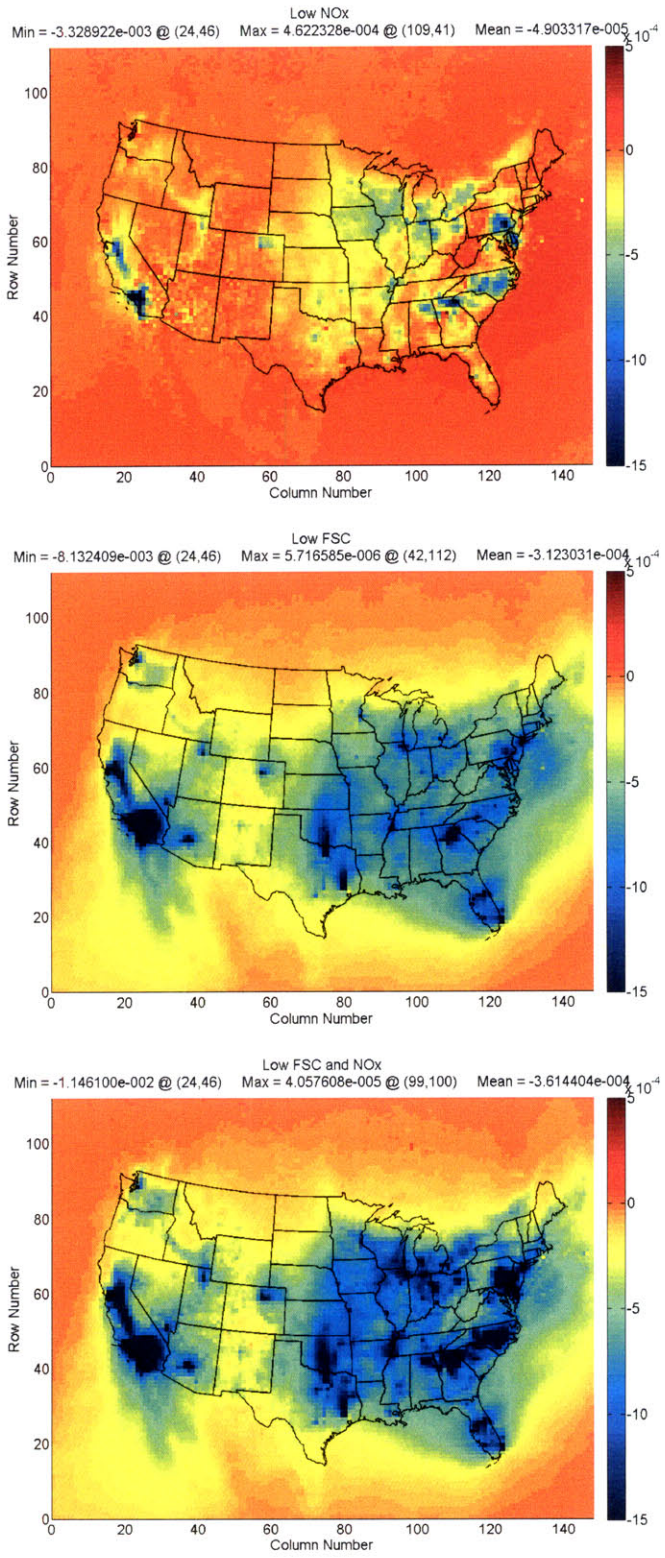

Figure 18 : Policy effect for: 10% NO_x reduction scenario (top), 60% FSC reduction scenario (center), and combined NO_x and FSC stringency (bottom). Changes in concentration of PM2.5 (μg/m3) compared to baseline aviation are plotted across the United States, Y2005.

3.7.1.6 Discussion on RSM v2 and iF Results

The results of Section 3.7 have highlighted the utility of using reduced-order models to conduct the impact assessment analyses of policies. With the iF model and the RSM v2 model, we obtained estimates of various health endpoints due to subsonic aviation emissions below 3000 feet and monetized these impacts. The results of both models were on the same order of magnitude, with iF results about a factor of two larger than RSM v2 results. For both models, health impacts from secondary particulate matter dominated those from primary PM. These results support further investigation into ways to mitigate emissions of secondary PM precursors from aircraft.

In the same vein, RSM and iF values differ most substantially for secondary PM than for primary PM. While both models attributed the majority of health costs to ammonium-nitrate, the percentage contributions differed. In the iF model, secondary nitrates represented 54 % of health damages, roughly three-quarters of the contributions obtained in the RSM v2 model where they corresponded to 70 % of damages. Most significantly, the proportion of health damages attributed to secondary sulfates were 12 % for the RSM v2 compared to 33 % for the iF model. In both models, the CRFs used and the uncertainty distributions used were the same. These differences are mainly explained by the underlying construct of the source-receptor matrices on which the intake fractions are based versus the assumptions made in the CMAQ model and its complex chemical reactions. In addition, impacts from organic PM were not included in the iF modeling.

The overall higher health impacts from the iF model may be due to the intake fractions being developed for ground-level mobile sources. Rather than dispersing LTO emissions vertically over 3000 feet as was done in the CMAQ simulations, the iF model effectively assumes that all emissions are emitted at ground-level, as would be the case for automobiles. The concentration of PM being breathed in by humans if this were the case would be much greater, leading to an upward bias. Greco et al. found that when comparing intake fractions for ground-level sources with those for power plants having elevated smokestacks, the ground-level iFs for secondary nitrates were an average of 1.3 times larger than those of power plants and 1.5 times larger in the case of secondary sulfates (Greco et al., 2007). Both of these ratios are less than the factor of 2.2 difference found in our iF and RSM v2 analyses of the baseline aviation case for year 2005 (Table 27).

Another notable difference between the iF and the RSM v2 results surrounds the concept of "SMATing" (EPA, 2006a). The iF model accounts for SMATing through its use of source-receptor matrices which included SMATing and consideration of particle-bound water. Inclusion of particle-bound water to the $PM_{2.5}$ mass leads to higher concentrations (mass per volume) and hence higher health costs. The current version of the RSM does not include SMATing nor water mass, which may lead to a downward bias on estimated health impacts.

The RSM v2 results presented in this chapter for the 2005 baseline aviation case differ quite significantly from results presented in Sequeira's thesis (Sequeira, 2008). Refer to Appendix I for approximated changes in premature mortality. The EPAct and RSM analyses included in the thesis (and Appendix I) used different concentration response functions (CRFs) and population data. Sequeira used Pope et al. (Pope III et al., 2002) CRFs for premature mortality (beta distribution with mean of 0.6 % with standard deviation of 0.2 %) which is about 1.7 times lower than the triangular distribution with mean of 1% used in the iF and RSM models. In addition, the population used was obtained from 2001 U.S. census data whereas the iF and RSM models used population growth rates to approximate 2005 populations. Results obtained from RSM v2 using the EPAct CRFs and 2001 population for the baseline 2005 case yielded differences of 47 % for the adult mortality output with respect to those obtained with APMT settings, equivalent to a change of roughly 100 adult mortalities. Comparing the percent contributions per species found in Sequeira's thesis and those obtained by the RSM v2 for the baseline aviation case (RSM post-BPR) we find large discrepancies. Where we found a 70 % contribution from secondary nitrates, Sequeira reports a 20 % contribution. The main explanations for these differences are as follows:

- Results for the "RSM post-BPR" inventory in Sequeira's thesis were obtained using a linear scaling model based on the EPAct analysis done using CMAQ and SMATing;
- The EPA's SMATed CMAQ changes in concentration of AMM, PM Sulfates, and most significantly PM Nitrates differ significantly from the pre-SMATed CMAQ data;
- Sequeira used the SANDWICH model to attribute particle-bound water mass (Sequeira, 2008), leading to an increased contribution from secondary sulfates.

Considering that the RSM approximates changes in concentrations for the different PM species with very low errors compared to the high-fidelity CMAQ model, we are confident that our results are not the result of an approximation error.

Given that the "RSM post-BPR" results presented in Sequeira's thesis were obtained by linear scaling of EPAct results, comparisons with this inventory are not ideal as there is added uncertainty from the scaling. A more direct comparison can be done using EPAct results, pre- and post-SMATing, versus "RSM999" CMAQ results (Masek, 2008). Both the EPAct inventory and RSM999 inventories are pre-bypass-ratio correction (Sequeira, 2008). The EPAct inventory was based on FOA3a approximations while the RSM999 inventory was based on FOA3. Another difference is that the EPAct inventory erroneously had 400 ppm FSC at 25% of airports instead of 680 ppm, leading to 15% lower SO_x inventory. Comparison results including plots of changes in concentration of ammonium, PM Nitrates (NO_3), and PM Sulfates (SO_4) are given in Appendix J for the following three cases: 1) CMAQ results of EPAct analysis pre-SMATing; 2) CMAQ results of EPAct analysis post-SMATing; 3) CMAQ results of RSM999 analysis with no-SMATing. Appendix J.1 summarizes both inventories. Tables J.2, J.3, and J.4 compare domain-averaged changes in concentration of AMM, PM Nitrates, and PM Sulfates for the three analyses. Appendix J results reveal that the difference in proportions of sulfates and nitrates are minimal between EPAct pre-SMATed concentrations and RSM999 concentrations. The discrepancy becomes obvious upon inspection of EPAct post-SMATed concentrations and RSM999 concentrations. In the case of PM Sulfates, the average concentration over the U.S. is 1.7 times higher after SMATing. For PM Nitrates, the average concentration is 1.6 times lower after SMATing. The changes in spatial patterns caused by SMATing are also apparent in the plots shown in Appendix J. SMATing appears to have an especially large impact on spatial patterns of PM Nitrates.

By accounting for water, contributions of ammonium-sulfate become even more important. Figure 19 illustrates the contribution of water and ammonium to domain averaged changes in concentrations for the post-SMATed EPAct results. The SMATing and the water-apportionment differences explain why Sequeira reports higher contributions from secondary sulfates (46 %) than from secondary nitrates (18 %), while our non-SMATed CMAQ results for RSM999 report higher contributions from nitrates (56 %) than from secondary sulfates (16 %).

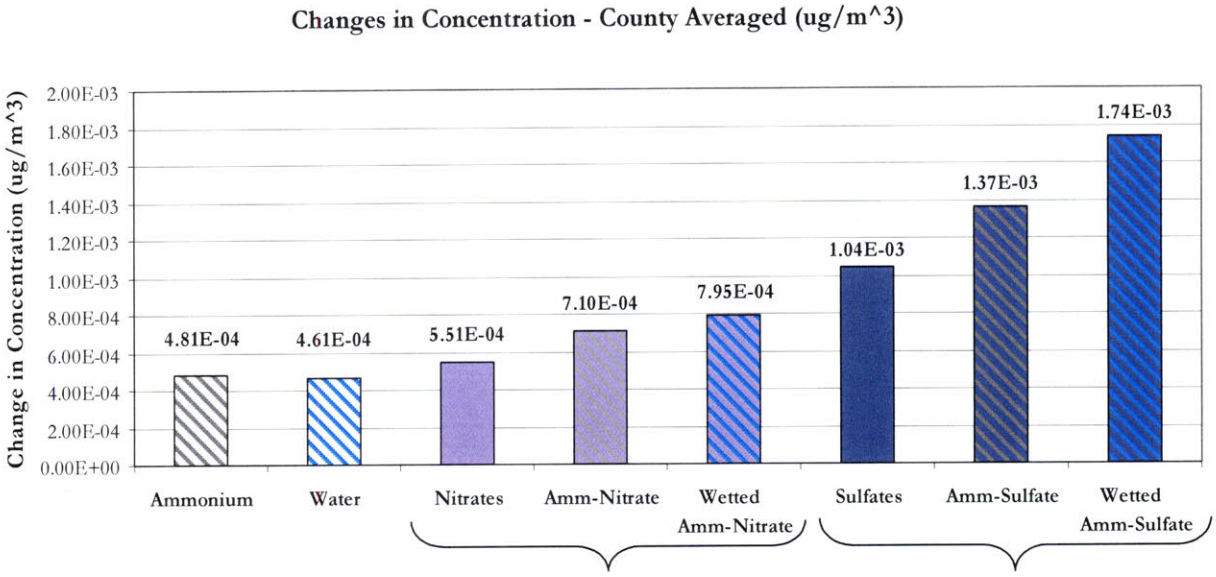

Figure 19: Post-SMATed EPAct changes in concentration of Nitrates and Sulfates before and after the addition of ammonium and water using the SANDWICH method. Results are county-averaged changes due to aircraft only (ug/m^3).

3.8 Uncertainty Assessment of RSM v2

The importance of a thorough uncertainty assessment for any complex model rests on its implications in terms of decision-making, model objectives, and future development. There are two types of uncertainty: aleatory uncertainty due to natural variability, and epistemic uncertainty due to a lack of knowledge. For an in-depth discussion of complex model uncertainty and assessment methods, the reader is referred to Allaire's Ph.D. thesis, *Uncertainty Assessment of Complex Models with Application to Aviation Environmental Systems* (Allaire, 2009). In this section, we present the results obtained by following Allaire's 7 step uncertainty assessment method. We conduct (n + 2) Monte Carlo evaluations, where "n" is the number of factors or parameters assessed. From the uncertainty analysis, two sensitivity analyses are then done:

1) Global sensitivity analysis:
    - Total sensitivity analysis;
    - Main effect sensitivity analysis;
2) Distributional sensitivity analysis.

Based on the results of the sensitivity analyses, we suggest factors on which future research should be directed in order to reduce output variance and those that are non-influential.

Several variables and parameters in the aviation health impact pathway have inherently large uncertainty associated to them. In the APMT AQ models, we depict these uncertain parameters as probabilistic distributions rather than deterministic values, when possible. Monte Carlo simulations are then used to propagate uncertainties throughout the framework resulting in probabilistic distributions for the air quality health impacts and net present value (NPV) outputs. In cases where judgment, morals, or opinion may play a role in the selected parameter range, separate scenarios are modeled. Examples of such cases include the selection of discount rates, population growth factors and valuation costs per endpoint.

3.8.1 Factors and Outputs

The goals of the uncertainty assessment having been stated above and the assumptions and limitations of the AQ model having been treated in theses by Rojo and Masek and complemented by Chapter 3 of this thesis, we now jump to Steps 3 and 4 of the method of Allaire. The two main

outputs of the APMT AQ model (RSM v2) are the number of adult mortalities and the total health costs (NPV). Table 32 presents the AQ model's factors and their characteristics:

Table 32: APMT Air Quality model factors and characterization.

Factor	Units	Uncertainty Distribution	Source	Uncertainty Type	Outputs Affected
SOx inventory (paired with fuelburn)	Uncertainty coefficient from 0 to 1	Uniform 0.92 – 1.12	(Rojo, 2007)	Epistemic: modeled inventory is not exactly equal to true emitted amounts in that year	Mortalities, NPV
NOx inventory	Uncertainty coefficient from 0 to 1	Uniform 0.83 – 1.23	(Rojo, 2007)	Epistemic: modeled inventory is not exactly equal to true emitted amounts in that year	Mortalities, NPV
nvPM inventory	Uncertainty coefficient from 0 to 1	Uniform 0.52 – 2.06	(Rojo, 2007)	Epistemic: modeled inventory is not exactly equal to true emitted amounts in that year	Mortalities, NPV
FSC variability	ppm	Weibull $\lambda = 0.0627$ (scale) $k = 1.268$ (shape)	(DESC, 2002-2007)	Aleatory: natural variability of sulfur content due to location of fuel source and natural formation processes; Epistemic: distribution comes from military survey, size of sample	Mortalities, NPV
RSM linear regression	Uncertainty multiplier for the sqrt(MSE)	Normal $\mu = 0$ $\sigma^2 = 1$	(Masek, 2008)	Aleatory: uncertainty multiplier sampled randomly from standard normal distribution	Mortalities, NPV
CRF adult mortality	% per $\mu g \cdot m^{-3}$ $PM_{2.5}$	Triangular 1.0 (0.6 – 1.7)	(Rojo, 2007)	Aleatory: PM effects will vary naturally depending on the individual Epistemic: more epidemiological studies would refine CRF values	Mortalities, NPV
VSL	Million U.S. Y2000 $	Lognormal Mean = $ 6.3 M Std. dev. = $2.8 M	(DOT, 2008)	Aleatory: Value of a statistical life is specified by the policy-makers using the model.	NPV

3.8.2 Uncertainty analysis

Visual inspection of Figure 20 reveals that 3000 simulations are adequate for convergence of the mean number of mortalities and NPV, with an acceptable variance. Needless to say, there is a tradeoff between the level of convergence attained by a high number of runs and the simulation run time. For the RSM impact analyses presented in the previous sections, we opted for 3000 Monte Carlo simulations, an acceptable number for convergence of the mean number of mortalities and NPV.

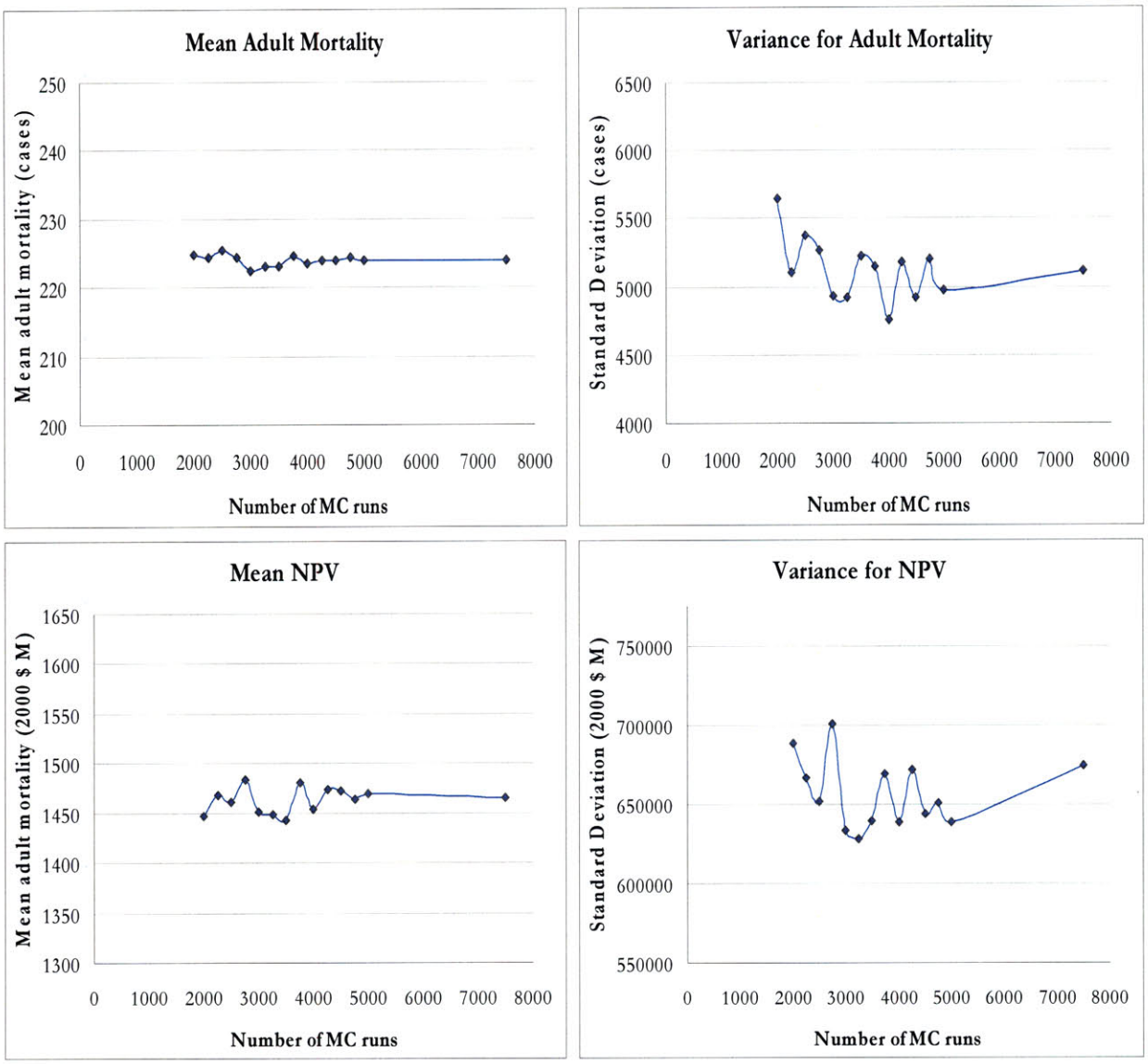

Figure 20: Convergence test for RSM v2 outputs of number of premature mortalities and NPV. We find that 3000 MC draws is an acceptable number, with acceptable variance and adequate runtime.

Table 33 presents the means and standard deviations of the outputs based on 3000 Monte Carlo simulations of the baseline. Output histograms for the baseline case are shown in Figure 21.

Table 33: Statistics of 3000 Monte Carlo simulations for 2005 baseline case.

Premature Adult Mortality		NPV ($B)	
Mean	Std. dev.	Mean	Std. dev.
210	64	1.4	0.78

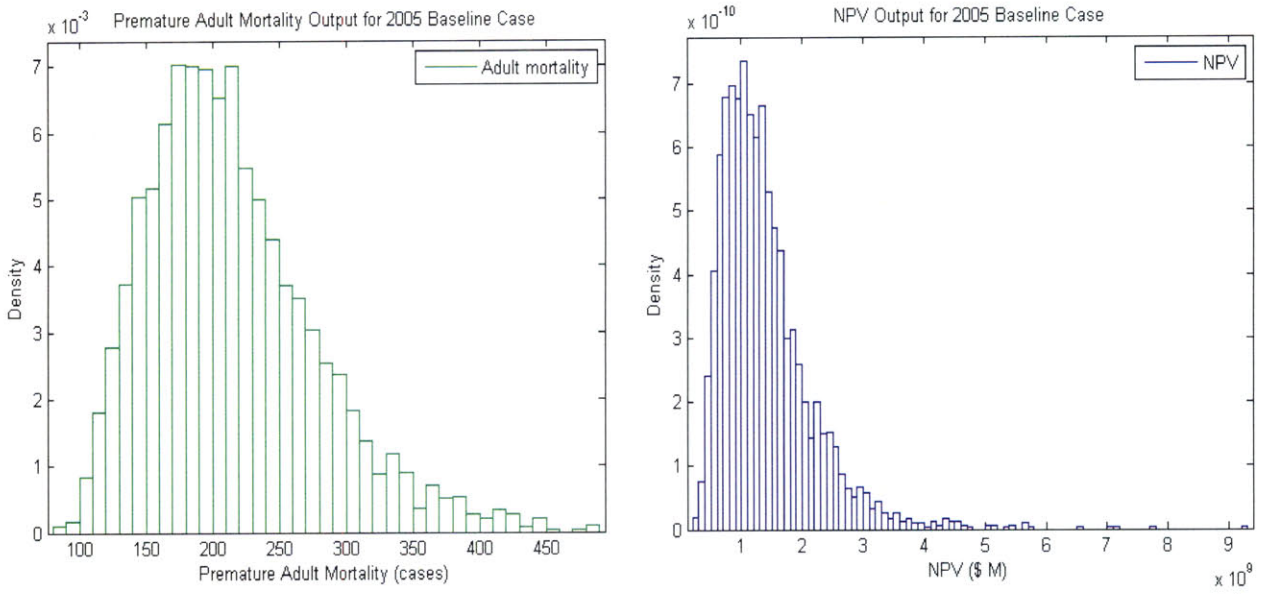

Figure 21: Output distributions for premature mortality and NPV. Results obtained with 3000 MC simulations.

From Table 32, we find 7 major factors influencing output uncertainty. The uncertainty analysis therefore consists of 7 + 2 Monte Carlo evaluations. After conducting convergence tests on the global and distributional sensitivity indices which we present in the following section, we concluded that using 10,000 simulations in the uncertainty assessment step ensured better convergence of the indices. RSM v2 assessment results that follow are therefore based on (7 + 2) Monte Carlo evaluations with 10,000 simulations each.

3.8.3 Sensitivity analysis

Allaire dictates that if the standard deviation of the outputs is large with respect to the mean, there is a need for an uncertainty assessment. As this is the case for both of our outputs, we continue with global and distributional sensitivity analyses (refer to Allaire (2009) and references within).

3.8.3.1 Global sensitivity analysis

Results of the global sensitivity analysis (GSA), i.e. main effect sensitivity indices and total effect sensitivity indices are show in Table 34. In order to maximize the convergence of the S_i's, 10,000 Monte Carlo simulations were generated for each n + 2 evaluation.

Table 34: Global sensitivity analysis results for AQ model: main effect and total effect sensitivity indices.

Factor	Adult Mortality Main Effect Sensitivity Index (S_i)	Adult Mortality Total Effect Sensitivity Index (τ_i)	NPV Main Effect Sensitivity Index (S_i)	NPV Total Effect Sensitivity Index (τ_i)
SOx inventory	0.01	0.00	0.01	0.00
NOx inventory	0.04	0.04	0.02	0.01
nvPM inventory	0.03	0.03	0.01	0.01
FSC variability	0.44	0.47	0.14	0.18
RSM linear regression	0.00	0.00	0.01	0.00
CRF adult mortality	0.48	0.50	0.14	0.17
VSL	0.00	0	0.65	0.70

In the case of the main effect sensitivity analysis, distributions for all parameters except the factor being investigated are re-sampled. For example, to obtain the main effect sensitivity index for the "VSL" parameter, the VSL distribution is assumed to be fixed and the other parameters are varied.

Conversely, in the case of the total effect sensitivity analysis, all parameters are kept fixed except the one in question which is re-sampled.

For premature mortality, the global sensitivity analysis (Table 34) has revealed that the CRF coefficient for premature mortality dominates the contribution to *output variability*. The second major contributor is the variability in Fuel Sulfur Content. To a much lesser extent, uncertainty on the NO_x, nvPM and SO_x inventories also have a small contribution. Contributions from the RSM linear regression uncertainty are not significant to the second significant digit. As VSL does not affect the premature mortality output, its total sensitivity index (τ_i) is zero.

For NPV, the VSL is the largest contributor to the *output variability*, according to the global sensitivity analysis. The CRF variability as well as the FSC variability are the next highest ranked contributors to total NPV variability. NO_x, nvPM and SO_x inventories also have a small contribution, as was the case for the mortality output. Contributions from the RSM linear regression uncertainty are not significant to the second significant digit.

The sum of the τ_i's is 1.03 for premature mortality, and 1.07 for NPV. This indicates that there are larger interaction effects for NPV than for premature mortality. A τ_i sum of one corresponds to no interaction between factors.

3.8.3.2 Distributional sensitivity analysis

As defined by Allaire, a distributional sensitivity analysis (DSA) is better suited to determine which factors should be the topic of further research. Compared to the main effect sensitivity index which assumes that all the variance of a factor can be reduced to zero, the "average adjusted main effect sensitivity index" obtained from a DSA treats the factor's reduction in variability as a random variable. In the DSA, we only look at epistemic sources of uncertainty, such that further research would effectively reduce the variability of this factor. Therefore, we do not assess the FSC, VSL, and RSM parameters in this assessment. The variability of FSC is mainly aleatory due to the natural difference in sulfur content of fuels from around the country. Considering that commercial jet fuel is processed from the same sources as military jet fuel, the variability in FSC between military and commercial fuels would not be reduced much by further research. As for the VSL, policy-makers typically set the distribution of this factor. Variability would not be reduced by further research.

Similarly, the uncertainty on the RSM is entirely aleatory by design. Monte Carlo simulations for the RSM factor are based on a random sampling of the standard normal distribution. This uncertainty coefficient is then multiplied with the RSM's standard deviations in each cell. While the standard deviation of the RSM regressions can be reduced, the aleatory uncertainty distribution applied will not.

Results of the DSA are shown in Figure 22 where adjusted main effect S_i's are plotted versus $(1 - \delta)$ (refer to Allaire (2009)). Of note, for $(1 - \delta)$ equal to one, the adjusted main effect sensitivity indices equal the unadjusted main effect indices. Taking the average of the adjusted S_i's, we obtain the "average adjusted main effect sensitivity indices." Adjusted and unadjusted S_i's are compared in Table 35.

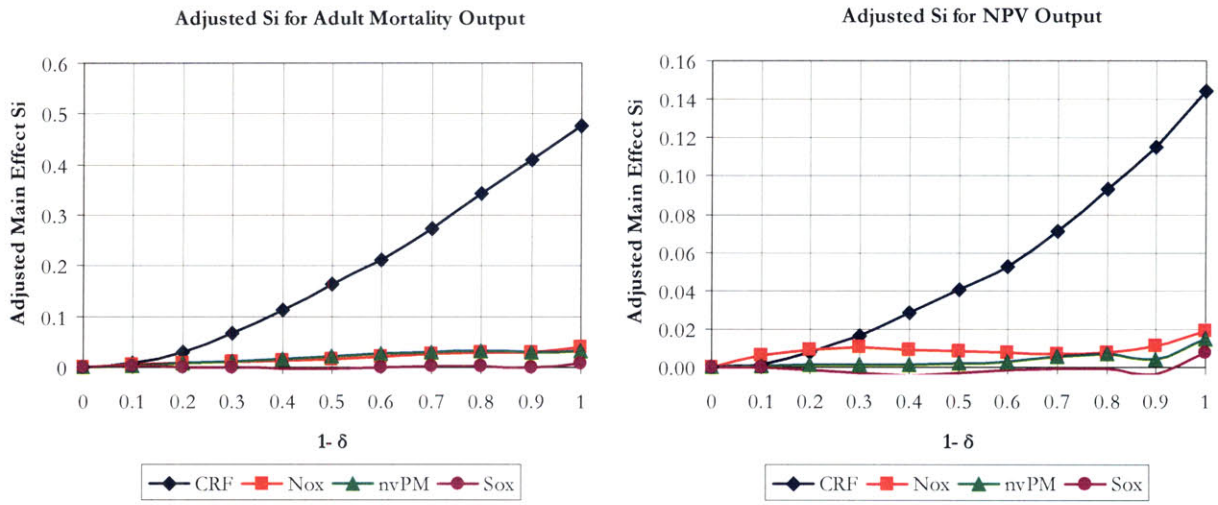

Figure 22: Distributional Sensitivity Analysis (DSA) results. Adjusted main effect Si's are plotted for both outputs, mortality (left) and NPV (right).

From the DSA results (Table 35), we find that the ranking of the model's epistemic uncertainty factors in terms of average adjusted main effect sensitivity indices (AAS) for adult mortality is CRF mortality in first followed by NO_x inventory uncertainty and nvPM inventory uncertainty. The epistemic factors are those for which additional research could help in reducing variability. This information should be used in prioritizing future research efforts. Inspection of the AAS' for the NPV output reveals that only CRF mortality and NO_x emissions uncertainties are worthwhile reducing with future research. The largest contributors to output uncertainty as found by the GSA were VSL and FSC variability, both of which additional research would not reduce variability.

Table 35: Distributional sensitivity analysis results for AQ model: average adjusted main effect sensitivity indices, with un-adjusted main effect indices (Si's).

Factor	Adult Mortality Average Adjusted Main Effect Sensitivity Index (AAS)	Adult Mortality Main Effect Sensitivity Index (S_i)	NPV Average Adjusted Main Effect Sensitivity Index (AAS)	NPV Main Effect Sensitivity Index (S_i)
SOx inventory (paired with fuelburn)	0.00	0.01	0.00	0.01
NOx inventory	0.02	0.04	0.01	0.02
nvPM inventory	0.02	0.03	0.00	0.01
FSC variability	n/a	0.44	n/a	0.14
CRF adult mortality	0.19	0.48	0.05	0.14
VSL	n/a	0.00	n/a	0.65

3.9 Limitations of RSM v2 and Future Work

With the successful implementation of RSM v1 into APMT followed by that of the speciated RSM v2, in this section we explore the possible improvements to be included in the design of a new RSM v3. An overview of the latest model's limitations serves as an introduction to our suggested improvements.

3.9.1 Limitations of the current model

The uncertainties of the underlying CMAQ CTM model are in large part unquantified and have not been included in the uncertainty analysis of the APMT AQ model. However, for other sources of uncertainty, we have quantified them to the extent to which the state of the science has allowed us and propagated the uncertainty throughout the impact pathway by means of Monte Carlo simulations.

The spatial interpolation scheme is presently determined by the user (Section 3.5.3.3) who specifies α and β values. As was stated in Masek's thesis, the optimal choice of α and β values to use in this context is unknown (Masek, 2008).

Another limitation of the model is the lack of "SMATing" of approximated changes in PM concentrations. As explained in Section 3.7.1.6 and shown in Appendix J, SMATing has the potential of affecting both the magnitude of sulfate and nitrate concentrations and the spatial patterns of the changes in concentration (especially for nitrates). Also as described in Masek's thesis, the changes in concentration approximated by CMAQ and hence by the RSM are for so-called "dry PM," which is in contrast to "wet-PM" for which the concentration-response functions (CRFs) are derived. By not considering the added mass of water particles becoming bound to the dry PM, our estimates for health impacts due to aviation are likely biased downwards. In order to include particle-bound water, the CMAQ run scripts would have to be modified such that C_{H2O}, the concentration of PM-bound water, would be an output. This way, the RSM could model changes in C_{H2O} just as it does for NH_4 in the present version.

Currently, the model uses CRFs for $PM_{2.5}$ assuming equal toxicity between PM species. In other words, the same health impacts are associated to one $\mu g/m^3$ of $PM_{2.5}$ regardless of whether the

contribution is from secondary nitrates or primary PM. This limitation can be resolved in the future as more epidemiological studies in the area are made available and CRFs per species are obtained.

The APMT air quality health impact analysis focuses on particulate matter and does not include ozone or hazardous air pollutants (HAPs) impacts. The choice to focus on $PM_{2.5}$ was justified in Rojo's thesis and was based on an analysis that found that impacts of ozone due to aviation were about 49 cases of acute mortality (90 % CI: 3 to 95 cases) in 2002 compared to 670 mortalities from $PM_{2.5}$, for an ozone contribution equal to 7% of $PM_{2.5}$ mortalities (Rojo, 2007). This choice to omit ozone impacts is further justified in the EPAct final report where the authors explain that "the modeled ozone changes (...) are small enough that they challenge the resolution and accuracy of the modeling methods" (Ratliff et al., 2009).

As was discussed previously in Section 3.5.3.2, the assumption of a constant HC EI has lead to less accurate regressions for PM Organics compared to other species. The dependency of PM Organics on HC EI is not being captured despite the fact that NO_x is acting as a surrogate variable.

Another limitation of the RSM v2 surrounds the underlying CMAQ training runs where all multipliers were varied at a national-scale. As we know, this introduces added uncertainties when the RSM is used for regional level policies where multipliers in only one region are changing. To introduce regional variability, a much larger number of CMAQ training runs would be required. Not only would the independent variables be sampled for values within their design space, but they would also be varied in different regions of the geographic domain.

The model currently only covers the United States domain. Air quality health impacts from U.S. aviation in Canada and Mexico are not accounted for in the current model. As well, the costs and benefits of world-wide regulations on the global population cannot be assessed with the current AMPT AQ model.

The numerous sources of uncertainties described in Section 3.8, not to mention the unquantifiable uncertainties, lead to somewhat large confidence intervals and could be seen as limitations of the model. On the other hand, in a policy assessment context these uncertainties are common between policy and baseline. Consequently, when the effects of a policy are compared to a baseline case,

common uncertainties are captured by paired Monte Carlo simulations, i.e. the same random draws are used for the policy and baseline cases. Results for the "policy effect," meaning policy minus baseline impacts, have much narrower distributions. Section 3.7.1.5 illustrates this principle whereby for three policies results with respect to the baseline case are shown with relatively smaller confidence intervals than those for the baseline case alone.

Finally, the model is designed to suit the EPA's guidelines which dictate that only emissions below 3,000 feet be considered when assessing health impacts. A recent study by Barrett et al. has determined that cruise emissions may contribute to approximately a factor of 2 to 10 times the health impacts of landing, takeoff and taxi particulate matter (Barrett et al., 2009). These health impacts from cruise emissions are not being captured by the current APMT Impacts Air Quality module.

3.9.2 Future work

To conclude the chapter, we emphasize four different model limitations which should be addressed in future work and make suggestions.

3.9.2.1 Cruise Emissions

The results of a recent study by Barrett et al. warrant further investigation into the inclusion of the health impacts related to emissions produced by aircraft at cruise altitude. While the EPA does not currently include these emissions in its inventory preparation guidelines for air quality assessment, doing so would paint a more complete portrait of the health impacts of a policy.

There would be different ways to include cruise emissions. One way would be to produce a new RSM based on nested GEOS-Chem (global CTM) and CMAQ simulations. Another way would be simply to first quantify the health impacts due to cruise emissions with respect to those due to LTO emissions and secondly, assuming linearity, scale total health impacts from LTO to include cruise. This simpler approach would require an appropriate sensitivity analysis.

3.9.2.2 HC EI

The inclusion of a fifth independent variable will provide higher fidelity in the prediction of changes in PM Organics. More numerous CMAQ training runs will be necessary in the design of

experiments of this version of the RSM compared to previously, as we would be adding an extra dimension. At the same time, it should be noted that contributions from PM Organics are estimated to represent about 4% of to total $PM_{2.5}$ impacts (Section 3.7.1.2). The benefits of adding a new variable should therefore be weighed with respect to the resource costs of a higher number of simulations.

3.9.2.3 SMATing and water mass

The SMATing and addition of water mass to the outputs of the RSM would contribute to making the results of the model aligned with the EPA's methodology. For future work, a method or software should be implemented to SMAT the RSM outputs (changes in concentration). Apportioning water to PM particles would be done before health impacts were computed. Consideration should nonetheless be given to the fact that CRFs are derived based on dry-PM.

3.9.2.4 Model Applicability to ULS Scenarios

In Section 3.7.1.5, the analysis of low fuel sulfur scenarios revealed that population-weighted changes in concentration (dC·P) from PM Sulfates were negative for low SO_x emissions. As well, decreases in SO_x emissions led to decreases in PM Nitrate concentrations. CMAQ noise and RSM under-sampling are the most plausible explanations for these results. As was discussed, the observed behavior of PM Sulfates and PM Nitrates at low FSC multiplier levels warrants more CMAQ simulations to bolster the RSM DOE points in this region.

3.9.2.5 Increasing Model Efficiency by Removing RSM Uncertainty Factor

Based on the results of the global sensitivity analysis presented in Section 3.8.3.1, it can be concluded that the aleatory Gaussian uncertainty factor applied to the RSM standard deviation has very little influence on total output variability. The RSM uncertainty had a total sensitivity index of 0.00 for the premature mortality output and an index of 0.01 for the NPV output.

The RSM uncertainty is applied independently for each grid-cell and for each Monte Carlo simulation. This amounts to unnecessarily large data files and is responsible for slowing down the model run time. For 3,000 Monte Carlo runs, it is required to store $148 \times 112 \times 3{,}000$ uncertainty multipliers which alone necessitate about 370 MB of disk space. With this setup, the computation of health impacts is done cell by cell, for each Monte Carlo run, i.e. 4.97×10^7 times.

It would be advantageous to remove the uncertainty distribution applied to the RSM regression's standard deviation. Based on the global sensitivity results, this would lead to approximately zero loss of variability for the premature mortality output, and only about 1 % loss of variability for the NPV output. Model runtime would be decreased and storage space would be significantly reduced. In addition, the model assessment process which currently takes over 4 hours of computer runtime for the simulations described in Section 3.8.3 would be drastically shortened.

3.9.2.6 RSM for Europe

Expanding the domain of the APMT AQ capabilities to include Europe would be a clear benefit in terms of analyzing global policies. The same principles used for the U.S. version can be easily transferred to Europe. A series of CMAQ (or other air quality modeling tool) simulations can be used to produce a training set. A response surface model can then be developed by linearly regressing on the outputs and inputs of the training set.

4 Conclusion

Aircraft NO_x was shown to help decrease premature mortality cases due to skin cancer while aircraft emissions of primary particulate matter (mainly soot) and secondary particulate matter precursor gases (NOx and SOx and organics) were shown to increase cases of premature mortality due to respiratory and cardiac ailments. An overview of the health costs and health benefits of aviation emissions follows, drawing from the UV irradiance impacts from Chapter 2 and the air quality impacts from Chapter 3.

It is apparent from the analyses presented in Chapters 2 and 3 that the aviation health costs due to changes in air quality outweigh the health benefits due to increases in ozone column. In year 2005, the aviation health costs related to air quality impacts in the U.S. were estimated at $1.4 billion in year 2000 U.S. dollars (90% confidence interval: $550 million – $2.8 billion). In comparison, the 2002 net benefits from subsonic aircraft NO_x on nonmelanoma skin cancer incidences and associated mortalities in the U.S. are estimated at $130 M (90 % confidence interval : $68 – $220 M) in 2000 dollars. Despite the fact that these analyses were done for two different years, they both constitute impact assessments for the U.S. baseline commercial aviation case with a time difference of three years. In light of this, we can conclude that the health costs from air quality impacts of aviation are an order of magnitude larger than the health benefits from changes in UV irradiance due to ozone column variation. The benefits obtained from aircraft NO_x on skin cancer incidence and mortality effectively offset the air quality costs by about 9 %.

While this work touched upon the health impacts of aviation and aviation-related policies, it is important to consider impacts on climate and noise in any rigorous cost-benefit analysis for a given policy. A policy targeting fuel sulfur content, for example, may have both health benefits as well as climate dis-benefits, for the reason that sulfates act as a cooling agent in the atmosphere while causing respiratory ailments at ground-level. Reduced order models for quickly assessing environmental impacts of a policy are of prime importance in capturing as many impacts as possible.

APPENDICES

APPENDIX A.1

Non-melanoma skin cancer mortality rates published by Lewis and Weinstock. Upper table is from their 2004 study and the lower table is from their 2007 study. Rates are age-adjusted to 2000 U.S. Standard population.

Table 3. Mortality Rates (No. of Deaths) for Nonmelanoma Skin Cancers*

Variable	Nongenital SCC	BCC	Other NMSC	Genital Carcinoma		Total NMSC
				Vulvar	Penile	
Overall rates, age adjusted to the:						
US 2000 standard	0.29 (44)	0.08 (12)	0.09 (13)	0.45 (66)		0.91 (135)
US 1970 standard	0.21	0.05	0.06	0.32		0.65 (135)
World standard	0.15	0.04	0.05	0.23		0.47 (135)
Sex†						
Male	0.50 (27)	0.13 (6)	0.12 (7)	NA	0.24 (13)	0.99 (53)
Female	0.18 (17)	0.06 (6)	0.06 (6)	0.56 (53)	NA	0.86 (82)
Year of death†						
1988-1991	0.28 (12)	0.02 (1)	0.07 (3)	0.53 (15)	0.26 (4)	0.81 (35)
1992-1996	0.28 (16)	0.11 (6)	0.09 (5)	0.65 (22)	0.33 (8)	1.04 (57)
1997-2000	0.32 (16)	0.11 (5)	0.10 (5)	0.48 (16)	0.07 (1)	0.86 (43)
Age, y‡						
0-54	0.02 (2)	0.00 (0)	0.02 (2)	0.08 (4)	0.02 (1)	0.09 (9)
55-64	1.10 (6)	0.01 (1)	0.09 (1)	0.48 (3)	0.55 (3)	1.21 (14)
65-74	0.46 (5)	0.21 (2)	0.19 (2)	1.53 (9)	1.10 (5)	2.21 (23)
75-84	2.27 (16)	0.40 (3)	0.45 (3)	4.34 (19)	0.90 (2)	6.21 (43)
≥85	6.31 (15)	2.88 (6)	2.06 (5)	10.3 (18)	3.32 (2)	19.7 (46)

Abbreviations: BCC, basal cell carcinoma; NA, not applicable; NMSC, nonmelanoma skin cancer; SCC, squamous cell carcinoma.
*Rates refer to the number of deaths per 100 000 persons per year.
†Rates are age-adjusted to the 2000 US standard population.
‡Rates are not adjusted.

Source: (Lewis and Weinstock, 2004)

APPENDIX A.2

Age-adjusted NMSC mortality rates in the United States, 1969–2000

	1969–1974	1975–1984	1985–1994	1995–2000
Genital				
Men	0.42 (*n*=1,688)	0.32 (2,463)	0.25 (2,238)	0.22 (1,402)
Whites	0.37 (1,306)	0.29 (1,982)	0.23 (1,877)	0.21 (1,213)
Blacks	1.0 (369)	0.67 (455)	0.44 (328)	0.31 (164)
Women	0.67 (3,558)	0.54 (6,021)	0.50 (6,907)	0.48 (4,665)
Whites	0.65 (3,175)	0.54 (5,479)	0.50 (6,230)	0.50 (4,305)
Blacks	0.76 (363)	0.52 (515)	0.53 (625)	0.37 (316)
Nongenital				
Men	1.14 (4,154)	1.08 (7,962)	1.02 (9,360)	0.79 (5,128)
Whites	1.20 (3,923)	1.14 (7,535)	1.10 (8,793)	0.87 (4,880)
Blacks	0.63 (231)	0.55 (427)	0.59 (567)	0.36 (248)
Women	0.58 (2,873)	0.49 (5,486)	0.42 (5,743)	0.37 (3,631)
Whites	0.58 (2,648)	0.50 (5,073)	0.44 (5,319)	0.40 (3,414)
Blacks	0.51 (225)	0.42 (413)	0.35 (424)	0.25 (217)

Rates are age-adjusted to the 2000 US standard population and are expressed as the number of deaths per 10^5 at-risk individuals per year.

Source: (Lewis and Weinstock, 2007)

APPENDIX B

Nationwide cancer mortality rates for non-melanoma skin cancer in white females (right) and white males (left). Rates are taken from 1990-1994 data (most recent NCI data available) and have been age-adjusted to US 1970 population. Source: National Cancer Institute (NCI), Cancer Mortality Maps and Graphs.

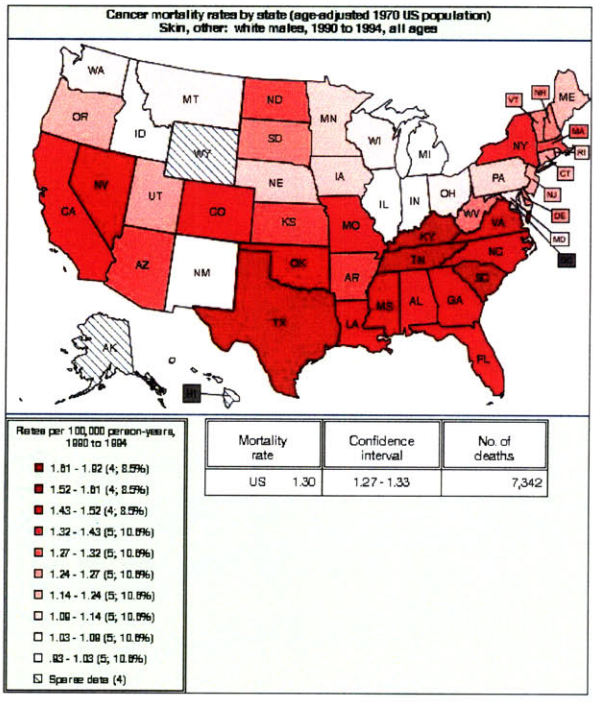

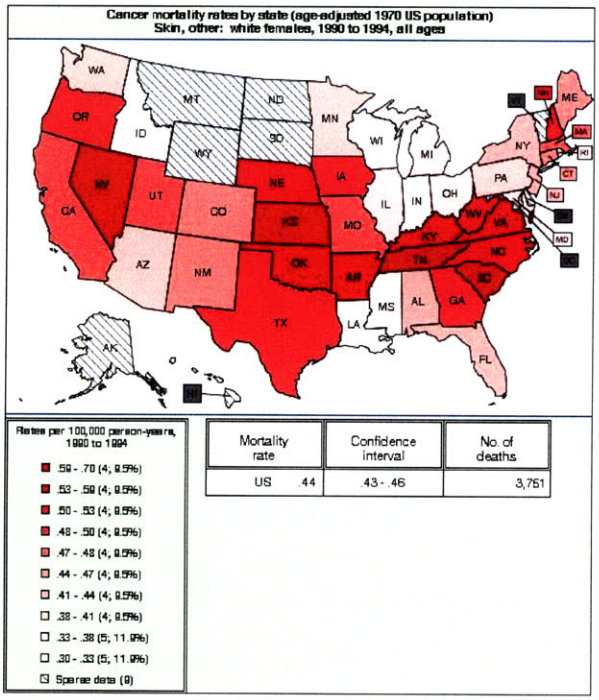

APPENDIX C

Copy of Appendix B of the AHEF model description document *Human Health Benefits of Stratospheric Ozone Protection* (ICF, 2006) listing the U.S. states included in each latitude band.

Table B-1. Regional Definitions for Mortality Data Set

40° N to 50° N	30° N to 40° N	20° N to 30° N
Alaska	California (North)*	Alabama
Connecticut	Colorado	Arizona
Idaho	Delaware	Arkansas
Maine	District of Columbia	California (South)*
Massachusetts	Illinois	Florida
Michigan	Indiana	Georgia
Minnesota	Iowa	Hawaii
Montana	Kansas	Louisiana
New Hampshire	Kentucky	Mississippi
New York	Maryland	New Mexico
North Dakota	Missouri	South Carolina
Oregon	Nebraska	Texas
Rhode Island	Nevada	
South Dakota	New Jersey	
Vermont	North Carolina	
Washington	Ohio	
Wisconsin	Oklahoma	
	Pennsylvania	
	Tennessee	
	Utah	
	Virginia	
	West Virginia	
	Wyoming	

* Counties in California were segregated into either the South or Middle region. The population was split based upon county population data from the Demographic Research Unit of the California Department of Finance.

APPENDIX D

Figures taken from Köhler et al. 2008.

Results from panel b) are used in the 2002 case study, section 2.4.2.

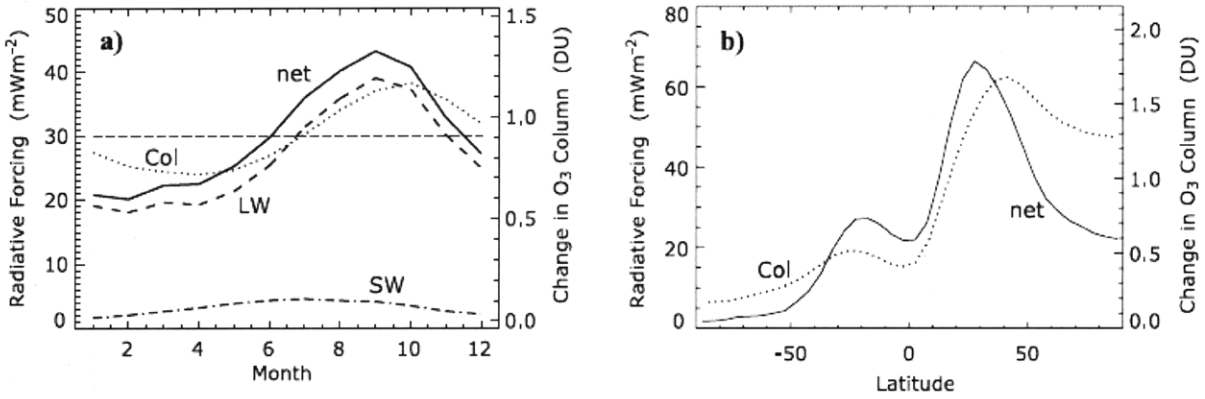

Figure 9. (a) Seasonal variation in global O_3 column in p-TOMCAT and global mean adjusted radiative forcing at the tropopause due to O_3 changes from inclusion of aircraft emissions, for longwave, shortwave and net forcings. (b) Zonal and annual mean changes in O_3 column and associated radiative forcing.

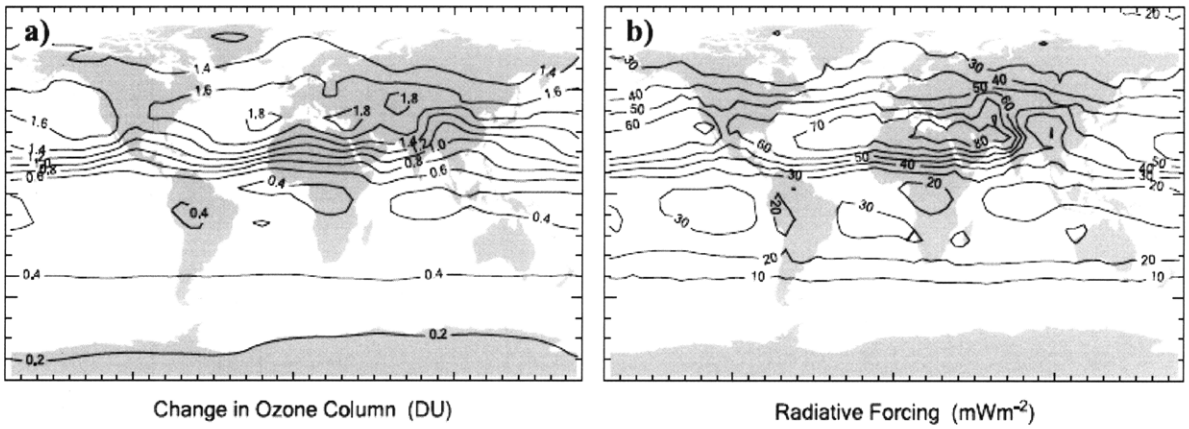

Figure 10. Geographical distribution of (a) annual mean O_3 column changes (in DU) from inclusion of aircraft emissions in p-TOMCAT and (b) annual mean radiative forcing due to ozone changes (in mWm^{-2}).

APPENDIX E

Figure taken from NOAA Climate Prediction Center. Spatial plot of standard total ozone column in Dobson Units.

Stand used in the 2002 case study, section 2.4.2.

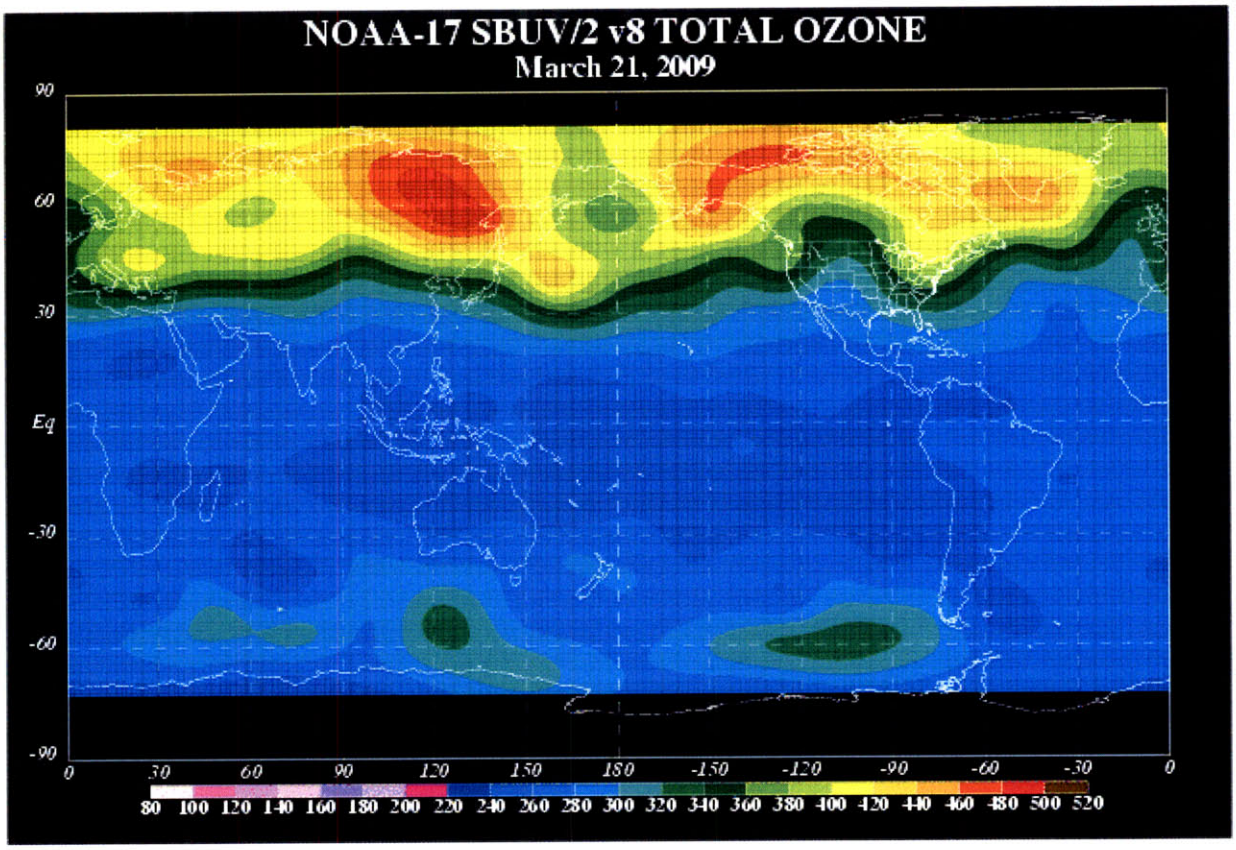

APPENDIX F

BAFs used in the AHEF model, as found in the *Human Health Benefits of Stratospheric Ozone Protection* description document (ICF, 2006).

Table 6. Summary of Calculated BAFs and Key Inputs

Health Effect	Data Sources[a]	Selected Action Spectrum	BAF: Used in AHEF (Annual Exposures)		BAF: Not Used in AHEF (Peak Clear Day Exposures)	
			Males	Females	Males	Females
CMM Incidence/ Mortality	*Incidence*: Ratios from SEER data set (see Section 3.2) *Mortality*: EPA/NCI data set (see Section 3.1) *BAF*: Developed using econometric analysis (described in Section 5.3.1)	SCUP-h (1993)	0.5846	0.5047	1.444	1.310
BCC Incidence	*Incidence*: Based on methods used in U.S. EPA (1987) and Fears and Scotto (1983) (see Section 3.4) *BAF*: de Gruijl and Forbes (1995)	SCUP-h (1993)	1.5	1.3	NA	NA
SCC Incidence	*Incidence*: Based on methods used in U.S. EPA (1987) and Fears and Scotto (1983) (see Section 3.4) *BAF*: de Gruijl and Forbes (1995)	SCUP-h (1993)	2.6	2.6	NA	NA
NMSC Mortality	*Mortality*: EPA/NCI data set (see Section 3.3) *BAF*: Developed using econometric analysis (described in Section 5.3.1)	SCUP-h (1993)	0.7094	0.4574	2.068	1.565

NA = Not available.

[a] For all health effects, the Serafino and Frederick model (1987) was used by independent researchers to derive the BAFs used in the AHEF. The Serafino and Frederick model is a radiative transfer model that translates ozone measurements from the Nimbus-7 satellite into ground-level solar UV irradiance, similar to the TUV model used in the AHEF.

APPENDIX G.1

Patch plots of CMAQ results over 25 simulations with omission of RSM012 and RSM019. Changes in PM concentration per species are plotted versus emissions multipliers. Linearity is demonstrated for all species and appears more clearly than when the two questionable simulations were included (Figure 13).

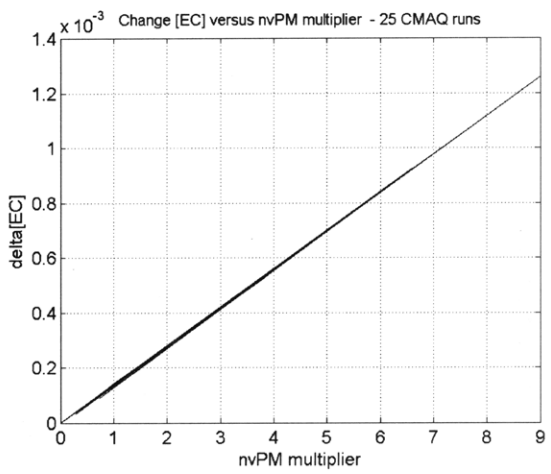

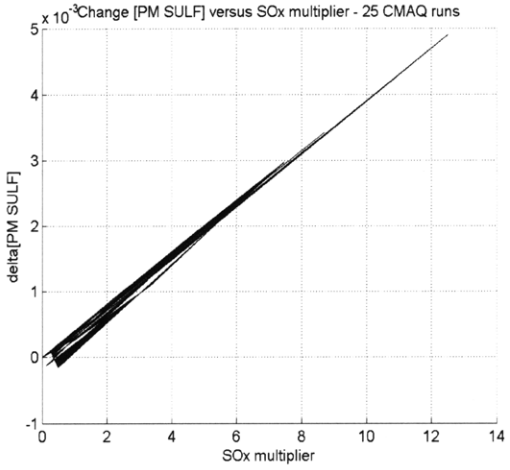

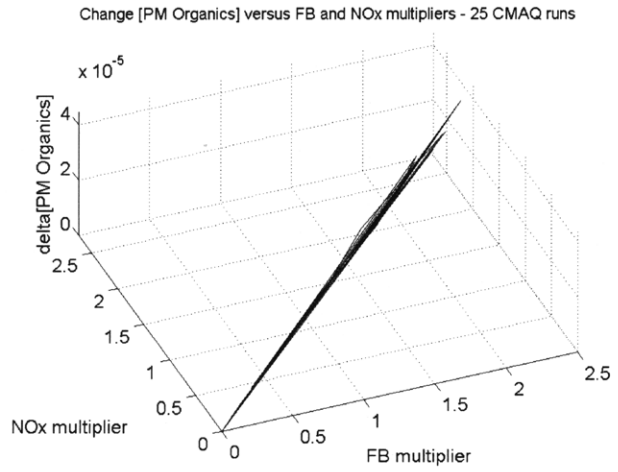

APPENDIX G.2

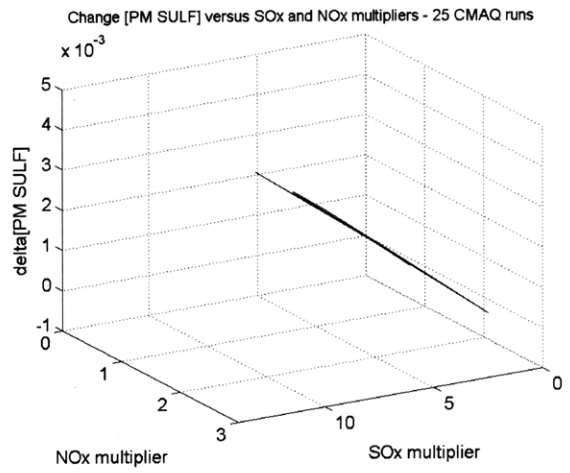
Change [PM SULF] versus SOx and NOx multipliers - 25 CMAQ runs
x 10^-3
delta[PM SULF]
NOx multiplier
SOx multiplier

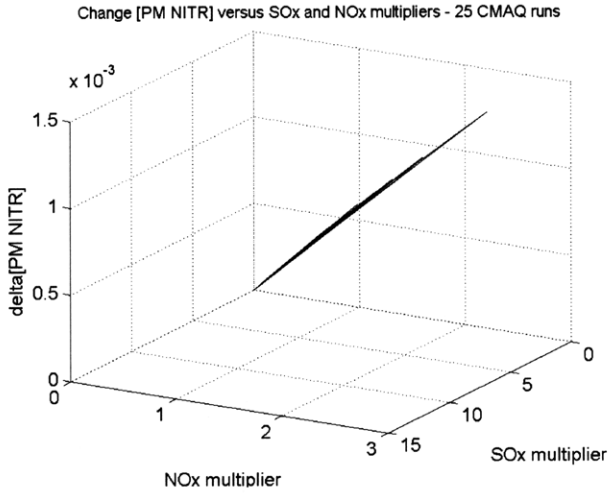
Change [PM NITR] versus SOx and NOx multipliers - 25 CMAQ runs
x 10^-3
delta[PM NITR]
NOx multiplier
SOx multiplier

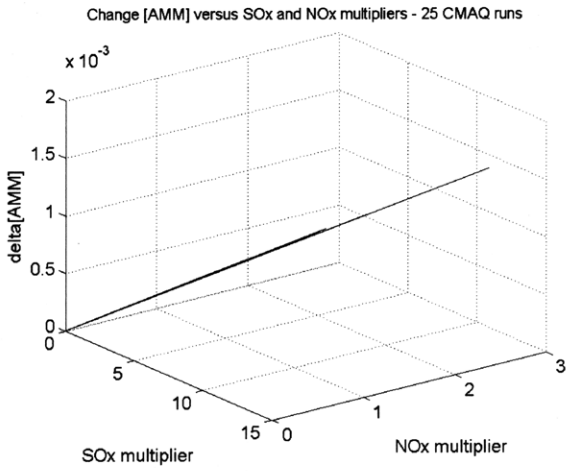
Change [AMM] versus SOx and NOx multipliers - 25 CMAQ runs
x 10^-3
delta[AMM]
SOx multiplier
NOx multiplier

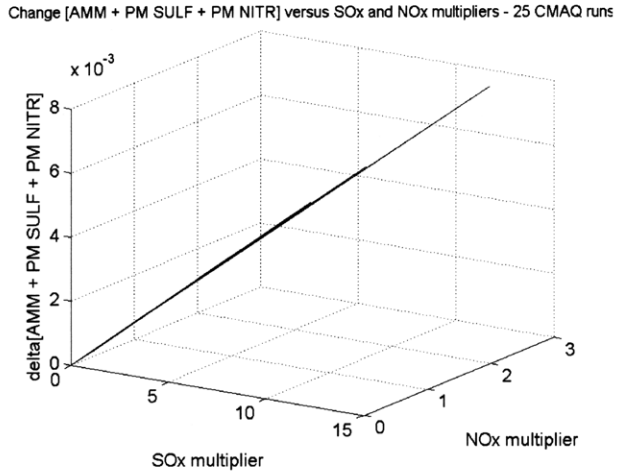
Change [AMM + PM SULF + PM NITR] versus SOx and NOx multipliers - 25 CMAQ runs
x 10^-3
delta[AMM + PM SULF + PM NITR]
SOx multiplier
NOx multiplier

APPENDIX H

Maps of changes in concentration for elemental carbon and PM organics for baseline aviation, 2005. Plots are the same as those presented in Figure 15, but on finer scales.

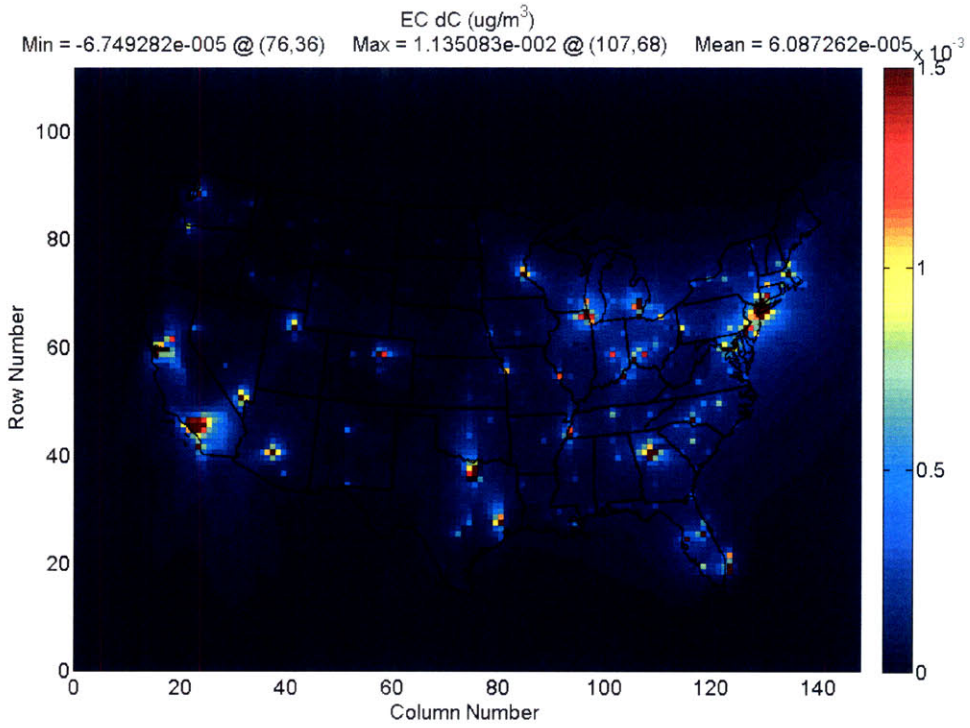

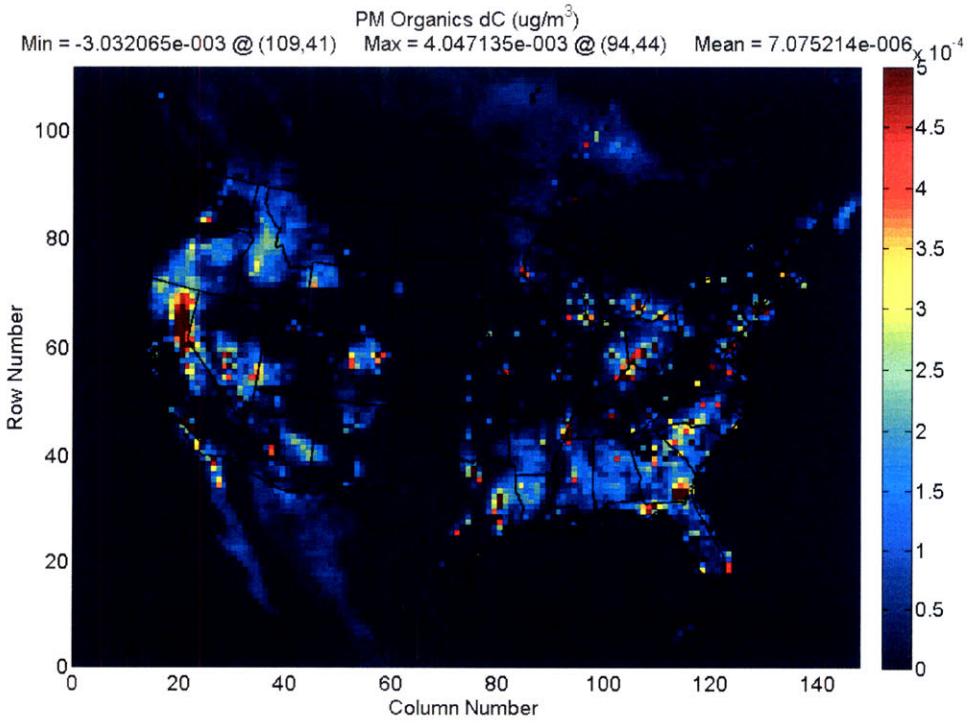

APPENDIX I

Results from Sequeira (2008) analyses compared to RSM v2 analyses. The "RSM post-BPR" inventory used by Sequeira is the same inventory as the 2005 baseline aviation inventory used in the RSM analysis.

Approximated number of premature mortalities from Sequeira (2008).

	nvPM	Vol-PM Organics	Amm-Nitrate	Amm-Sulfate	Vol-PM Amm-Sulf
EPAct	23 (14 %)	30 (18 %)	30 (18 %)	75 (46 %)	6 (4 %)
RSM post-BPR	8 (6 %)	9 (6 %)	29 (20 %)	97 (67 %)	1 (1 %)

Approximated number of premature mortalities per PM species, as obtained from the RSM v2. Baseline aviation case, Y2005.

	EC	PM Organics	PM Nitrates	PM Sulfates
RSM v2	30 (14%)	9 (4 %)	150 (70%)	26 (12%)

APPENDIX J.1

EPAct June 2005– May 2006 study : Comparison of EPA's pre-SMATed CMAQ results with post-SMATed changes in concentration of ammonium, PM nitrates, and PM sulfates. CMAQ results obtained for a comparable scenario (RSM run999) are also shown. Inventories used are compared in Table J.1. Both the EPA and the run999 simulations were done using CMAQ, with EPA NEI 2001 (no aviation) as background. Inventories used in the EPAct study and in run999 are pre-bypass-ratio correction. Both inventories have an assumed FSC of 680 ppm, however the EPAct inventory erroneously had 25% of airports at 400 ppm, leading to 15% lower SOx inventory. Results shown are contributions from aircraft only.

Table J.1 : Inventory comparison between EPAct and RSM – Run999 (tones/year)

Inventory	Nonvolatile Primary PM	Volatile Primary PM	Total Primary PM	NOx	SOx	Total PM
EPAct Pre-BPR correction (FOA3a)	928	1,190	2,120	79,100	8,800	90,000
RSM - Run999 Pre-BPR correction (FOA3)	850	207	1,060	78,900	10,400	90,400

APPENDIX J.2

Change in concentration of Ammonium

EPAct | **RSM999**

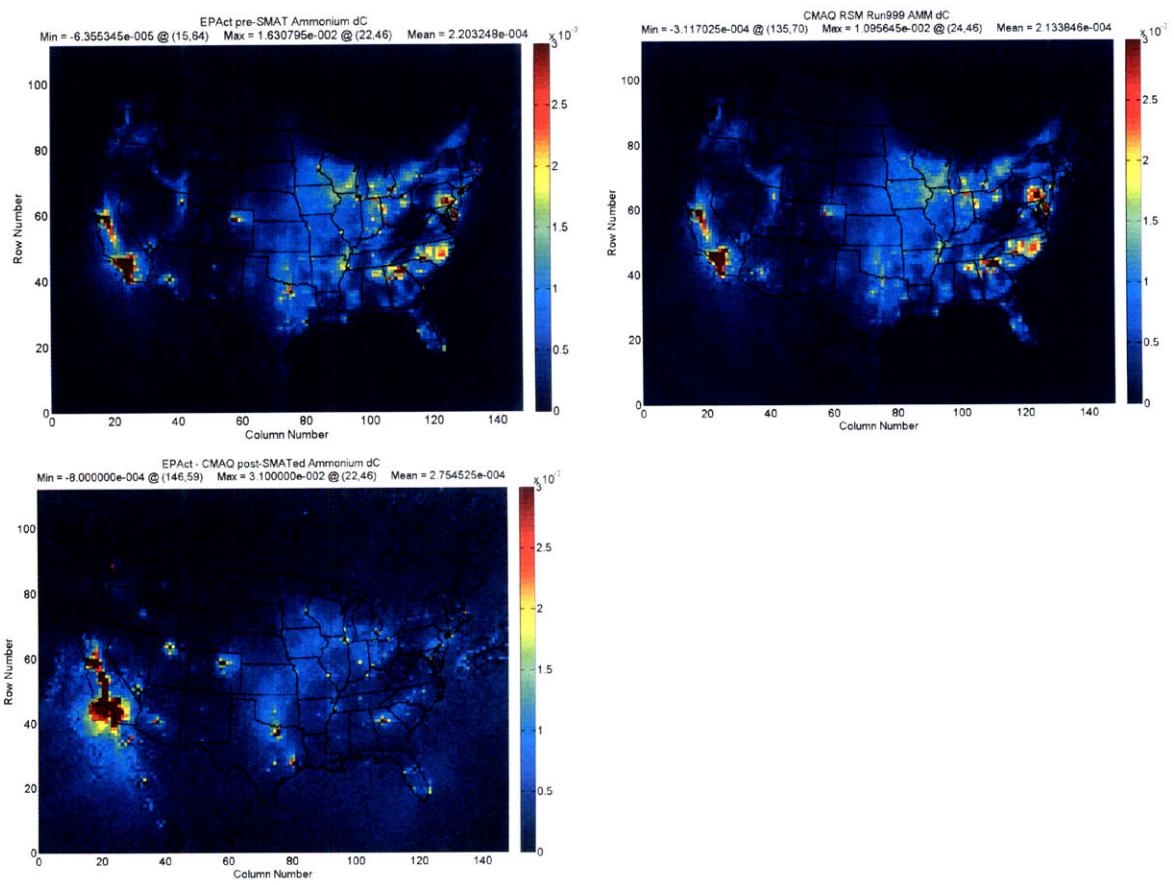

Table J.2 : Mean change in Ammonium concentration for 3 maps shown above.

Inventory / Process	Mean change in AMM concentration ($\mu g/m^3$) over U.S. domain
EPAct / pre-SMATing	2.20×10^{-4}
EPAct / post-SMATing	2.75×10^{-4}
RSM Run 999 / pre-SMATing	2.13×10^{-4}

APPENDIX J.3

Change in concentration of PM Nitrates

EPAct | **RSM999**

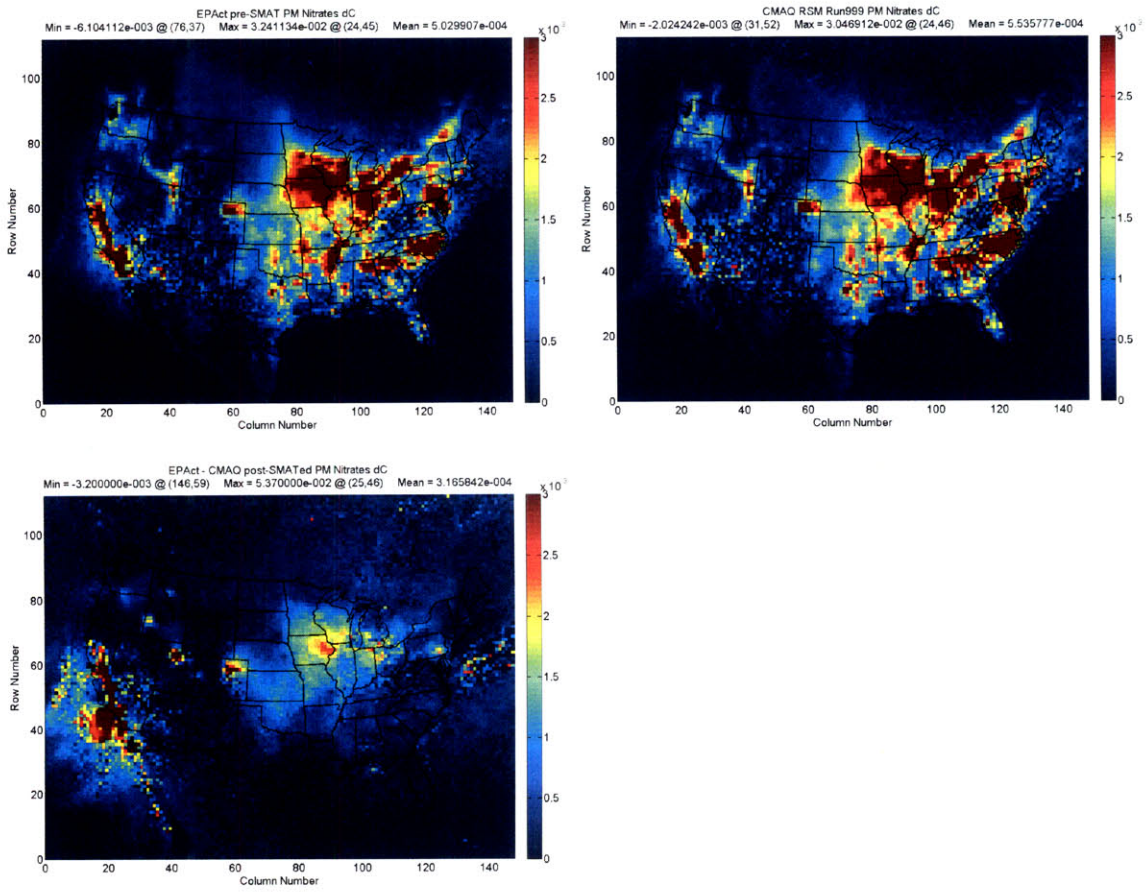

Table J.3 : Mean change in PM Nitrates concentration for 3 maps shown above.

Inventory / Process	Mean change in PM Nitrates concentration ($\mu g/m^3$) over U.S. domain
EPAct / pre-SMATing	5.03×10^{-4}
EPAct / post-SMATing	3.17×10^{-4}
RSM Run 999 / pre-SMATing	5.54×10^{-4}

APPENDIX J.4

Change in concentration of PM Sulfates

EPAct | **RSM999**

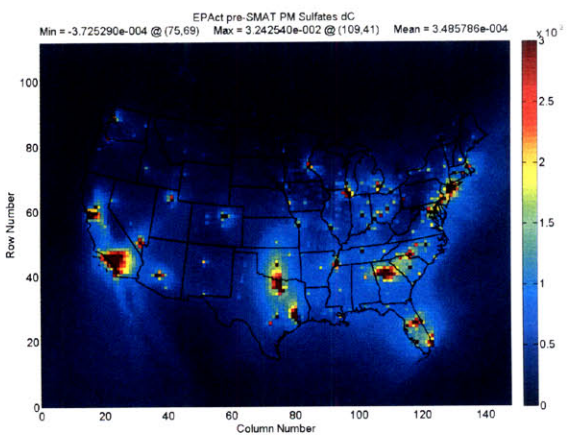

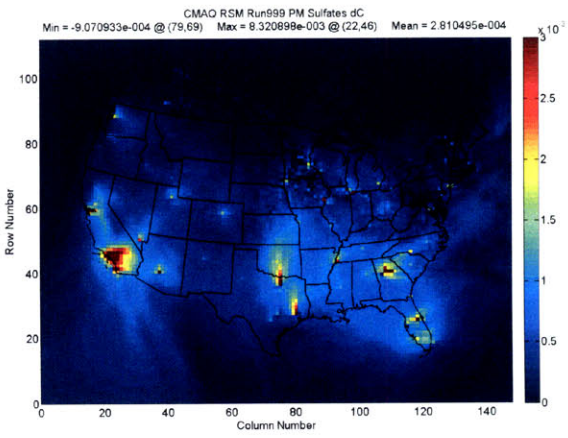

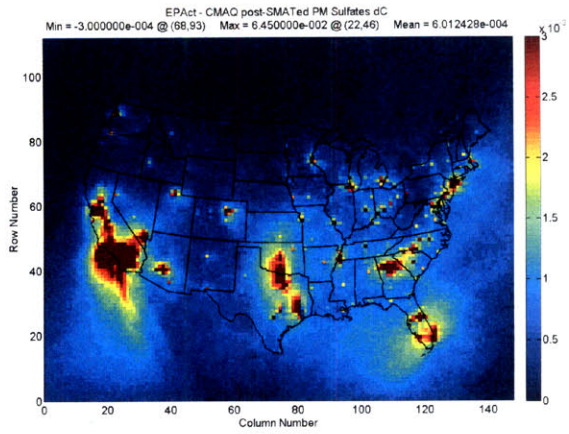

Table J.4 : Mean change in PM Sulfates concentration for 3 maps shown above.

Inventory / Process	Mean change in PM Sulfates concentration ($\mu g/m^3$) over U.S. domain
EPAct / pre-SMATing	3.49×10^{-4}
EPAct / post-SMATing	6.01×10^{-4}
RSM Run 999 / pre-SMATing	2.18×10^{-4}

Bibliography

ABT 2005. BenMAP environmental benefits mapping and analysis program user's manual. Bethesda, MD: Abt Associates, Inc. Prepared for U.S. Environmental Protection Agency Office of Air Quality and Standards.

ACS. 2008a. *Overview: Skin Cancer - Basal and Squamous Cell* [Online]. American Cancer Society. Available: www.cancer.org/docroot/CRI/content/CRI_2_2_1X_How_many_people_get_nonmelanoma_skin_cancer_51.asp?sitearea= [Accessed March 10 2009].

ACS. 2008b. *Overview: Skin Cancer - Melanoma* [Online]. American Cancer Society. Available: http://www.cancer.org/docroot/CRI/CRI_2_1x.asp?dt=39 [Accessed March 10 2009].

ALLAIRE, D. L. 2009. *Uncertainty Assessment of Complex Models with Application to Aviation Environmental Systems.* Ph.D., Massachusetts Institute of Technology.

ALMAHROOS, M. & KURBAN, A. 2004. Ultraviolet carcinogenesis in nonmelanoma skin cancer. Part I: incidence rates in relation to geographic locations and in migrant populations. *SKINmed,* 3, 29-35; first page 29.

AMANN, M., COFALA, J., HEYES, C., KLIMONT, Z., MECHLER, R., POSCH, M. & SCHOEPP, W. 2004. The RAINS model. Documentation of the model approach prepared for the RAINS peer review 2004. *International Institute for Applied Systems Analysis, Laxenburg, Austria.*

BARRETT, S. R. H., BRITTER, R. E. & WAITZ, I. A. 2009. Global mortality attributable to aircraft cruise emissions. *Submitted to Environmental Science & Technology.*

BAS 2008. Science Briefing 2008: The Ozone Hole. *It's over twenty years since the discovery of the ozone hole drew world attention to the impact of human activity on the global environment.* British Antarctic Survey, National Environment Research Council.

BENNETT, D. H., MCKONE, T. E., EVANS, J. S., NAZAROFF, W. W., MARGNI, M. D., JOLLIET, O. & SMITH, K. R. 2002. Defining Intake Fraction. *Environmental Science & Technology,* 36, 207-216.

BRASH, D., RUDOLPH, J., SIMON, J., LIN, A., MCKENNA, G., BADEN, H., HALPERIN, A. & PONTÉN, J. 1991. A role for sunlight in skin cancer: UV-induced p53 mutations in squamous cell carcinoma. *Proc Natl Acad Sci U S A,* 88, 10124-8.

BRUNELLE-YEUNG, E., MASEK, T., ROJO, J. J., LEVY, J. I., ARUNACHALAM, S., MILLER, S. M. & WAITZ, I. A. In preparation. The magnitude and distribution of fine particle-related public health impacts of aircraft emissions in the United States.

BUREAU, U. S. C. 2000. *1990 to 1999 Annual Time Series of County Population Estimates By Age, Sex, Race, and Hispanic Origin* [Online]. Available: http://www.census.gov/popest/archives/1990s/CO-99-12.html [Accessed March 2009].

BYUN, D. & SCHERE, K. L. 2006. Review of the Governing Equations, Computational Algorithms, and Other Components of the Models-3 Community Multiscale Air Quality (CMAQ) Modeling System. *Applied Mechanics Reviews,* 59, 51-77.

BYUN, D. W. & CHING, J. K. S. 1999. *Science Algorithms of the EPA Models-3 Community Multiscale Air Quality (CMAQ) Modeling System,* US Environmental Protection Agency, Office of Research and Development.

CAEP 2006. Report of WG2 TG4 - Airport Air Quality: Emissions LAQ Guidance. *In:* COMMITTEE ON AVIATION ENVIRONMENTAL PROTECTION (CAEP), S. M., CAEP/7-WP/28 (ed.).

CAFE 2006. Service Contract for carrying out cost-benefit analysis of air quality related issues, in particular in the clean air for Europe (CAFE) programme: An update on cost-benefit analysis of the CAFE programme. *AEA Technology Environment.*

CEC 2005a. Commission staff working paper: Annex to: The Communication on Thematic Strategy on Air Pollution and The Directive on "Ambient Air Quality and Cleaner Air for Europe": Impact Assessment. Brussels: Commission of the European Communities.

CEC 2005b. Communication from the Commission to the Council and the European Parliament: Thematic Strategy on air pollution. Brussels: Commission of the European Communities.

CHEN, G. J., YELVERTON, C. B., S POLISETTY, U. S., HOUSMAN, T. S., WILLIFORD, P. M., TEUSCHLER, H. V. & FELDMAN, S. R. 2006. Treatment Patterns and Cost of Nonmelanoma Skin Cancer Management. *Dermatologic Surgery,* 32**,** 1266-1271.

CHEN, J., FLEISCHER, A. J., SMITH, E., KANCLER, C., GOLDMAN, N., WILLIFORD, P. & FELDMAN, S. 2001. Cost of nonmelanoma skin cancer treatment in the United States. *Dermatol Surg,* 27**,** 1035-8.

CODE, U. S. 1955 with Amendments in 1990. The Clean Air Act (42 U.S.C. 7401-7626). *In:* CONGRESS, U. S. (ed.) *42, Chapter 85.* Washington, DC.

CRUTZEN, P. 1973. A discussion of the chemistry of some minor constituents in the stratosphere and troposphere. *Pure and Applied Geophysics,* 106**,** 1385-1399.

CSSI 2007. Emissions and Dispersion Modeling System (EDMS) User's Manual. Washington, DC, Prepared for the FAA Office of Environment and Energy.

DE GRUIJL, F. & FORBES, P. 1995. UV-induced skin cancer in a hairless mouse model. *Bioessays,* 17**,** 651-60.

DE GRUIJL, F. & VAN DER LEUN, J. 1994. Estimate of the wavelength dependency of ultraviolet carcinogenesis in humans and its relevance to the risk assessment of a stratospheric ozone depletion. *Health Phys,* 67**,** 319-25.

DESC 2002-2007. Petroleum Quality Information Systems (PQIS) Report. Defense Energy Support Center (DESC-BP).

DOT, U. S. 2008. Revised Departmental Guidance: Treatment of the Value of Preventing Fatalities and Injuries in Preparing Economic Analyses. *Memorandum to Secretarial Officers, Modal Administrators; Re: Treatment of the Economic Value of a Statistical Life in Departmental Analyses.* Washington, D.C.: Office of the Secretary of Transportation.

EPA 1992. Procedures for Emission Inventory Preparation - Vol IV: Mobile Sources. U.S. Environmental Protection Agency (EPA 420-R-92-009).

EPA 1999. Regulatory Impact Analysis - Control of Air Pollution from New Motor Vehicles: Tier 2 Motor Vehicle Emissions Standards and Gasoline Sulfur Control Requirements. Washington, D.C.: US Environmental Protection Agency, Air and Radiation EPA420.

EPA 2000. Final Regulatory Analysis: Clean Diesel Trucks, Buses, and Fuel: Heavy-Duty Engine and Vehicle Standards and Highway Diesel Fuel Sulfur Control Requirements. Washington, DC: U.S. Environmental Protection Agency Office of Air and Radiation (EPA420-R-00-026).

EPA 2001. Human Health Effects of Ozone Depletion From Stratospheric Aircraft. Washington, DC: U.S. Environmental Protection Agency, National Aeronautics and Space Administration.

EPA 2004a. Air Quality Criteria for Particulate Matter (Final Report, Oct 2004). Washington, DC: U.S. Environmental Protection Agency (EPA/600/P-99/002aF).

EPA 2004b. Air Quality Criteria for Particulate Matter (Final Report, Oct 2004) Volume I. Washington, DC: U.S. Environmental Protection Agency (EPA/600/P-99/002aF).

EPA 2004c. Final regulatory impact analysis: Control of emissions from nonroad diesel engines. Washington, DC: U.S. Environmental Protection Agency Office of Air and Radiation (EPA420-R-04-007).

EPA 2005a. Regulatory Impact Analysis for the Final Clean Air Interstate Rule. Washington, DC: U.S. Environmental Protection Agency Office of Air and Radiation (A.2005.4 A).

EPA 2005b. Regulatory Impact Analysis for the Final Clean Air Visibility Rule or the Guidelines for Best Available Retrofit Technology (BART) Determinations Under the Regional Haze Regulations, Final. Washington, DC: U.S. Environmental Protection Agency Office of Air and Radiation (EPA-452/R-05-004).

EPA 2006a. EPA procedures for estimating future PM2.5 values for the CAIR final rule by application of the (revised) speciated modeled attainment test (SMAT).

EPA 2006b. Regulatory Impact Assessment PM National Ambient Air Quality Standards. Washington, DC: U.S. Environmental Protection Agency Office of Air and Radiation.

EPA 2006c. Response Surface Modeling: Technical support document for proposed PM NAAQA Rule. Research Triangle Park, NC: U.S. EPA Office of Air Quality Planning and Standards.

EPA 2007a. Regulatory Impact Analysis for Final Rule: Control of Hazardous Air Pollutants from Mobile Sources (signed February 9, 2007). Washington, DC: U.S. Environmental Protection Agency Office of Air and Radiation (EPA420-R-07-002).

EPA 2007b. Regulatory Impact Analysis for the Proposed Revisions to the National Ambient Air Quality Standards for Ground-Level Ozone. Washington, DC: U.S. Environmental Protection Agency Office of Air and Radiation.

EPA 2008. Regulatory Impact Analysis: Control of Emissions of Air Pollution from Locomotive Engines and Marine Compression Ignition Engines Less than 30 Liters Per Cylinder. Washington, DC: U.S. Environmental Protection Agency Office of Transportation and Air Quality (EPA420-R-08-001a).

EPA 2009. Cost of Illness Handbook: Chapter II.6: Cost of Skin Cancer, pending.

EPSTEIN, J. 1996. Nonmelanoma skin cancer. *Compr Ther,* 22**,** 179-82.

FEARS, T. & SCOTTO, J. 1983. Estimating increases in skin cancer morbidity due to increases in ultraviolet radiation exposure. *Cancer Invest,* 1**,** 119-26.

FRANSSEN, E., VAN WIECHEN, C., NAGELKERKE, N. & LEBRET, E. 2004. Aircraft noise around a large international airport and its impact on general health and medication use. *Occup Environ Med,* 61**,** 405-13.

FUGLESTVEDT, J. S., SHINE, K. P., BERNTSEN, T., COOK, J., LEE, D. S., STENKE, A., SKEIE, R. B., VELDERS, G. J. M. & WAITZ, I. A. 2009. Transport impacts on atmosphere and climate: Metrics. *Atmospheric Environment,* In publication**,** 30.

GAUSS, M., ISAKSEN, I. S. A., LEE, D. S. & S\'BFVDE, O. A. 2006. Impact of aircraft NOx emissions on the atmosphere – tradeoffs to reduce the impact. *Atmos. Chem. Phys.*\, 6\, 1529\-1548\.

GRANT, W., MOAN, J. & REICHRATH, J. 2007. Comment on "the effects on human health from stratospheric ozone depletion and its interactions with climate change" by M. Norval, A. P. Cullen, F. R. de Gruijl, J. Longstreth, Y. Takizawa, R. M. Lucas, F. P. Noonan and J. C. van der Leun, Photochem. Photobiol. Sci., 2007, 6, 232. *Photochem Photobiol Sci,* 6**,** 912-5; discussion 916-8.

GRECO, S. L., WILSON, A. M., SPENGLER, J. D. & LEVY, J. I. 2007. Spatial patterns of mobile source particulate matter emissions-to-exposure relationships across the United States. *Atmospheric Environment,* 41**,** 1011-1025.

HALTON, J. H. 1960. On the efficiency of certain quasi-random sequences of points in evaluating multi-dimensional integrals. *Numerische Mathematik,* 2**,** 84-90.

HOLLAND, M., HUNT, A., HURLEY, F., NAVRUD, S. & WATKISS, P. 2005. Final Methodology Paper (Volume 1) for Service Contract for carrying out cost-benefit analysis of air quality related issues, in particular in the clean air for Europe (CAFE) programme, report to ECDG Environment. *AEA Technology Environment.*

HOLVE, D. J. & CHAPMAN, J. 2005. Real-Time Soot (black carbon) Concentration and Size by Light Scattering, Aircraft Particle Emissions eXperiment (APEX). presentation at the American Association for Aerosols Reseach.

HURLEY, F., HUNT, A., COWIE, H., HOLLAND, M., MILLER, B., PYE, S. & WATKISS, P. 2005. Methodology Paper (Volume2) for Service Contract for carrying out cost-benefit analysis of air quality related issues, in particular in the clean air for Europe (CAFÉ) programme. *AEA Technology Environment.*

HUSSEIN, M. 2005. Ultraviolet radiation and skin cancer: molecular mechanisms. *J Cutan Pathol,* 32, 191-205.

IARC 1992. Monographs on the evaluation of carcinogenic risks to humans. Lyon, France.

ICAO 2007. Outlook for Air Transport to the Year 2025. International Civil Aviation Organization, United Nations.

ICF 2006. Human Health Benefits of Stratospheric Ozone Protection: Peer Reviewed Report. *Prepared for the Office of Air and Radiation, U.S. EPA.* Washington, DC: ICF Consulting.

ISAKSEN, I., SAUSEN, R. & PYLE, J. 2003. The EU project TRADEOFF Aircraft emissions: Contributions of various climate compounds to changes in composition and radiative forcing tradeoff to reduce atmospheric impact. *Project Final report, Contract No. EVK2-CT-1999-0030,* 158.

KARAGAS, M., GREENBERG, E., SPENCER, S., STUKEL, T. & MOTT, L. 1999. Increase in incidence rates of basal cell and squamous cell skin cancer in New Hampshire, USA. New Hampshire Skin Cancer Study Group. *Int J Cancer,* 81, 555-9.

KELFKENS, G., DE GRUIJL, F. & VAN DER LEUN, J. 1990. Ozone depletion and increase in annual carcinogenic ultraviolet dose. *Photochem Photobiol,* 52, 819-23.

KYLE, J., HAMMITT, J., LIM, H., GELLER, A., HALL-JORDAN, L., MAIBACH, E., DE FABO, E. & WAGNER, M. 2008. Economic evaluation of the US Environmental Protection Agency's SunWise program: sun protection education for young children. *Pediatrics,* 121, e1074-84.

KÖHLER, M. O., RÄDEL, G., DESSENS, O., SHINE, K. P., ROGERS, H. L., WILD, O. & PYLE, J. A. 2008. Impact of perturbations to nitrogen oxide emissions from global aviation. *J. Geophys. Res.,* 113.

LANE, T., DONAHUE, N. & PANDIS, S. 2008. Effect of NOx on secondary organic aerosol concentrations. *Environ Sci Technol,* 42, 6022-7.

LEWIS, K. & WEINSTOCK, M. 2004. Nonmelanoma skin cancer mortality (1988-2000): the Rhode Island follow-back study. *Arch Dermatol,* 140, 837-42.

LEWIS, K. G. & WEINSTOCK, M. A. 2007. Trends in Nonmelanoma Skin Cancer Mortality Rates in the United States, 1969 through 2000. *J Invest Dermatol,* 127, 2323-2327.

LIU, S. C., TRAINER, M., FEHSENFELD, F. C., PARRISH, D. D., WILLIAMS, E. J., FAHEY, D. W., HÜBLER, G. & MURPHY, P. C. 1987. Ozone Production in the Rural Troposphere and the Implications for Regional and Global Ozone Distributions. *J. Geophys. Res.,* 92.

LONGSTRETH, J. D., DE GRUIJL, F. R., KRIPKE, M. L., TAKIZAWA, Y. & VAN DER LEUN, J. C. 1994. Environmental effects of ozone depletion: 1994 Assessment, Chapter 2 Effects of Increased Solar Ultraviolet Radiation on Human Health. Nairobi, Kenya: United Nations Environmental Programme.

MADRONICH, S. 1992. Implications of recent total atmospheric ozone measurements for biologically active ultraviolet radiation reaching the earth's surface. *Geophysical Research Letters,* 19.

MADRONICH, S. 1993. UV radiation in the natural and perturbed atmosphere. *Environmental Effects of UV (Ultraviolet) Radiation,* 17–69.

MADRONICH, S. & DE GRUIJL, F. 1993. Skin cancer and UV radiation. *Nature,* 366, 23-23.

MADRONICH, S., MCKENZIE, R. L., BJÖRN, L. O. & CALDWELL, M. M. 1998. Changes in biologically active ultraviolet radiation reaching the Earth's surface. *Journal of Photochemistry and Photobiology B: Biology,* 46, 5-19.

MADRONICH, S., WEATHERHEAD, E. & FLOCKE, S. 1996. Trends in UV radiation. *International journal of environmental studies,* 51, 183-198.

MASEK, T. 2008. *A Response Surface Model of the Air Quality Impacts of Aviation.* Master's, Massachusetts Institute of Technology.

MCKINLAY, A. 1987. F., and BL Diffey, 1987: A reference action spectrum for ultraviolet induced erythema in human skin. *CIE-Journal,* 6, 17-22.

MURDOCH, J. C. & THAYER, M. A. 1990. The Benefits of Reducing the Incidence of Nonmelanoma Skin Cancers: a Defensive Expenditure Approach. *Journal of Environmental Economics and Management,* 18, 107-119.

NCI. 2009a. *Cancer Mortality Maps & Graphs : Other (Non-Melanoma) Skin Cancer* [Online]. National Cancer Institute. Available: http://dceg.cancer.gov/cgi-bin/atlas/ca-type?site=osk [Accessed March 2009].

NCI. 2009b. *Treatment Options for Nonmelanoma Skin Cancer* [Online]. Available: http://www.cancer.gov/cancertopics/pdq/treatment/skin/Patient/page4 [Accessed March 2009 2009].

NENES, A., PANDIS, S. N. & PILINIS, C. 1998. ISORROPIA: A New Thermodynamic Equilibrium Model for Multiphase Multicomponent Inorganic Aerosols. *Aquatic Geochemistry,* 4, 123-152.

NOAA. 2006. *Latest SBUV/2 Analyses* [Online]. Camp Springs: National Oceanic and Atmospheric Administration. Available: http://www.cpc.noaa.gov/products/stratosphere/sbuv2to/sbuv2to_latest.shtml [Accessed March 21 2009].

NORVAL, M., CULLEN, A., DE GRUIJL, F., LONGSTRETH, J., TAKIZAWA, Y., LUCAS, R., NOONAN, F. & VAN DER LEUN, J. 2007. The effects on human health from stratospheric ozone depletion and its interactions with climate change. *Photochem Photobiol Sci,* 6, 232-51.

NORVAL, M. & GRUIJL, F. 2007. Reply to the Comment on "The effects on human health from stratospheric ozone depletion and its interactions with climate change" by WB Grant, J. Moan and J. Reichrath, Photochem. Photobiol. Sci., 2007, 6, DOI: 10.1039/b705482c. *Photochemical & Photobiological Sciences,* 6, 916-918.

NRC 2007. *Models in Environmental Regulatory Decision Making,* Washington, D.C., National Academic Press.

PEARCE, D. 2000. Valuing Risks to Life and Health - Towards Consistent Transfer Estimates in the European Union and Accession States. *Paper prepared for the European Commission (DGXI) Workshop on Valuing Mortality and Valuing Morbidity.* University COllege London.

PENNER, J. E., LISTER, D. H., GRIGGS, D. J., DOKKEN, D. J. & MCFARLAND, M. 1999. *Aviation and the global atmosphere. A special report of IPCC Working Groups I and III.,* UK, Cambridge University Press.

PERLIS, C. & HERLYN, M. 2004. Recent advances in melanoma biology. *Oncologist,* 9, 182-7.

PITCHER, H. M. & LONGSTRETH, J. D. 1991. Melanoma mortality and exposure to ultraviolet radiation: an empirical relationship. *Environ Int,* 17, 7–21.

POPE III, C., BURNETT, R., THUN, M., CALLE, E., KREWSKI, D., ITO, K. & THURSTON, G. 2002. Lung cancer, cardiopulmonary mortality, and long-term exposure to fine particulate air pollution. Am Med Assoc, Vol. 287, No. 9, p.1132-1141.

RATLIFF, G., SEQUEIRA, C., WAITZ, I., OHSFELD, M., THRASHER, T., GRAHAM, M., THOMPSON, T., GILLETTE, W., GUPTA, M., IOVINELLI, R., HOLSCLAW, C., MANNING, B., DOLWICK, P. & DAVIDSON, K. 2009. Aircraft Impacts on Local and Regional Air Quality in the United States: A Response to Section 753 of the Energy Policy Act of 2005 (DRAFT). Cambridge, MA: Massachusetts Institute of Technology.

ROJO, J. J. 2007. *Future Trends in Local Air Quality Impacts of Aviation.* S.M., Massachusetts Institute of Technology.

SCOTTO, J. & FEARS, T. R. 1981. Incidence of nonmelanoma skin cancer in the United States. NIH Publication ed. Washington, D.C.: U.S. Department of Health and Human Services, Issue 82, p.2433.

SCOTTO, J., PITCHER, H. & LEE, J. 1991. Indications of future decreasing trends in skin-melanoma mortality among whites in the United States. *Int J Cancer,* 49, 490-7.

SEQUEIRA, C. J. 2008. *An assessment of the health implications of aviation emissions regulations.* S.M., Massachusetts Institute of Technology.

SERUP-HANSEN, N., GUDUM, A. & SØRENSEN, M. M. 2004. Valuation of Chemical Related Health Impacts. *Estimation of direct and indirect costs for asthma bronchiale, headache, contact allergy, lung cancer and skin cancer.* Danish Ministry of the Environment Environmental Protection Agency.

SETLOW, R. 1974. The wavelengths in sunlight effective in producing skin cancer: a theoretical analysis. *Proc Natl Acad Sci U S A,* 71, 3363-6.

SETLOW, R. 1999. Spectral regions contributing to melanoma: a personal view. *J Investig Dermatol Symp Proc,* 4, 46-9.

STANG, A. 2007. Genital and Nongenital Nonmelanoma Skin Cancer: More Epidemiological Studies Are Needed. *J Invest Dermatol,* 127, 2296-2299.

TANG, J., SO, P. & EPSTEIN, E. J. 2007. Novel Hedgehog pathway targets against basal cell carcinoma. *Toxicol Appl Pharmacol,* 224, 257-64.

VAN DER LEUN, J. C., LONGSTRETH, J. D., DE GRUIJL, F. R., KRIPKE, M. L., ABSECK, S., ARNOLD, F., SLAPER, H. I., G., V. & TAKIZAWA, Y. 1998. Environmental effects of ozone depletion: 1998 Assessment, Chapter 2 Health Risks. *In:* PROGRAMME, U. N. E. (ed.). Nairobi.

WAITZ, I., LUKACHKO, S., GO, Y., HOLLINGSWORTH, P., HARBACK, K. & MORSER, F. 2006a. Requirements Document for the Aviation Environmental Portfolio Management Tool. PARTNER-COE-2006-001, June 2006.

WAITZ, I., LUKACHKO, S., WILLCOX, K., BELOBABA, P., GARCIA, E., HOLLINGSWORTH, P., MAVRIS, D., HARBACK, K., MORSER, F. & STEINBACH, M. 2006b. Architecture Study for the Aviation Environmental Portfolio Management Tool. PARTNER-COE-2006-002, June 2006.

WEINSTOCK, M., BOGAARS, H., ASHLEY, M., LITLE, V., BILODEAU, E. & KIMMEL, S. 1991. Nonmelanoma skin cancer mortality. A population-based study. *Arch Dermatol,* 127, 1194-7.

WOODY, M. 2009. Secondary Organic Aerosol produced from Aircraft Emissions at the Atlanta Airport - An Advanced Diagnostic Investigation using Process-based and Reaction-based approaches. University of North Carolina at Chapel Hill, Paper submitted to the Partnership

for AiR Transportation Noise and Emissions Reduction (PARTNER): Joseph A. Hartman Student Paper Competition.

WORLD_BANK 2007. *The Cost of Pollution in China: economic estimates of physical damage*, World Bank, Rural Development, Natural Resources and Environment Management Unit., East Asia and Pacific Region.

ZIEGLER, A., LEFFELL, D., KUNALA, S., SHARMA, H., GAILANI, M., SIMON, J., HALPERIN, A., BADEN, H., SHAPIRO, P. & BALE, A. 1993. Mutation hotspots due to sunlight in the p53 gene of nonmelanoma skin cancers. *Proc Natl Acad Sci U S A,* 90**,** 4216-20.